Molecular genetic studies on autoregulation of nodulation and nitrate-induced control of root nodule symbiosis in *Lotus japonicas*

NISHIDA HANNA

Doctor of Philosophy

Department of Basic Biology
School of Life Science
SOKENDAI (The Graduate University for Advanced Studies)

Molecular genetic studies on autoregulation of nodulation and nitrate-induced control of root nodule symbiosis in *Lotus japonicus*

Nishida, Hanna

PhD Dissertation
2017

SOKENDAI (The Graduate University for Advanced Studies)
School of Life Science
Department of Basic Biology

TABLE OF CONTENTS

Chapter 1

GENERAL INTRODUCTION 1

Figures 10

Chapter 2

A *NIN-LIKE PROTEIN* mediates nitrate-induced control of root nodule symbiosis in *Lotus japonicus*

2.1 Introduction 12

2.2 Results 13

2.3 Discussion 21

2.4 Methods 24

Figures and Tables 29

Chapter 3

Expression of the *CLE-RS3* gene suppresses root nodulation in *L. japonicus*

3.1 Introduction 58

3.2 Results 61

3.3 Discussion 64

3.4 Methods 66

Figures and Tables 69

Chapter 4

GENERAL DISCUSSION 83

Figures 90

ACKNOWLEDGEMENTS 94

REFERENCES 95

Chapter 1
GENERAL INTRODUCTION

Root nodule symbiosis

As a component of essential amino acids, nucleic acids, chlorophyll, coenzymes, and numerous plant secondary products, nitrogen is an indispensable inorganic nutrient required by plants throughout their life (Frink et al., 1999). Although nitrogen gas occupies about 78% of the atmosphere, most plant species are unable to directly assimilate atmospheric nitrogen. In addition, while the main sources of nitrogen for land plants are nitrate and ammonium in the soil, their abundance is not stable and is dependent on the environment, suggesting that nitrogen is a critical limiting element for the growth of most plants. Root nodule symbiosis is an important strategy mainly adopted by legumes to enhance nitrogen acquisition. The interaction between legumes and nitrogen-fixing rhizobia results in the formation of root-derived specialized symbiotic organs called root nodules. Symbiotic nitrogen fixation in root nodules containing rhizobia enables legumes to thrive in nitrogen-deficient soil.

The first report on root nodule symbiosis probably dates back to 1838. Boussingault reported that legumes could obtain nitrogen source from atmospheric nitrogen. Fifty-years later, Hellriegel and Wilfarth found that root nodules were responsible for the conversion of atmospheric nitrogen to ammonia (Hellriegel and Wilfarth, 1888). In 1889, the existence of bacteria was reported from nodules, and they were designated as *Rhizobium leguminosarum* by Frank (Frank, 1889). To date, physiological aspects of root nodule symbiosis have been delineated on the basis of histology and biochemical approaches using leguminous plants, including *Glycine max, Medicago sativa, Pisum sativum, Vicia species, Astragalus sinicus,* and *Trifolium repens*. Studies using two model legumes, *Lotus japonicus* and *Medicago truncatula*, have facilitated our understanding of molecular genetic mechanisms that regulate the symbiosis. These two plant species differ in terms of the morphology of their nodules (Ferguson et al., 2010). *L. japonicus* produces typical sphere-shaped determinate nodules. Determinate-type nodules are developed by cell divisions of root cortical cells and subsequent cell expansion. Once sufficient mass is established, cells in developing nodules lose their ability to divide. Conversely, indeterminate nodules of *M. truncatula* maintain meristematic activity at the tip of elongated nodules throughout nodule development, which allows semi-permanent growth of the nodule. Although developmental patterns differ somewhat between the two types of nodules, there are no significant

differences in the molecular mechanisms involved in nodulation and their fundamental functions as symbiotic organs (Suzaki et al., 2015).

Nodulation begins with mutual recognition between host plants and rhizobia (Fig. 1-1) (Kouchi et al., 2010; Oldroyd, 2013). First, free-living rhizobia in the soil sense host plant-derived-specific flavonoids. Flavonoids such as luteolin penetrate into bacterial cells and stimulate binding of NodD transcription factor to *cis*-elements on *Nod* (nodulation) genes promoter (Peters et al., 1986; Peck et al., 2006), resulting in the production of specific lipochito-oligosaccharides, called Nod factors (Lerouge et al., 1990), which serve as bacterial nodulation signals. Then, perception of the Nod factors by plants elicits symbiotic signaling pathways in the root epidermis, which induces several sequential physiological and morphological alternations in the roots, including oscillation of calcium levels in epidermal cells defined as calcium spikes, root hair deformation, such as curling, and re-initiation of cell division in the root cortex to form nodule primordia (Ehrhardt et al., 1996, Esseling et al., 2003). During early nodulation processes, rhizobia trapped at the tip of the root hair invade into plant cells through plant-derived specialized intracellular tube-like structures, termed infection threads (Fournier et al., 2008; Murray, 2011). Infection threads guide bacteria into inner tissues of host roots. When infection threads reach developing nodules, rhizobia are released into host cells as a compartment surrounded by a host membrane, termed a symbiosome (Limpens et al., 2005). Then, each bacterium in the infected cells takes on a morphologically and physiologically different form called bacteroid. This is a terminally differentiated form of rhizobia that is capable of fixing nitrogen to ammonia via nitrogenase (Mergaert et al., 2006). Although aerobic conditions are required for bacteria to produce sufficient ATP for nitrogen fixation, nitrogenase activity is very vulnerable to oxygen. To overcome this, plants accumulate leghemoglobin, a nodule-specific oxygen-binding protein, in mature nodules. They also maintain low oxygen partial pressure, which permits the production of energy for nitrogen fixation using oxygen, without direct contact between oxygen and nitrogenase (Ott et al., 2005).

Autoregulation of nodulation (AON)

Nodules function as an organ that supplies a source of nitrogen to host plants. Conversely, hosts consume photosynthetic products as an energy source for nodule development and nitrogen fixation. Therefore, from a plant perspective, a balance between the benefits of obtaining nitrogen sources and the cost of losing carbon sources that should be used for growth, needs to be maintained.

In 1952, Nutman showed that surgical excision of effective nodules in red clover promoted the formation of new nodules, suggesting that the effective nodules could inhibit further nodulation (Nutman, 1952). Bhuvaneswari et al. found that the root region was susceptible to rhizobial infection near the root tip in soybean roots. In addition, those authors showed that nodulation frequency in the susceptible zone developed lately after nodulation took place in root regions developed early (Bhuvaneswari et al., 1980; Pierce and Bauer, 1983). Similar phenomena have been observed in alfalfa, clover, and cowpea (Bhuvaneswari et al., 1981). Interpretation of these results led to the proposal that legumes possess a conserved self-regulatory mechanism to suppress nodulation, which is, autoregulation of nodulation (AON). Subsequently, a split-root experiment provided important information, where soybean roots were divided into two parts and each root was infected with a time lag. The experiment showed that previous inoculation of half of the root system suppressed the nodule development of later-inoculated roots in the other half (Kosslak and Bohlool, 1984). This was the first evidence to show that early-forming nodules can suppress subsequent nodulation events through systemic long-range signaling between roots and shoots. In 1985, Carroll et al. screened for soybean mutants under high nitrate conditions and identified several hypernodulation mutants named *nitrate-tolerant symbiotic* (*nts*) (Carroll et al., 1985). These mutants formed excessive nodules irrelevant to nitrate. A split-root experiment indicated that the *nts* mutant is defective in AON (Olsson et al., 1989). Furthermore, by reciprocal grafting between *nts* mutants and wild type (WT) plants, Delves et al. showed that the hypernodulation phenotype of *nts* mutants was caused by a mutation in the shoot (Delves et al., 1986).

In a current model of AON, two types of long-distance mobile signaling factors have been postulated. Rhizobial infection induces production of signaling molecules called roots-derived signals, which move from the root to shoot through the xylem. Then, the root-derived signals are recognized by their receptors in the shoot, and activate the production of secondary signaling molecules called shoot-derived inhibitors (SDIs), which in turn are transported from the shoot to root through the phloem to restrict further nodulation (Fig. 1-2). Thus far, analyses of several hypernodulation mutants, mainly in model legumes, have provided great insight into the molecular mechanisms of AON. *L. japonicus HYPERNODULATION ABERRANT ROOT FORMATION 1* (*HAR1*) was identified as the first AON-related gene in plants, which encodes a putative leucine-rich repeat receptor-like kinase (LRR-RLK) (Kawaguchi et al., 2002; Krusell et al., 2002; Nishimura et al., 2002; Wopereis et al., 2000). The *har1* mutants exhibit reduced plant growth due to the formation of a markedly increased number of nodules. Reciprocal grafting

experiments using WT and *har1* mutants confirmed that the defect of shoot-acting HAR1 is responsible for the hypernodulation phenotype, because the excessive nodulation phenotype was observed only when *har1* plants were used as the scion. After identification of *HAR1*, *M. truncatula SUPER NUMERIC NODULES* (*SUNN*) (Schnabel et al., 2005), *G. max NODULE AUTOREGULATION RECEPTOR KINASE* (*NARK*), one of the genes responsible for *nts* mutants (Searle et al., 2003), and *P. sativum SYM29* (Krusell et al., 2002) were found to control the number of nodules. HAR1, SUNN, NARK, and PsSYM29 are orthologous to Arabidopsis CLAVATA1 (AtCLV1), which functions as a key negative regulator of stem cell homeostasis in the shoot apical meristem (Clark et al., 1997).

In Arabidopsis, AtCLV3, which is a small peptide belonging to the CLAVATA3/ENDOSPERM SURROUNDING REGION (CLE) family, acts as a ligand of AtCLV1 (Fletcher et al., 1999; Ogawa et al., 2008). Based on these findings, Okamoto et al. focused on *L. japonicus CLE* genes; their expression and subsequent functional analyses resulted in the identification of two *LjCLE* genes, *CLE-ROOT SIGNAL 1* (*CLE-RS1*) and *CLE-RS2*, which were strongly induced in roots in response to rhizobial infection (Okamoto et al., 2009). Constitutive expression of the *CLE-RS1* or *CLE-RS2* gene in transgenic hairy roots suppressed nodulation in a HAR1-dependent manner. The effect of suppression was systemically transmitted from transformed to untransformed roots generated in the same plants (Okamoto et al., 2009). They further determined the structure of the active form of CLE-RS2, which is an arabinosylated glycopeptide consisting of 12 amino acids derived from the CLE domain, and the mature CLE-RS2 peptide was found to directly bind to HAR1. Furthermore, CLE-RS2 was shown to be transported from the root to the shoot through the xylem, suggesting that CLE-RS2 is a strong candidate for a root-derived signal (Okamoto et al., 2013).

Recently, a transcription factor involved in the expression of *CLE-RS1* and *CLE-RS2* in response to rhizobial infection was identified. This factor is known as NODULE INCEPTION (NIN), which is a RWP-RK type transcription factor, and is essential for infection thread development and cortical cell division to produce nodule primordia (Schauser et al., 1999; Marsh et al., 2007). Constitutive expression of *LjNIN* in the absence of rhizobia induced spontaneous cortical cell division (Soyano et al., 2013; Yoro et al., 2014), indicating that LjNIN is a necessary and sufficient factor for initiating nodule organogenesis. However, constitutive expression of *LjNIN* suppressed nodulation in the presence of rhizobia. *CLE-RS1/2* are direct targets of LjNIN. Constitutive *LjNIN* expression activates *CLE-RS1/2*, and downregulates its own expression

systemically in a HAR1-dependent manner (Soyano et al., 2014). Thus, in addition to its positive role for nodulation, LjNIN negatively regulates nodulation through AON activation.

In *L. japonicus*, *KLAVIER* (*KLV*), *LjCLV2*, and *TOO MUCH LOVE* (*TML*) have been identified as components of the AON. Double mutant analyses indicated that *KLV*, *LjCLV2*, *TML,* and *HAR1* function in the same genetic pathway. *KLV* and *LjCLV2* each encodes an LRR-RLK belonging to a different subfamily from the HAR1 and LRR-RL proteins, and they are proposed to form a receptor complex with HAR1 (Miyazawa et al., 2010; Krusell et al., 2011). The results of an inverted-Y grafting approach suggested that *TML*, encoding an F-box/Kelch-repeat protein, acts in roots downstream of CLE-RS1/2-HAR1 signaling (Magori et al., 2009; Takahara et al., 2013). Sasaki et al. showed that rhizobial infection induced the expression of *ISOPENTENYL TRANSFERASE 3* (*LjIPT3*) in shoots in a *HAR1*-dependent manner; this gene encodes an enzyme involved in the cytokinin biosynthetic pathway. They also showed that cytokinin applied from cotyledons could be transported to roots and subsequently inhibit nodulation in a *TML*-dependent manner (Sasaki et al., 2014). However, it remains unknown how shoot-derived cytokinins inhibit nodulation. Thus, the identification of SDI in studies on AON remains to be determined.

Nitrate-induced control of root nodule symbiosis

As another strategy to fulfill the nitrogen demands of plants without unnecessary loss of carbon, plants control root nodule symbiosis in response to nitrogen availability in the soil. Most chemical forms of nitrogen are rapidly converted to nitrate in the aerobic soil, and thus plants are most likely to be exposed to nitrate among diverse nitrogen derivatives (Crawford and Forde, 2002). For this reason, many studies investigating the response to nitrogen nutrition have focused on nitrate. In 1916, Fred and Graul reported that a sufficient nitrogen source, such as nitrate, in the soil inhibited root nodule symbiosis, where the application of nitrate affected multiple stages of root nodule symbiosis (Fig.1-1) (Fred and Graul, 1916). For example, high levels of nitrate inhibited the production of flavonoids, which are involved in Nod factor synthesis, rhizobial infection, nodule initiation, nodule growth, and nitrogen fixation activity (Streeter and Wong, 1988; Carroll and Mathews, 1990; Coronado et al., 1995). Furthermore, high nitrate accelerated nodule senescence or disintegration (Matamoros et al., 1999). In soybean, nodule growth and nitrogen fixation activity were immediately stopped upon nitrate application, and these response were quickly reversible when nitrate was removed (Fujikake et al., 2002; Fujikake et al., 2003; Saito et al., 2014). Thus, plants seem to reversibly regulate symbiosis depending on the nitrate status in their environment. The results of split-root and two-layered pot experiments indicated

that root nodule symbiosis is inhibited in the root in direct contact with nitrate and in other roots in the absence of nitrate (Cho and Harper, 1991; Jeudy et al., 2010; Yashima et al., 2003). This led to a model being proposed on the local and systemic effects of nitrate on nodulation, whereby plants can sense the nitrogen status in whole roots and control root nodule symbiosis.

Interestingly, hypernodulation mutants, such as *har1*, *klv,* and *tml* in *L. japonicus*, *sunn* in *M. truncatula*, and *nark* in *G. max* exhibited marked increases in the number of nodules and also formed nodules under high nitrate concentrations (Wopereis et al., 2000; Oka-Kira et al., 2005; Magori et al., 2009; Schnabel et al., 2005; Searle et al., 2003). In addition, *CLE-RS2*, which encodes a root-derived signal in AON, responds not only to rhizobial infection but also to nitrate (Okamoto et al., 2009). Based on these observations, the molecular mechanism underlying the control of nodulation by nitrate involves a system similar to AON (Okamoto et al., 2009). On the other hand, high nitrate application was found to reduce the number of infection threads (Soyano et al., 2015) and inhibit nodule growth (Okamoto and Kawaguchi, 2015; Jeudy et al., 2010) in *har1* and *sunn* mutants, suggesting that the responsible genes are not required for the two nitrate-affected processes. Hence, AON alone is insufficient to fully explain nitrate-induced pleiotropic control of the root nodule symbiosis. Although nitrate application is reported to inhibit the expression of rhizobia-inducible genes, such as *LjNIN* and *LjNF-YA* (Barbulova et al., 2007; Soyano et al., 2015), the underlying molecular basis is unknown.

Several hypotheses have been proposed to explain the pleiotropic effects of nitrate. First, inhibition of nodule growth and nitrogen fixation by nitrate may be related to the diversion of photoassimilates. Fujikake et al. investigated the partitioning pattern of photoassimilates in soybean roots by applying ^{14}C-labeled carbon dioxide, and found that the distribution of ^{14}C to nodules was decreased by nitrate treatment, whereas that to lateral roots was increased. These results are consistent with nitrate application promoting lateral root growth (Fujikake et al., 2003; Saito et al., 2014). Second, closure of the putative oxygen diffusion barrier, or reduced oxygen permeability by nitrate, inhibits the supply of oxygen to bacteroids, thereby reducing the nitrogenase activity. (Vessey and Waterer, 1992; Minchin, 1997). Alternatively, the nitrate-induced inhibition of nitrogenase activity may result from the formation of a complex involving nitric oxide, an assimilation product of nitrate, and leghemoglobin (Kato et al., 2010). Further studies focusing on the underlying molecular mechanisms are needed to validate the hypotheses.

It has also been suggested that nitrate-induced control of root nodule symbiosis is associated with phytohormones. Ethylene is one of the well-known a negative factor of root nodule symbiosis. Loss-of-function mutants of *M. truncatula SICKLE*, which encodes a protein

involved in ethylene signaling, resulted in an excessive nodulation phenotype (Penmetsa and Cook, 1997). Exposure to exogenous ethylene negatively affects both Nod factor-elicited calcium spiking and root hair infection (Oldroyd et al., 2001). In alfalfa, nitrate application was found to enhance the production of ethylene in the root. In addition, the inhibitory effect of nitrate on nodule formation can be partially suppressed by aminoethoxyvinylglycine, an inhibitor of ethylene biosynthesis (Caba et al., 1998; Ligero et al., 1991). During nodule organogenesis, an auxin response is activated during cortical cell division and the establishment of localized auxin response in cortical cells may be important for nodule primordium formation (Suzaki et al., 2012). In soybean, rhizobial infection was shown to increase the auxin concentration in the root system; however, this was inhibited under high nitrate levels (Caba et al., 2000). Thus, nitrate is likely to interact with auxin signaling in the roots, although it remains unknown whether this is a direct or indirect interaction.

Recently, comprehensive approaches have been used to identify factors that may be involved in the nitrate-induced control of root nodule symbiosis, which includes RNA sequencing (RNA-seq) transcriptome profiling and proteome analysis of *M. truncatula* (Cabeza et al., 2014; van Noorden et al., 2016). Notably, proteins involved in flavanoid biosynthesis were identified in response to nitrate during early nodule development. Flavonoids secreted from host roots stimulate rhizobia to produce Nod factors. However, application of flavonoids to rhizobia did not rescue the nitrate-induced inhibition of nodulation. Thus, lack of *Nod* gene induction in rhizobia due to the reduced expression of flavonoid-related enzymes may not fully explain nodule inhibition by nitrate (van Noorden et al., 2016). A RNA-seq approach investigating the inhibition of nitrogen fixation activity by nitrate found that nitrate could down-regulate the expression of genes encoding nodule-specific cysteine-rich peptides (NCRs) and leghemoglobins. (Cabeza et al., 2014). NCRs are involved in bacterial differentiation into bacteroids, and symbiosome development (Wang et al., 2010; Van de Velde et al., 2010). The transformation into bacteroids is necessary to activate nitrogenase activity (Becker et al., 2004; Horváth et al., 2015). Nitrate may target bacterioid metabolism through NCRs. However, the presence of NCRs is restricted to legumes that form indeterminate nodules. Legumes such as *L. japonicus* and soybean lack NCRs. Thus, the finding from *M. truncatula* may not be a general mechanism explaining the nitrate-induced control of nitrogen fixation.

Nitrate responses in plants

Most nitrogen in soil is present as nitrate. Nitrogen is converted to ammonium by soil bacteria and fungi through mineralization. Ammonium is then oxidized via nitrite to nitrate through a process known as nitrification. Nitrate is taken up by roots mainly by the NITRATE TRANSPORTER 1 (NRT1) and NRT2 family of nitrate transporters. Next, nitrate is first reduced to nitrite by NITRATE REDUCTASE (NIA) in the cytosol, and further reduced to ammonium occurs by NITRITE REDUCTASE (NIR) in plastids. Then, ammonium is assimilated into glutamine by the GLUTAMINE SYNTHETASE/GLUTAMINE OXOGLUTARATE AMINOTRANSFERASE cycle (Miller and Cramer, 2005; Guan, 2017). Nitrate is an essential nutrient for most plants; however, the supply from soils is not stable. Nitrate concentrations in soil solution vary from a few micromolar to several millimolar for several reasons, including leaching, plant absorption, and nitrification burst (Crawford and Glass, 1998; Miller et al., 2007). In order to cope with fluctuating nitrate environments, plants reprogram genome-wide gene expression in response to nitrate availability in the soil, and regulate diverse plant developmental processes such as seed germination (Alboresi et al., 2005; Yan et al., 2016), shoot growth (Walch-Liu et al., 2000; Rahayu et al., 2005), root growth (Sun et al., 2017), flowering (Castro Marín et al., 2011; Yuan et al., 2016), and stomatal opening (Guo et al., 2003). Transcriptome analysis using the Arabidopsis NIA-null (*Atnia1 Atnia2*) mutant showed that, although this mutant lacked NIA activity and could not reduce nitrate, numerous genes including the key nitrate assimilatory genes, responded to nitrate. Thus, nitrate itself acts as a signal, and nitrate signaling is activated independently of nitrate metabolism (Wang et al., 2004).

The control of nitrate transporters governs nitrate uptake. Plants have two uptake systems depending on the nitrate concentration, namely, a high-affinity transport system (HATS) in the low concentration range (<0.5 mM), and a low-affinity transport system (LATS) in the high concentration range (>0.5 mM). HATS can transport ions from the soil at concentrations as low as 1 μM. Most characterized nitrate transporters are either high- or low-affinity transporters, and HATS and LATS are thought to involve different transporters. However, Arabidopsis *NRT1.1* and *M. truncatula NRT1.3* provide two exceptions, which appear to act as dual affinity transporters (Wang et al., 1998; Liu et al., 1999; Morère-Le Paven et al., 2011). AtNRT1.1 (also known as CHLORATE RESISTANT 1 [CHL1] or NRT1/PTR FAMILY 6.3 [NPF6.3]) was the first nitrate transporter to be identified and characterized in plants (Tsay et al., 1993). This transporter can switch between high- or low-affinity transport activity depending on phosphorylated or non-phosphorylated status of the protein (Liu and Tsay, 2003; Ho et al., 2009).

Moreover, AtNRT1.1 functions as a nitrate sensor to trigger nitrate responses independently of its nitrate uptake function (Remans et al., 2006; Ho et al., 2009; Wang et al., 2009).

Changes in root architecture, obtained by adjusting lateral root development, affect the efficiency of nitrate acquisition from the soil. Under low nitrate conditions, plants develop more exploratory root systems by stimulating the initiation and elongation of lateral roots. (Krouk et al., 2010; Gruber et al., 2013). However, the total length and formation of lateral roots are inhibited under severe nitrogen deficiency (Gruber et al., 2013). Therefore, different mechanisms may control lateral root development depending on the degree of nitrogen deficiency. In contrast, a uniform supply of high nitrate inhibit both the formation and elongation of lateral root through effects on phytohormone, such as auxin, abscisic acid, and ethylene (Tian et al., 2008; Signora et al., 2001; Tian et al., 2009). In this condition, plants may conserve energy for other uses by inhibiting lateral root development (Sun et al., 2017). In environments where nitrate is unevenly distributed, Arabidopsis stimulates lateral root elongation in nitrate-rich zones to compensate for nitrogen deficiency in nitrate deficient zones (Zhang et al., 1999). A similar increase in lateral roots in response to local nitrate supply has been reported in maize, rice, and barley (Yu et al., 2014; Huang et al., 2015; Drew and Saker, 1975). Based on these plant responses to nitrogen availability, it is thought that nitrate responses are controlled by local signaling pathways, which are sensitive to local changes in the external nitrate concentration and long-range signaling pathways that transmit the nitrogen status to spatially separated roots (Sun et al., 2017).

In this dissertation, I studied two strategies developed in plants to balance the benefits and costs associated with root nodule symbiosis; plants can negatively regulate nodule number through AON and/or stop the symbiosis in response to nitrate. In Chapter 2, to elucidate the genetic mechanism relevant to the control of root nodule symbiosis by nitrate, I screened mutants using *L. japonicus*, resulting in the identification of the *nitrate unresponsive symbiosis 1* (*nrsym1*) mutant. Detailed phenotypic analysis of this mutant and functional analysis of NRSYM1 indicated that this factor acts as a key regulator in the nitrate-induced pleiotropic control of root nodule symbiosis. In Chapter 3, five new *CLE* genes were identified from the *L. japonicus* genome through an *in silico* search. Among these newly identified *CLE* peptides genes, *CLE-RS3* was shown to be a novel component of AON, which may act as a potential root-derived signal.

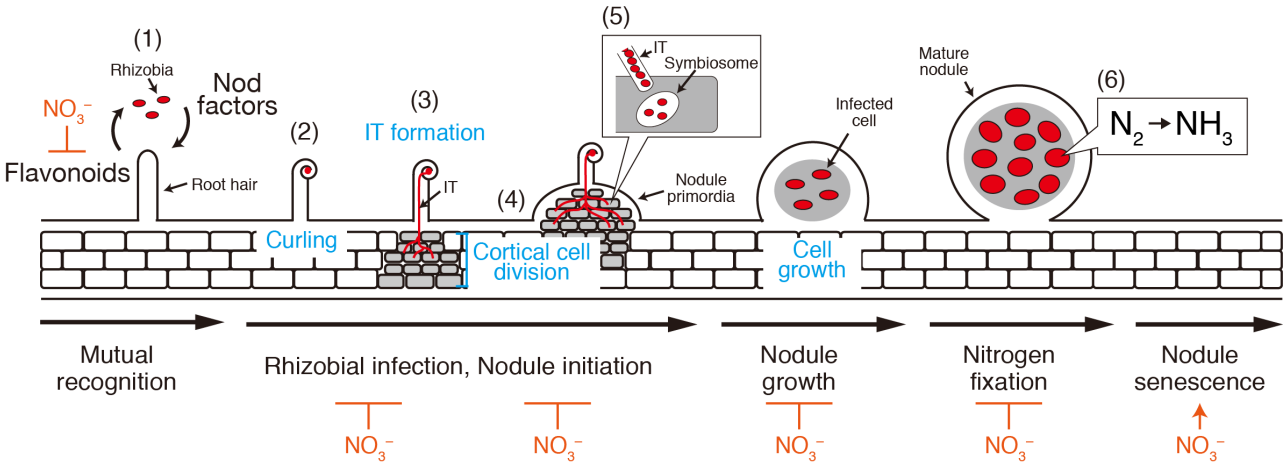

Figure 1-1. Schematic diagram of root nodule symbiosis and the sites of nitrate action during nodulation.

Sequential processes of determinate-type nodulation are shown. (1) Rhizobia synthesize and secret Nod factors in response to flavonoids derived from host roots. The perception of Nod factors triggers nodulation processes. After mutual recognition between host plants and rhizobia, (2) rhizobia are trapped at the tip of the root hair by its curling. (3) Plants then form infection threads (ITs) that guide rhizobia into inner tissue layers of the host. (4) Simultaneously, de-differentiation of the cortical root cells is induced, and these cells proliferate to form nodule primordia. (5) During the course of nodule development, rhizobia are endocytotically released into the nodule cells and (6) acquire the ability to fix atmospheric nitrogen. High nitrate inhibits pleiotropic phases of root nodule symbiosis, including the production of flavonoids, rhizobial infection, nodule initiation, nodule growth, and nitrogen fixation activity, and accelerates nodule senescence.

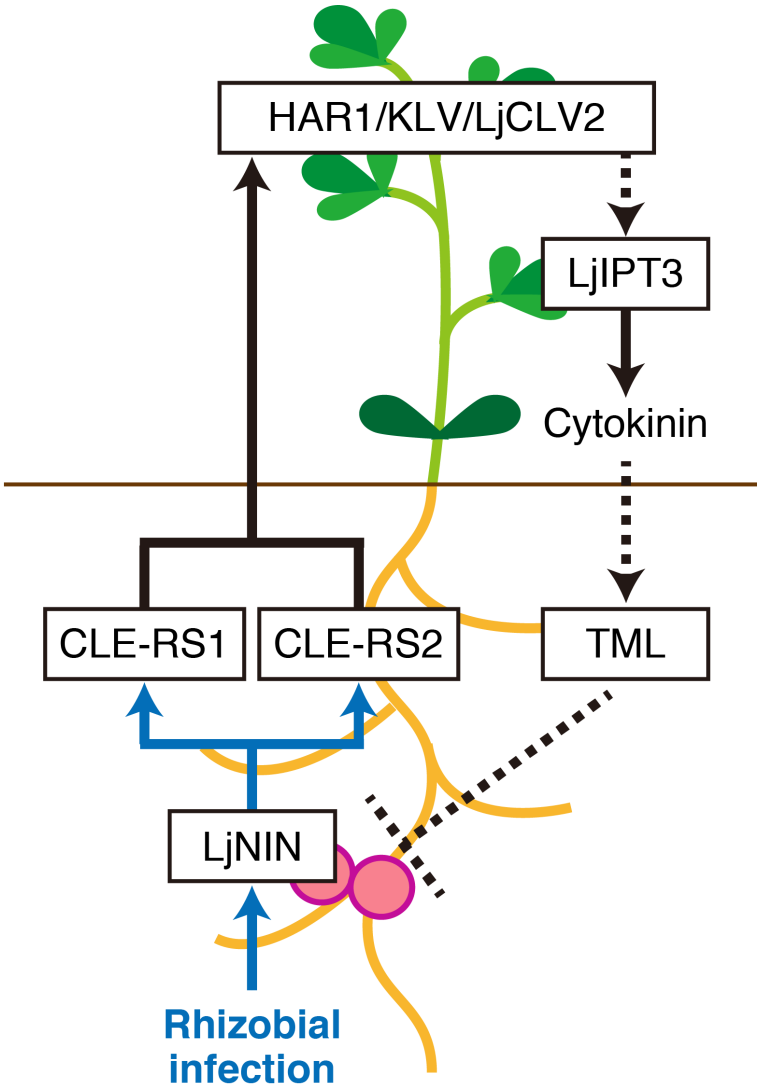

Figure 1-2. A current model of autoregulation of nodulation in *L. japonicus*

The expression of *LjNIN* is induced upon rhizobial infection. LjNIN transcription factor stimulates cortical cell division, and directly induces *CLE-RS1/2* genes. Modified CLE peptides are transmitted from the roots to the shoots through the xylem, and are recognized by the HAR1/KLV/LjCLV2 putative receptor complex. Expression of *LjIPT3*, which encodes a cytokinin biosynthesis enzyme, is induced in a HAR-dependent manner. Shoot-derived cytokinin is transported to the root through the phloem, and directly or indirectly inhibits nodulation in a TML-dependent manner, which may be involved in the down-regulation of *LjNIN*.

Chapter 2

A *NIN-LIKE PROTEIN* mediates nitrate-induced control of root nodule symbiosis in *Lotus japonicus*

2.1 Introduction

In a nitrogen-deficient environment, legumes can form specialized symbiotic organs, root nodules, through association with rhizobia. Root nodules enable plants to obtain a nitrogen source fixed from atmospheric nitrogen. To establish the root nodule symbiosis, a sequential progression of several key processes needs to occur in the root. Upon the perception of a signal from rhizobia, plants form intracellular tube-like structures called infection threads that are used to accommodate rhizobia within the host cells. Simultaneously, dedifferentiation of the cortical root cells is induced, and these cells proliferate to form nodule primordia. During the course of nodule development, rhizobia are endocytosed into the nodule cells and are able to fix nitrogen (Kouchi et al., 2010; Oldroyd, 2013). Owing to the symbiosis, legumes can grow in soil without a nitrogen source; however, the symbiosis is known to be an energy-consuming activity in which photosynthates are used as an energy source to drive processes such as cortical cell proliferation and nitrogen fixation (Kouchi et al., 2010; Tjepkema and Winship, 1980). Therefore, to optimize their growth, plants need to maintain a balance of benefits and costs; that is, the nitrogen demands of plants must be fulfilled without unnecessary loss of carbon. To this end, plants have developed two major ways to negatively regulate the symbiosis.

First, legumes control the number of nodules per root system through a mechanism called AON, a systemic long-range signaling between roots and shoots (Caetano-Anolles and Gresshoff, 1991; Oka-Kira and Kawaguchi, 2006; Suzaki et al., 2015). In the model legume *L. japonicus*, expression of two *LjCLE* genes, *CLE-RS1*, and *CLE-RS2*, is induced by rhizobial infection of the roots (Okamoto et al., 2009). The resulting CLE-RS1/2 peptides, presumably root-derived mobile signals, negatively affect nodulation and may interact with a shoot-acting LRR-RLK named HAR1 that is proposed to form a receptor complex with other LRR-RLK, KLV (Miyazawa et al., 2010) and LRR-RL protein, LjCLV2 (Krusell et al., 2011). As a result, the production of secondary shoot-derived signals is induced, and these signals are transported down to the root to block further nodule development (Krusell et al., 2002; Nishimura et al., 2002; Okamoto et al., 2013). Loss-of function mutations in any gene involved in the AON commonly result in deficient plant growth due to the formation of an excess number of nodules (Wopereis et al., 2000; Oka-Kira et al., 2005; Magori et al., 2009), demonstrating the importance of

maintaining a symbiotic balance through AON. Systemic negative feedback control appears to have a conserved molecular mechanism among leguminous species, as functional counterparts of HAR1 and CLE-RS1/2 have been identified in other legumes such as *M. truncatula* and *G. max* (Schnabel et al., 2005; Searle et al., 2003; Mortier et al., 2010; Reid et al., 2013).

Second, plants have the ability to control root nodule symbiosis in response to nitrogen availability in the soil. Plants may cease the symbiosis if there is a sufficient nitrogen source available in their environment, thereby enabling plants to save the cost associated with nodulation. In this context, plants can regulate each of the multiple phases of root nodule symbiosis, including rhizobial infection, nodule initiation, nodule growth, and nitrogen fixation activity, in response to nitrate, a major form of inorganic nitrogen in soil (Streeter and Wong, 1988; Carroll and Mathews, 1990). High nitrate is also known to accelerate nodule senescence or disintegration (Matamoros et al., 1999). In addition to their hypernodulating-phenotypes, mutations in key LRR-RLKs involved in the AON in several legumes, such as *L. japonicus* HAR1 and KLV, *M. truncatula* SUNN and *G. max* NARK, retain nodule formation even in the presence of a high nitrate concentration (Wopereis et al., 2000; Oka-Kira et al., 2005; Schnabel et al., 2005; Carroll et al., 1985). Furthermore, expression of the *CLE-RS2* gene is induced not only by rhizobial infection but also by nitrate application. These observations suggest that the mechanism for nitrate-induced control of nodulation shares common elements with the AON (Okamoto et al., 2009). In contrast, some findings suggest that fundamental knowledge of AON is insufficient to account for a pleiotropic regulatory mechanism (Jeudy et al., 2010; Okamoto and Kawaguchi, 2015), indicating that new factors await discovery.

In this study, I identify a novel *L. japonicus* mutant, *nitrate unresponsive symbiosis 1* (*nrsym1*). The *nrsym1* mutants are unable to cease root nodule symbiosis under nitrate-sufficient conditions. It was shown that *NRSYM1* encodes a NIN-LIKE PROTEIN (NLP) transcription factor and mediates nitrate-induced pleiotropic control of root nodule symbiosis. In addition, the specific role of AON components in this process was determined. That is, NRSYM1 directly regulates *CLE-RS2* expression in response to nitrate, thereby triggering the negative regulation of nodule number.

2.2 Results

NRSYM1 mediates the nitrate-induced control of root nodule symbiosis

To elucidate the genetic mechanism relevant to the nitrate-induced control of root nodule symbiosis, I screened for mutants involved in the nitrate response during nodulation using EMS-

treated *L. japonicus* WT MG-20 plants. Two allelic recessive mutants named *nitrate unresponsive symbiosis 1-1* (*nrsym1-1*) and *nrsym1-2* were identified. F1 plants derived from a cross between *nrsym1-1* and the WT MG-20 parental line normally responded to nitrate. In the F2 population, nitrate-sensitive and nitrate-tolerant plants segregated in an ~3:1 ratio (17 nitrate-sensitive and 7 nitrate-tolerant plants). These results indicate that the *nrsym1* mutation is inherited as a recessive trait. The *nrsym1-1* mutants exhibited normal nodulation under nitrate-free conditions. Although 10 mM nitrate significantly attenuated nodulation in WT, the *nrsym1-1* plants formed mature nodules in the presence of a high nitrate concentration (Fig. 2-1a). To establish root nodule symbiosis, a sequence of key processes, including nodule initiation, rhizobial infection, nodule growth, and nitrogen fixation activity, are essential and are under nitrate control (Streeter and Wong, 1988; Carroll and Mathews, 1990). The nodule number of WT gradually decreased with increasing concentrations of nitrate, and the formation of small and immature nodules suggested that premature arrest of nodule development had occurred. In contrast, in the *nrsym1-1* mutant, nodule number was primarily normal and mature nodules formed even in the presence of 10 mM nitrate. Under 50 mM nitrate conditions, nodulation was attenuated even in the *nrsym1-1* mutants (Fig. 2-1b). In WT, the number of infection threads, an indicator of rhizobial infection foci, was significantly reduced by nitrate, but the nitrate-induced reduction of infection thread number was not observed in the *nrsym1-1* mutants (Fig. 2-1c). Next, to focus on the effect of nitrate on nodule growth, plants were first grown with rhizobia on nitrate-free agar plates. After 7 days, by which time nodule primordia had formed, the plants were transferred to new agar plates containing 0 mM or 10 mM nitrate, and nodule sizes were measured every 5 days. Whereas WT nodule size under the nitrate-free condition increased with time, 10 mM nitrate arrested nodule growth. In contrast, in the *nrsym1-1* mutant, nodule growth was not affected by high nitrate (Fig. 2-1d). Finally, the effect of nitrate on the nitrogen fixation activity of nodules was investigated (Fig. 2-1e). Plants were grown with rhizobia in the absence of nitrate for 21 days, by which time mature nodules had formed. Then, 0 mM or 10 mM nitrate was supplied to the plants. After 3 days, the acetylene reduction activity (ARA) of nodules was measured for each plant. In WT, nitrate significantly reduced the ARA of nodules. In contrast, the inhibitory effect was not observed in the *nrsym1-1* mutants. The *nrsym1-2* mutants had a nitrate-tolerant phenotype similar to *nrsym1-1* (Fig. 2-1a,b, 2-2a-c). These data indicate that the *nrsym1* mutation eliminates the pleiotropic nitrate-induced inhibition of root nodule symbiosis.

I next examined the effects of the *nrsym1* mutation on plant growth. Whereas nitrate promoted shoot growth of both WT and *nrsym1-1*, in the absence of rhizobia *nrsym1-1* had a

smaller fresh shoot weight than WT (Fig. 2-1f). The shoot–root fresh weight ratio, a representative marker for nutrient starvation status (Lawlor et al., 2001), was lower in *nrsym1-1* compared with WT under nitrate-sufficient conditions (Fig. 2-1g). Thus, in addition to its symbiotic roles, NRSYM1 seems to function in non-symbiotic nitrate-related processes. In the presence of nitrate, the shoot weight of inoculated WT was indistinguishable from that of uninoculated WT plants. Of note, simultaneous application of rhizobia and nitrate to *nrsym1-1* caused about a 22% reduction in shoot growth compared with uninoculated and nitrate-treated *nrsym1-1* plants (Fig. 2-1f). The *nrsym1-2* mutants had a shoot phenotype similar to that of *nrsym1-1* (Fig. 2-2d,e). These results indicate that nodulation in a nitrate-sufficient condition can be harmful to plant growth.

In addition to nitrate, plants are known to control root nodule symbiosis in response to ammonium (Barbulova et al., 2007). I then analyzed nodulation of *nrsym1* under ammonium-sufficient conditions (Fig. 2-2f). In the presence of 10 mM ammonium, nodulation of *nrsym1* and WT was attenuated. This result suggests that NRSYM1 is not involved in the ammonium-induced control of nodulation.

High nitrate conditions reduce nodule cell size

To characterize the effect of nitrate on nodule growth in more detail, I observed nodule sections of WT and the *nrsym1-1* mutants grown in the presence of 0 or 10 mM nitrate. WT nodules formed in the presence of 10 mM nitrate were obviously small (Fig. 2-1a). Examination of WT nodule sections from plants grown in nitrate revealed that rhizobia-colonized infected cells were recognizable, but their size was much smaller compared with the WT nitrate-free nodules (Fig. 2-3a). Then, the number and size of cells located in the inner region of nodule parenchyma were measured. In WT nodules grown in the presence of nitrate, the number of cells was comparable to that of nitrate-free nodules (Fig. 2-3b). On the other hand, nitrate reduced the cell sizes of both infected and uninfected cells (Fig. 2-3c), suggesting that the reduction in nitrate-induced nodule size was due to a smaller cell size rather than cell number. Sections from *nrsym1-1* nodules developed in the presence of nitrate were largely indistinguishable from the *nrsym1-1* nodules developed in the absence of nitrate (Fig. 2-3a). Although nitrate reduced the cell sizes of both infected and uninfected *nrsym1-1* cells, the number of infected cells increased (Fig. 2-3b,c).

***NRSYM1* encodes an NLP transcription factor**

I first sought to isolate *NRSYM1* by a map-based cloning approach. The *NRSYM1* locus was

mapped to a region between two simple sequence repeat markers, TM1417 and TM0366, on chromosome 5 (Fig. 2-4). Subsequently, a genome-resequencing approach using the *nrsym1-1* and *nrsym1-2* mutants (Table 2-1) identified point mutations in the gene, chr5.CM0148.170.r2.a, which was previously identified as *LjNLP4* (Suzuki et al., 2013). There are two nucleotide substitutions in the gene: a C-to-T substitution causing the formation of a stop codon Q327STOP (*nrsym1-1*) and a G-to-A substitution causing the replacement of valine by isoleucine V283I (*nrsym1-2*) (Fig. 2-5a,b). A 7.5-kb genomic fragment encompassing the entire *NRSYM1* locus was introduced into the *nrsym1-1* mutants by *Agrobacterium rhizogenes*-mediated hairy root transformation. The mutant roots carrying the complementation construct normally responded to nitrate (Fig. 2-5c), indicating that the *nrsym1* phenotype results from mutation of the gene. *NRSYM1* encodes a protein with sequence similarity to Arabidopsis NLP transcription factors (Schauser et al., 2005). In Arabidopsis, NLPs have a role as master regulators of nitrate-inducible gene expression (Konishi and Yanagisawa, 2013). Phylogenetic analysis showed that NRSYM1 belongs to a clade containing AtNLP6 and AtNLP7 (Fig. 2-6). Constitutive expression of *AtNLP6* or *AtNLP7* by the *LjUBQ* promoter partially rescued the nodule number phenotype of *nrsym1-1*. On the other hand, mature nodules still formed on the roots (Fig. 2-7). These results suggest that the functions of NRSYM1 and AtNLP6/7 are partially conserved. NRSYM1 consists of an N-terminal conserved domain, an RWP-RK DNA-binding domain, and a conserved PB1 domain (Fig. 2-5b). Placement of a premature stop codon in the N-terminal conserved domain of *nrsym1-1* implies that *nrsym1-1* is a null mutant. The amino acid residue (V283) that is mutated in *nrsym1-2* is highly conserved among NLPs (Fig. 2-8) and the severity of the *nrsym1-2* mutation is similar to that of *nrsym1-1* (Fig. 2-1a,b, 2-2a-e), suggesting that V283 is a critical amino acid residue for NRSYM1 function.

I then analyzed the expression pattern of *NRSYM1* in some vegetative and reproductive organs by real-time RT-PCR. *NRSYM1* expression was widely observed in the organs examined (Fig. 2-9a). The level of *NRSYM1* expression was unchanged by nitrate treatment and seemed to be unaffected by rhizobial inoculation, at least at the whole root level (Fig. 2-9a,b). Reporter gene analysis using a *pNRSYM1::β-glucuronidase* (*GUS*) construct showed that *NRSYM1* was expressed in the root vascular tissue (Fig. 2-9c), nodule primordia (Fig. 2-9d) and mature nodules (Fig. 2-9e).

HAR1 regulates the nitrate-induced control of nodule number but not other processes

Several observations suggest that AON is implicated in nitrate-induced control of root nodule symbiosis (Oka-Kira et al., 2005; Barbulova et al., 2007). To assess the potential genetic interaction between NRSYM1 and HAR1, a key regulator of AON, I analyzed the *nrsym1 har1* double mutant phenotype (Fig. 2-10a-d). Under nitrate-free and -sufficient conditions, *nrsym1-1 har1-7* mutants formed an excess number of nodules that were similar to those of the *har1-7* mutants (Fig. 2-10b). In the presence of 10 mM nitrate, however, the *har1-7* mutants continued to produce an elevated number of small, white immature nodules (Fig. 2-10b) similar to those formed in WT in the presence of high nitrate. In *har1-7*, infection thread number and nodule size were significantly reduced by nitrate (Fig. 2-10a,c). In contrast, the nitrate-induced reduction in infection thread number and nodule size was masked by the presence of the *nrsym1* mutation (Fig. 2-10a,c). In the *har1-7* mutants, nitrate reduced the nitrogen fixation activity, but the *nrsym1-1 har1-7* mutants were tolerant of the reduction (Fig. 2-10d). Hence, these results indicate that HAR1 may be involved in the regulation of nitrate-induced inhibition of nodule number, but rhizobial infection, nodule growth, and nitrogen fixation activity are controlled through a mechanism independent of HAR1.

Reciprocal grafting experiments were then performed using WT, *nrsym1-1* and *har1-7* (Fig. 2-10e). Whereas WT(scion)/*nrsym1-1*(rootstock)-grafted plants showed a nitrate-tolerant phenotype in the presence of 10 mM nitrate, nodulation of *nrsym1-1*/WT-grafted plants was nearly eliminated. Thus, root-acting NRSYM1 seems to have a role in the nitrate-induced control of nodulation. HAR1 was previously shown to act in the shoot (Nishimura et al., 2002). Whereas *nrsym1-1*/*har1-7*-grafted plants exhibited reduced nodulation in the presence of nitrate, *har1-7*/*nrsym1-1*-grafted plants had a nodule number similar to *har1-7*/*har1-7*-grafted plants. In the *har1-7*/*nrsym1-1*-grafted plants, mature nodules formed in the presence of high nitrate but were rarely observed in the *har1-7*/*har1-7*-grafted plants.

NRSYM1 controls nitrate-inducible gene expression

The expression of *CLE-RS2* is induced not only by rhizobia inoculation but also by nitrate application (Okamoto et al., 2009). To gain insight into the role of NRSYM1 in the nitrate response, I investigated the expression of a nitrate-inducible symbiotic gene (*CLE-RS2*) and two non-symbiotic genes (*LjNIA* and *LjNIR1*) by real-time RT-PCR. *LjNIA* and *LjNIR1*, respectively, encode nitrate and nitrite reductase involved in nitrate assimilation (Prosser et al., 2006, Orea et al., 2001). The expression of *CLE-RS2*, *LjNIA* and *LjNIR1* was strongly induced in WT by a 24-

h nitrate treatment, but the induction levels were much lower in *nrsym1-1* roots (Fig. 2-11a-c). The *nrsym1-2* mutants had a defect similar to that in *nrsym1-1* (Fig. 2-12a-c). I next examined nitrate-inducible gene expression at shorter time points (Fig. 2-12d-f). Whereas the *LjNIA* and *LjNIR1* genes in WT were upregulated 30 min after nitrate treatment, the induction of *CLE-RS2* was detectable 6 h after nitrate treatment. The induction levels of these genes in *nrsym1-1* roots were lower than those of WT at all time points. In addition, I examined the effects of lower concentrations of nitrate that do not inhibit nodulation on gene expression. Application of 200 μM nitrate induced *CLE-RS2*, *LjNIA* and *LjNIR1* expression in a NRSYM1-dependent manner (Fig. 2-12g-i). Whereas *LjNIA* and *LjNIR1* induction by nitrate was dependent on having NRSYM1 in roots (Fig. 2-11b,c), NRSYM1 was not required for inducing expression of the two genes in leaves (Fig. 2-12j,k). Next, the effect of *NRSYM1* constitutive expression on the expression of these genes was investigated. Under nitrate-free conditions, all the tested genes had similar expression levels in hairy roots transformed with control *pLjUBQ::GUS* or *pLjUBQ::NRSYM1* constructs (Fig. 2-11e-h). In contrast, nitrate application significantly activated *CLE-RS2*, *LjNIA* and *LjNIR1* in the roots that constitutively expressed *NRSYM1* (Fig. 2-11e-g), suggesting that NRSYM1 plays a role in the regulation of *CLE-RS2, LjNIA* and *LjNIR1* expression in response to nitrate. Nitrate application, *nrsym1* mutation nor *NRSYM1* expression affected *CLE-RS1* expression (Fig. 2-11d,h).

NIN is a key transcription factor that regulates nodule organogenesis (Schauser et al., 1999; Marsh et al., 2007; Soyano et al., 2013; Vernié et al., 2015). The expression of *LjNIN* tended to be downregulated by nitrate in WT as previously shown (Barbulova et al., 2007), and the effect was not observed in *nrsym1-1* roots (Fig. 2-12l).

NRSYM1 directly regulates *CLE-RS2* and *LjNIR1* expression in a nitrate-dependent manner

An observation of the *NRSYM1*-dependent expression of some nitrate-inducible genes (Fig.2-11a-c,e-g) led me to postulate that NRSYM1, an NLP transcription factor, directly regulates the expression of these genes. I then investigated whether these genes are direct targets of NRSYM1 by chromatin immunoprecipitation (ChIP)-qPCR analysis using transgenic hairy roots carrying the *pLjUBQ::NRSYM1-myc* construct. As the *nrsym1-1* mutant roots carrying the construct normally responded to nitrate, the NRSYM1-myc translational fusion seemed to be functional (Fig. 2-13a). NRSYM1 and LjNIN belong to the NLP family whose members are characterized by the presence of a conserved RWP-RK DNA-binding domain (Suzuki et al., 2013; Schauser et

al., 2005). In Arabidopsis, NLPs bind to the nitrate-responsive *cis*-element (NRE) of a number of nitrate-inducible genes (Konishi and Yanagisawa, 2013). Recently, LjNIN was shown to bind to the so-called NIN-binding nucleotide sequence (NBS) in the *CLE-RS2* and *LjNIR1* promoters, a sequence that is structurally similar to the NRE (Fig. 2-13b; Soyano et al., 2014; Soyano et al., 2015). Thus, I designed primer sets in the *CLE-RS2* and *LjNIR1* promoter region based on the presence of NRE/NBS (region 1, 3, 4 of the *CLE-RS2* promoter and region 3 of the *LjNIR1* promoter) and used them for qPCR analysis after ChIP (Fig. 2-13c). Chromatin suspensions were prepared from *pLjUBQ::NRSYM1-myc* roots that were incubated with 10 mM nitrate or without nitrate for 24 h, and ChIP was performed with polyclonal anti-myc antibodies. The *CLE-RS2* promoter region 1 was significantly enriched in nitrate-treated roots compared with that of roots receiving no nitrate (Fig. 2-13c,d). *LjNIR1* promoter region 3 was also enriched in nitrate-treated roots (Fig. 2-13c,e). These results suggest that NRSYM1 can directly bind to the promoter regions of *CLE-RS2* and *LjNIR1* in a nitrate-dependent manner.

To verify physical interaction between NRSYM1 and NRE/NBS of the *CLE-RS2* and *LjNIR1* promoters, I further carried out an electrophoretic mobility shift assay (EMSA). The mobility of the probes, CLE-RS2-1, CLE-RS2-3, CLE-RS2-4 and LjNIR1-3, specifically shifted when the samples were incubated with NRSYM1(531-976)-myc. In contrast, use of mutated probes, CLE-RS2-1m and LjNIR1-3m1, did not shift the mobility (Fig. 2-13b,f; Table 2-2). The band shift disappeared by the addition of competitor probes, CLE-RS2-1 or LjNIR1-3. On the other hand, the addition of a mutant competitor probe, CLE-RS2-1m, did not affect the band shift (Fig. 2-13g). The EMSA results showed that NRSYM1 specifically binds to NRE/NBS in the *CLE-RS2* promoter regions 1, 3, 4 and in *LjNIR1* promoter region 3. Addition of competitor CLE-RS2-3 probe inhibited the interaction between NRSYM1 and CLE-RS2-1, but the strength of competition was weaker than that of the competitor CLE-RS2-1 probe. Addition of the competitor CLE-RS2-4 probe hardly inhibited NRSYM1-CLE-RS2-1 interaction (Fig. 2-13g). These results suggest that NRSYM1-binding to region 1 has the strongest affinity among the three regions of the *CLE-RS2* promoter that interact with NRSYM1.

Both NRSYM1 and LjNIN can directly bind to the *CLE-RS2* promoter (Soyano et al., 2014). Identical amounts of NRSYM1(531-976)-myc and LjNIN(520–878)-myc proteins were incubated with the probe CLE-RS2-1 (Fig. 2-13h). Regarding LjNIN-CLE-RS2-1 interaction, a shifted band was observed only when I used the greatest amount of LjNIN protein. In contrast, use of smaller amounts of NRSYM1 proteins caused a shift. Hence, NRSYM1 has a higher affinity for the region than LjNIN.

To investigate whether the identified NRE/NBS from the *CLE-RS2* and *LjNIR1* promoters are involved in NRSYM1-mediated transcriptional activation, several promoter-GUS constructs (Fig. 2-14a) were introduced into the roots of WT or *nrsym1-1*, and GUS activities were quantified by real-time RT-PCR (Fig. 2-14b). *GUS* expression levels in *nrsym1-1* mutant roots carrying *CLE-RS2-1* and *LjNIR1* promoter fragments were lower than those of WT. In addition, *GUS* expression in WT was significantly reduced when the NRE/NBSs were mutated. Taken together, these results indicate that NRSYM1 regulates *CLE-RS2* and *LjNIR1* expression through direct binding to their promoters.

CLE-RS2 is required for nitrate-induced control of nodule number

In the AON in *L. japonicus*, the CLE-RS1 and -RS2 peptides act as putative root-derived signals through interaction with their receptor, HAR1, in the shoot and transmit secondary signals that negatively regulate nodulation (Okamoto et al., 2013). To elucidate the precise functions of CLE-RS1 and CLE-RS2, I tried to determine the loss-of-function effects of *CLE-RS1* or *CLE-RS2* genes. The CRISPR/Cas9 genome-editing system made it possible to obtain stable transgenic plants with nucleotide deletions or insertions in both genes (Fig. 2-15a). Each gRNA to target the nucleotide sequence encoding amino acids constituting a CLE domain was designed. Each gRNA that targeted *CLE-RS*1 or *CLE-RS2* had the possibility to additionally target *LjCLE49* and *CLE-RS3* (see chapter 3) among the *LjCLE* genes (Hastwell et al., 2017), although their off-target scores were quite low. The *LjCLE49* and *CLE-RS3* genes were sequenced in the *cle-rs1* #16, *cle-rs2* #2, *cle-rs2* #5 lines that were used in this study and confirmed that the two *LjCLE* genes were unaffected in these plants. Each T0 generation of the CRISPR lines already had homozygous indel mutations (Fig. 2-15a), and no other mutations in *CLE-RS1* or *CLE-RS2* were detected. Thus, there were no chimeric mutations in the three lines. Under nitrate-free conditions, *cle-rs1* and *cle-rs2* plants had a normal nodulation phenotype (Fig. 2-16a,b), and nodule number was significantly increased in the *cle-rs1 cle-rs2* double mutant (Fig. 2-16a), indicating that CLE-RS1 and CLE-RS2 redundantly regulate nodule number. The nodule number for the *cle-rs1 cle-rs2* double mutants was reduced by introducing a 7.4-kb genomic fragment encompassing the entire *CLE-RS1* locus (Fig. 2-15b). In the presence of 10 mM nitrate, nodulation was inhibited in *cle-rs1* plants to the same level as that in the WT (Fig. 2-16a,b). In contrast, nitrate-induced reduction in nodule number was not observed in the *cle-rs2* plants (Fig. 2-16a), but their nodule size was reduced by nitrate (Fig. 2-16b). This result concluded that CLE-RS2 is involved in the nitrate-induced control of nodule number but not nodule size.

NRSYM1 accumulates in the nucleus in response to nitrate

Although it was shown that NRSYM1 can directly regulate nitrate-inducible gene expression (Fig. 2-13,14), *NRSYM1* expression *per se* was not affected by nitrate (Fig. 2-9a). The subcellular localization of AtNLP6 and AtNLP7 proteins that belong to the same clade as NRSYM1 is regulated by nitrate; nuclear localization of the proteins is retained in the presence of nitrate (Marchive et al., 2013; Guan et al., 2017). Thus, the subcellular localization of NRSYM1 was examined by immunohistochemistry. The subcellular localization of NRSYM1 was indirectly determined using transgenic roots carrying the *pLjUBQ::NRSYM1-myc* construct combined with detection with polyclonal anti-myc primary antibodies and secondary antibodies containing Alexa Fluor 488. Although NRSYM1 was barely detected in nuclei in nitrate-free conditions (Fig. 2-17a, f), the protein was predominantly localized in nuclei within 20 min of nitrate treatment (Fig. 2-17b, f). Nuclear localization was also observed after 24 h of nitrate treatment (Fig. 2-17c, f). Moreover, nuclear accumulation of NRSYM1 was reversible when nitrate was removed (Fig. 2-17d, f). The addition of leptomycin B (LMB), an inhibitor of nuclear export (Haasen et al., 1999), inhibited the export of NRSYM1 from nuclei when nitrate-supplied roots were moved to a N-free medium (Fig. 2-17e, f). Overall, it is likely that nuclear localization of NRSYM1 is regulated by nitrate as is the case for AtNLP6/7.

2.3 Discussion

To balance the benefits and costs associated with root nodule symbiosis, plants control the number of nodules per root system using the AON system. In addition, plants can stop the symbiosis and save the cost if sufficient nitrogen is available in their surrounding environment. In this study, NRSYM1 was identified that acts as a key regulator in the latter mechanism. Under nitrate-sufficient conditions, unstoppable nodulation in *nrsym1* mutants diminished shoot growth, demonstrating the significance of the NRSYM1-mediated control of root nodule symbiosis for plant growth. More than 30 years ago, a similar approach to this screening study isolated several soybean mutants that all had not only nitrate-tolerant phenotypes but also formed an excess number of nodules (Carroll et al., 1985). Indeed, it turned out that the gene responsible for some of the mutants encodes an LRR-RLK that acts as a pivotal factor in the AON (Searle et al., 2003). Since then the AON has been proposed to have another role in mediating the nitrate-induced control of root nodule symbiosis. Unlike the canonical AON mutants, the *nrsym1* mutants form a normal number of nodules and show tolerance to all examined nitrate-affected processes. Genetic analysis of *NRSYM1*, *HAR1* and *CLE-RS2* indicated that the three genes act in the same genetic

pathway. In addition, it is shown that NRSYM1 directly regulates *CLE-RS2* expression in response to nitrate, providing a direct molecular link between nitrate and nodulation. After the activation of *CLE-RS2*, the downstream signaling pathway may be identical to that for AON, where the produced CLE-RS2 peptide functions as a root-derived signal through the interaction with the shoot-acting HAR1. In nitrate-sufficient conditions, the *cle-rs2* or *har1* mutants showed tolerance to nitrate-induced control of nodule number but not to other nitrate-affected processes. Hence, I hypothesize that the nitrate-induced NRSYM1>CLE-RS2>HAR1 signaling pathway plays a role predominantly in the control of nodule number (Fig 2-18a). In contrast, NRSYM1 is likely to use different downstream targets to achieve AON-independent regulation of other processes such as rhizobial infection, nodule growth, and nitrogen fixation activity (Fig 2-18a). This notion is consistent with a previous suggestion that there are both an AON-dependent and an -independent mechanism in nitrate-induced control of root nodule symbiosis (Okamoto et al., 2009, Jeudy et al., 2010; Okamoto and Kawaguchi, 2015). In most experiments of this study, I used 10 mM KNO_3, a nitrate concentration sufficient to inhibit symbiosis. The application of much lower KNO_3 concentrations (for example, 200 μM) induced *CLE-RS2* expression in an NRSYM1-dependent manner. The activation of *CLE-RS2* by low concentrations of nitrate seems to be insufficient for inhibiting nodulation. Thus, there may be an unidentified mechanism in response to high nitrate concentration that plays a role in inhibiting nodulation in parallel or downstream of *CLE-RS2* activation.

The amino acid sequence of the CLE domain is indistinguishable between CLE-RS1 and CLE-RS2, and the two peptides have similar negative activity in the control of nodulation (Okamoto et al., 2009). In this study, the creation of loss-of-function mutants enabled us to understand the conserved and diverse functions of these genes. The *cle-rs1 cle-rs2* double mutants have more nodules, whereas the single mutations do not affect nodule number, demonstrating that CLE-RS1 and CLE-RS2 have redundant functions in controlling nodule number. However, the *cle-rs1 cle-rs2* double mutant phenotype is milder than that shown by their receptor mutant, *har1*. In Arabidopsis, although many AtCLE peptides are involved in diverse developmental processes and their putative receptors are identified (Endo et al., 2014), there is only one case where the loss-of-function phenotype of a ligand is almost identical to that of its receptor (Clark et al., 1997; Fletcher et al., 1999), implying that loss-of-function effects in a *CLE* gene are usually masked because of functional redundancy. Therefore, there may be a higher order functional redundancy in CLE peptides regarding their control of nodule number. Under nitrate-sufficient conditions, as mentioned above, the *cle-rs2* mutants can produce a normal number of nodules, whereas the *cle-*

rs1 mutants were affected by nitrate. These results indicate that CLE-RS2 has a dual role in regulating the AON and nitrate-induced control of nodule number; CLE-RS1's function is specific to the former process. The different roles of the two genes agree with the observation that the expression of *CLE-RS2* is induced by nitrate but not *CLE-RS1*.

The designation of the NLP family originates from the symbiosis-specific transcription factor NIN (Schauser et al., 2005). NLP consists of an N-terminal conserved domain responsible for nitrate response, an RWP-RK DNA-binding domain, and a conserved PB1 domain involved in protein-protein interaction (Suzuki et al., 2013). In Arabidopsis, a non-leguminous plant, AtNLPs are considered as master regulators of the nitrate response because AtNLP6/7 regulates many nitrate-responsive genes (Marchive et al., 2013; Konishi and Yanagisawa, 2014). In Arabidopsis nitrate signaling, AtNRT1.1 (CHL1/ NPF6.3) is thought to act as a nitrate sensor, and the functions of some *M. truncatula* proteins belonging to NRT1 family have been characterize (Ho et al., 2009; Pellizzaro et al., 2014; Bagchi et al., 2012). More recently, the molecular link between nitrate sensing and AtNLP7-mediated activation of nitrate-inducible genes has been elucidated, where Ca^{2+}-sensor protein kinases (AtCPKs) act as master regulators that orchestrate the primary nitrate response (Liu et al., 2017). *L. japonicus* has five LjNLPs and LjNIN; one of the LjNLP Lj1g3v2295200 (LjNLP1) is reported to bind to NRE and to respond to nitrate (Suzuki et al., 2013). The partial loss of amino acid residues in the N-terminal conserved domain of LjNIN is thought to be associated with the protein's loss of nitrate-responsiveness (Suzuki et al., 2013). Alternatively, NIN has a new function in playing a role as a necessary and sufficient factor for nodulation (Schauser et al., 1999; Marsh et al., 2007; Soyano et al., 2013; Vernié et al., 2015). Therefore, it seems that the basal function of NLPs in plants can be related to nitrate response. Thus, the emergence of NIN provides an example of neofunctionalization during the evolution of legumes, where after gene duplication one of the NLPs may have been released from functional constraints, enabling it to accumulate mutations and to acquire a new function (Force et al., 1999). The *nrsym1* mutation caused the *Atnlp7*-like nitrate starvation phenotypes in non-symbiotic conditions (Castaings et al., 2009), and NRSYM1 has a role in regulating the expression of general nitrate-responsive genes involved in nitrate assimilation. In addition, constitutive expression of *AtNLP6* or *AtNLP7* partially rescued the *nrsym1* nodulation phenotype. These observations suggest that the original function as a regulator of a general nitrate-response is maintained in NRSYM1. Furthermore, it is revealed that NRSYM1 has a crucial function relevant to root nodule symbiosis by regulating nodulation-specific genes such as *CLE-RS2* (Fig. 2-18b). Therefore, in terms of the evolution of the NLP family in legumes,

NLPs may have evolved toward opposite directions; that is, NRSYM1 and NIN have acquired negative and positive roles, respectively, in the control of root nodule symbiosis. Given that NRSYM1 and LjNIN share *CLE-RS2* as a direct target gene, the NRSYM1>CLE-RS2 transcriptional regulatory module may be a prototype for AON. In ChIP experiments, I did not detect NRSYM1-binding to region 3 or 4 of the *CLE-RS2* promoter, to which LjNIN binds (Soyano et al., 2014). In contrast, the EMSA results suggests that NRSYM1 can bind to regions 3 and 4 in addition to region 1. The difference in these results may be related to differences between *in vivo* and *in vitro* experiments. The EMSA competition assay showed that NRSYM1 had the strongest affinity for region 1 with lesser affinities for region 3 and 4. In addition, the promoter-GUS assay result suggests that interaction between NRSYM1 and region 1 is sufficient to activate *CLE-RS2*.

Like Arabidopsis NLP6/7, the expression of *NRSYM1* is not induced by nitrate, suggesting that post-translational regulation of NRSYM1 provides it with function (Konishi and Yanagisawa, 2013). As nuclear localization of NRSYM1 is regulated by nitrate as well as AtNLP6/7 (Marchive et al., 2013; Guan et al., 2017; Fig. 2-18b), the nitrate-induced nuclear localization may be a feature of the NRSYM1/AtNLP6/7 clade of the NLP family. Recently, CPK-dependent phosphorylation of AtNLP7 was reported to regulate its nuclear retention (Liu et al., 2017). AtNLP8, a master regulator of nitrate-promoted seed germination, was shown to be localized in nuclei independently of nitrate; this finding suggests that an unknown mechanism provides AtNLP8 with transcriptional regulatory activity (Yan et al., 2016). Nitrate-induced control of root nodule symbiosis is known to be a reversible process dependent on nitrate availability (Fujikake et al., 2003). Future investigations of the detailed mechanism for reversible NRSYM1 nuclear localization may provide great insight into the underlying mechanism of the phenomenon.

2.4 Methods

Plant materials and growth conditions

The Miyakojima MG-20 ecotype of *L. japonicus* (Kawaguchi, 2000) was used as WT in this study. The Gifu B-129 ecotype of *L. japonicus* (Handberg and Stougaard, 1992) was used as a crossing partner for map-based cloning of *NRSYM1*. The *nrsym1-1* and *nrsym1-2* mutants were isolated from the M_2 generation of WT that had been mutagenized with 0.4% ethylmethane sulfonate (EMS). M_2 seeds were collected from ~10,000 M_1 plants provided from LegumeBase. A description of the *har1-7* mutants was published previously (Miyazawa et al., 2010). Plants were

grown with or without *Mesorhizobium loti* MAFF 303099 as previously described (Suzaki et al., 2013). For the nitrate response assay, different concentrations of KNO_3 (0-50 mM) were supplemented into Broughton and Dilworth (B&D) solution (Broughton and Dilworth, 1971). The solution was exchanged every 7 days after inoculation with newly prepared B&D solution containing different concentrations of KNO_3 to maintain the original KNO_3 concentrations.

Acetylene reduction assay

The nitrogenase activity of nodules was indirectly determined by measuring the acetylene reductase activity according to a previously described method (Hakoyama et al., 2012).

Genome-resequencing of the *nrsym1* mutants

The leaves of the *nrsym1* mutants were ground in liquid nitrogen using a mortar and pestle. Genomic DNA was isolated using a DNeasy Plant Mini Kit (Qiagen). The quality of purified genomic DNA was evaluated by a Quant-iT dsDNA BR Assay Kit (Invitrogen). For whole-genome shotgun sequencing of the *nrsym1* mutants, a library was constructed using a TruSeq DNA Sample Prep kit (Illumina) following the manufacturer's instructions. The quality of the library was checked using an Agilent 2100 Bioanalyzer and quantified using a KAPA Library Quant Kit (Kapa Biosystems). Paired-end 101 bp × 2 sequencing was performed using an Illumina HiSeq 2000 instrument (Illumina). Short reads were mapped against the *L. japonicus* genome assembly build 2.5 (Sato et al., 2008) by Bowtie2 (Langmead and Salzberg, 2012). The resulting data in the SAM format were converted to a binary equivalent BAM format and sorted using the samtools software package (Li et al., 2009). Variant calling was performed with samtools and bcftools.

Constructs and hairy root and stable transformation of *L. japonicus*

The primers used for PCR are listed in Table 2-3. For the complementation analysis of the *nrsym1* mutants, a 7.5-kb genomic DNA fragment including the *NRSYM1* candidate gene was amplified by PCR from WT genomic DNA. This fragment, including a 2.3-kb sequence directly upstream of the initiation codon, was cloned into pCAMBIA1300-GFP-LjLTI6b (Suzaki et al., 2012). The coding sequences (cds) of *NRSYM1* or *AtNLP6/7* were respectively amplified by PCR from template cDNAs prepared from WT *L. japonicus* or Arabidopsis Col-0 plants and were cloned into the pENTR/D-TOPO vector (Invitrogen). The insert was transferred into pUB-GW-GFP (Maekawa et al., 2008) by the LR recombination reaction. For the *NRSYM1* expression analysis,

GUS gene in pENTR-gus (Invitrogen) was inserted into pCAMBIA1300-GW-GFP-LjLTI6b (Suzaki et al., 2014) by the LR recombination reaction to create the vector, pCAMBIA1300-GUS-GFP-LjLTI6b. a 2.3-kb fragment of the *NRSYM1* promoter region was amplified by PCR from WT genomic DNA and cloned upstream of the *GUS* gene in the pCAMBIA1300-GUS-GFP-LjLTI6b vector. For ChIP and immunohistochemistry analysis, the *NRSYM1* cds without a stop codon was amplified by PCR from template cDNA prepared from WT roots and cloned into the pENTR/D-TOPO vector. The insert was transferred into pGWB20 (Nakagawa et al., 2007) by the LR recombination reaction in order to express a C-terminal fusion to a 10xMyc (myc) tag. Using the resulting construct as a template, the *NRSYM1-myc* fragments were amplified by PCR and cloned into the pENTR/D-TOPO vector. The insert was transferred into pUB-GW-GFP by the LR recombination reaction. To make the construct for *in vitro* translation of NRSYM1, a part of the *NRSYM1* cds (1591-2931) was amplified by PCR from template cDNA prepared from WT. The fragment was replaced with LjNIN that had been previously cloned into the downstream region of a 3xMyc tag in the pENTR1A vector (Invitrogen) (Soyano et al., 2013). The resulting *NRSYM1* (1591-2931)-*myc* fragments were amplified by PCR and cloned into the pF3K-WG (BYDV) Flexi vector (Promega). The LjNIN-myc construct for *in vitro* translation was described previously (Soyano et al., 2013). For promoter-GUS analysis, a 2.7-kb fragment of the *LjNIR1* promoter region (pLjNIR1) was amplified by PCR from WT genomic DNA. To make the *LjNIR1* promoter region lacking NRE (pLjNIR1-3m2), genomic fragments of the regions upstream and downstream of NRE were respectively amplified by PCR from WT genomic DNA. Each fragment was inserted upstream of the *GUS* gene in the pCAMBIA1300-GUS-GFP-LjLTI6b vector. The *pCLE-RS2-1::GUS* and *pCLE-RS2-1m::GUS* constructs are identical to CLE-RS2 region1 and CLE-RS2 region1 S1m as described previously (Soyano et al., 2014). For the complementation analysis of the *cle-rs1 cle-rs2* double mutants, a 7.4-kb genomic DNA fragment including the *CLE-RS1* gene was amplified by PCR from WT genomic DNA. This fragment, including a 5.9-kb sequence directly upstream of the initiation codon, was cloned into pCAMBIA1300-GFP. The recombinant plasmids were introduced into *A. rhizogenes* and were transformed into roots of *L. japonicus* plants by a hairy root transformation method as previously described (Suzaki et al., 2012).

To create CRISPR/Cas9 constructs of *CLE-RS1* or *CLE-RS2*, targeting sites in the genes were designed using the CRISPR-P program (http://cbi.hzau.edu.cn/crispr/)(Lei et al., 2014). Oligonucleotide pairs (Table 2-3) were annealed and cloned into a single guide RNA (sgRNA) cloning vector, pUC19_AtU6oligo, as previously described (Ito et al., 2015). Then, the

sgRNA expression cassette prepared in pUC19_AtU6oligo was excised and replaced with OsU3::gYSA in pZH_gYSA_FFCas9, an all-in-one binary vector harboring a sgRNA, Cas9 and an *HYGROMYCINPHOSPHOTRANSFERASE* (HPT) expression construct, as previously described (Ito et al., 2015). The recombinant plasmids were introduced into *L. japonicus* plants by *A. tumefaciens*-mediated stable transformation as previously described (Suzaki et al., 2012).

Expression analysis

The primers used for PCR are listed in Table 2-3. Total RNA was isolated from respective organs using the PureLink Plant RNA Reagent (Invitrogen). First-strand cDNA was prepared using the ReverTra Ace qPCR RT Master Mix with gDNA Remover (Toyobo). Real-time RT-PCR was performed using a Light Cycler 96 System (Roche) or a 7900HT Real-Time PCR system (Applied Biosystems) with a THUNDERBIRD SYBR qPCR Mix (Toyobo) according to the manufacturer's protocol. The expression of *LjUBQ* was used as the reference.

Grafting

Grafting was performed according to a previously described method (Magori et al., 2009). Seeds were grown on a sterilized plate containing 1% agar for the first 2 days in darkness and the next 2 days in a light/dark cycle, followed by shoot-root grafting. Grafted plants were used for nodulation assays 3 days after grafting.

ChIP-qPCR assay

ChIP and subsequent qPCR was performed as previously described (Soyano et al., 2013). Chromatin suspensions were prepared from 1 g of hairy roots constitutively expressing *NRSYM1-myc* with or without 10 mM KNO_3. qPCR was performed using a Light Cycler 96 System (Roche) with a KOD SYBR qPCR Mix (Toyobo) according to the manufacturer's protocol. The primers used for PCR are listed in Table 2-3.

EMSA

The NRSYM1 (531–976)-myc and LjNIN (520–878)-myc proteins were synthesized using the TNT SP6 high-yield wheat germ protein expression system (Promega) according to the manufacturer's protocol. Western blotting was performed as described previously (Nishihama et al., 2001) with an adjustment for loading equal amounts of the proteins. Membranes were incubated with 0.5 μg/mL anti-myc polyclonal antibody (Santa Cruz Biotechnology, Inc) in TBST

for 2 h at 28 °C. Membranes were washed three times in TBST and incubated for 1 h with a 1:5000 dilution of goat anti-rabbit IgG antibodies (Amersham Pharmacia). EMSA was performed as described previously (Soyano et al., 2013). For preparing probes and competitors, single-strand oligonucleotides were annealed to form dsDNA. Probes were labeled with biotin. The *in vitro* translation products containing NRSYM1 (531–976)-myc or LjNIN (520–878)-myc were incubated with probes for 30 min at 28 °C. Membranes were then incubated with a 1:1000 dilution of streptavidin-horseradish peroxidase conjugate (Thermo) in Nucleic Acid Detection Blocking Buffer (Thermo) for 1 h at 28 °C. Signals were detected using the ECL Prime Western Blotting Detection Reagent (Amersham Pharmacia) and LAS-4000mini (Fujifilm). Oligonucleotides used for probe synthesis are listed in Table 2-2.

Immunohistochemistry

Plants with transgenic hairy roots carrying the *pLjUBQ::NRSYM1-myc* construct were nitrogen-starved by growing them in the absence of nitrate for 3 days, followed by the addition of 10mM KNO_3. 100 nM LMB (Sigma) was used for the nuclear export inhibition experiment. Immunohistochemistry was carried out as previously described (Van de Velde et al., 2010). The roots were fixed in 3% (w/v) paraformaldehyde in MTSB buffer for 40 min and then incubated with a 1:200 dilution of an anti-myc polyclonal antibody (Santa Cruz Biotechnology, Inc) in 3% (w/v) BSA in MTSB/0.1% (v/v) Triton X-100 at room temperature overnight. The signal was detected with a 1:500 dilution of anti-sheep IgG-Alexa fluor 488 (Invitrogen). Before observing the signal, the roots were stained with 5 μg/ml 4', 6-diamidino-2-phenylindole (DAPI, Dojindo) for 15 min. Fluorescent images were obtained using a LSM700 confocal laser-scanning microscope (Carl Zeiss) equipped with ZEN (Carl Zeiss). The obtained images were analyzed using Image J; first, the threshold of the green signals derived from NRSYM1-myc was set equally among the images, and then the ratio of the number of the nuclei with green signals was quantified against the number of the total, namely DAPI-stained, nuclei in every image.

Data availability

Sequence data from this article can be found in the GenBank/EMBL data libraries under the following accession number: NRSYM1, LC230020. Data from the short reads from the WT (MG-20), *nrsym1-1* and *nrsym1-2* genomic DNA were deposited in the DNA Data Bank of Japan Sequence Read Archive under the accession number DRA005940.

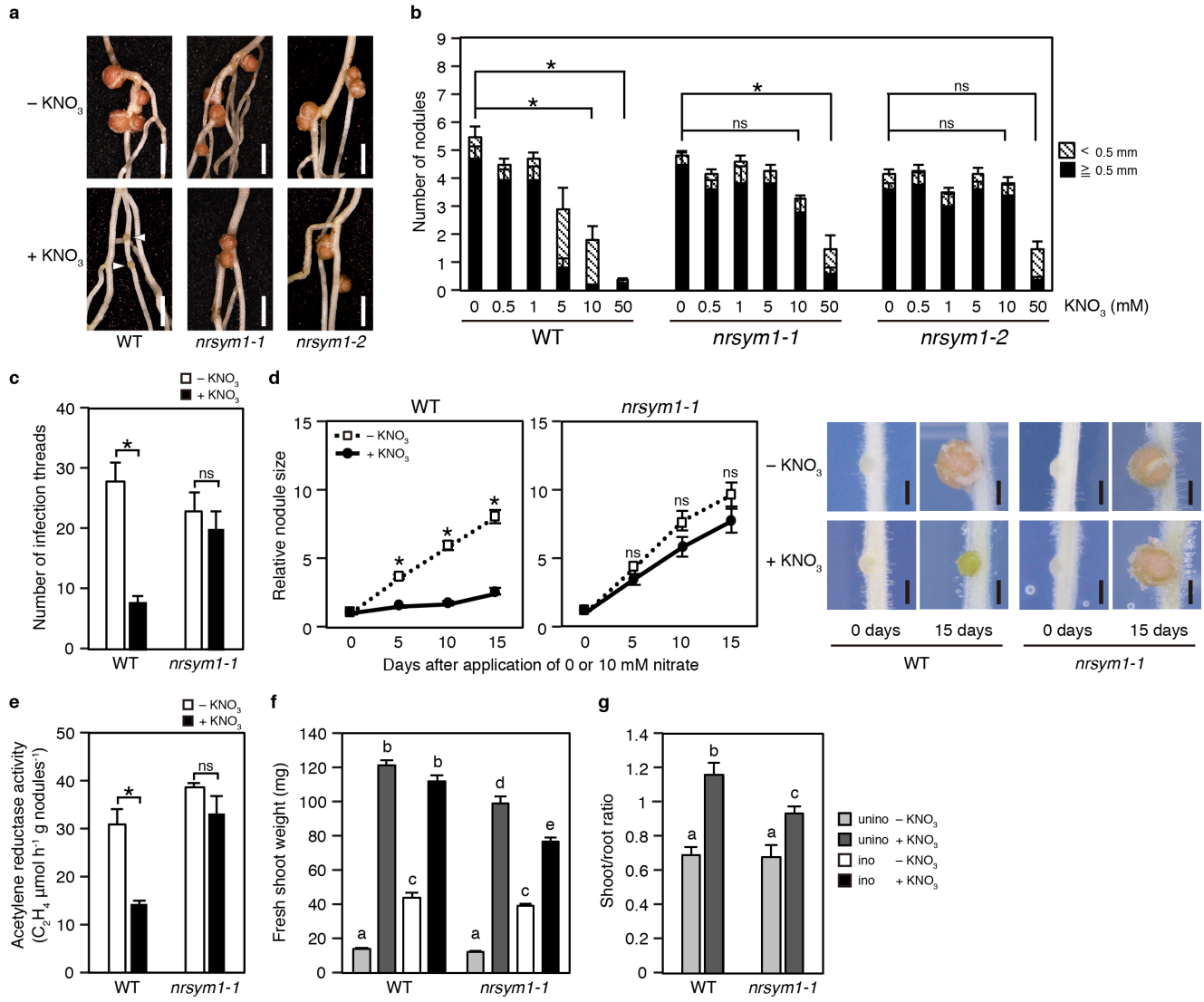

Figure 2-1. The effect of the *nrsym1* mutation on nodulation and plant growth.

For figure legend, see next page.

Figure 2-1. The effect of the *nrsym1* mutation on nodulation and plant growth.

(a) Nodule phenotypes of WT, the *nrsym1-1* mutant and the *nrsym1-2* mutant treated with 0 or 10 mM KNO_3 at 21 days after inoculation (dai). Arrowheads indicate small and premature nodules. Scale bars: 2 mm. (b) The number of nodules in WT, the *nrsym1-1* mutants and the *nrsym1-2* mutants in the presence of different concentrations of KNO_3 (0–50 mM) at 21 dai (n = 9 plants). (c) The number of infection threads in WT and the *nrsym1-1* mutants with 0 or 10 mM KNO_3 at 7 dai with rhizobia that constitutively express *LacZ* (n = 12 plants). (d) Relative nodule size (daily nodule size/nodule size at day 0) of WT and the *nrsym1-1* mutants (n = 13–19 nodules). Individual nodule size was measured at 0, 5, 10, and 15 days after the transfer to agar plates with 0 or 10 mM KNO_3. $*P < 0.05$ (Student's *t*-test compared 0 mM KNO_3-treated nodules with 10 mM KNO_3-treated nodules on the same day). ns, not significant. Scale bars: 0.5 mm. (e) Acetylene reduction activity (ARA) (μmol/ h, g nodules) of nodules formed on WT and the *nrsym1-1* mutants (n = 4 plants). Twenty-one dai plants without KNO_3 were supplied with 0 or 10 mM KNO_3, and after 3 days the ARA of nodules from each plant was measured. (f) Fresh shoot weight and (g) shoot to root fresh weight ratio of WT and the *nrsym1-1* mutants grown in 0 or 10 mM KNO_3 at 21 dai (ino) or without rhizobia (unino) (n = 10–12 plants). Error bars indicate SE. $*P < 0.05$ by Student's *t*-test. ns, not significant. (b-e). Columns with the same lower-case letter indicate no significant difference (Tukey's test, $P < 0.05$) (f, g).

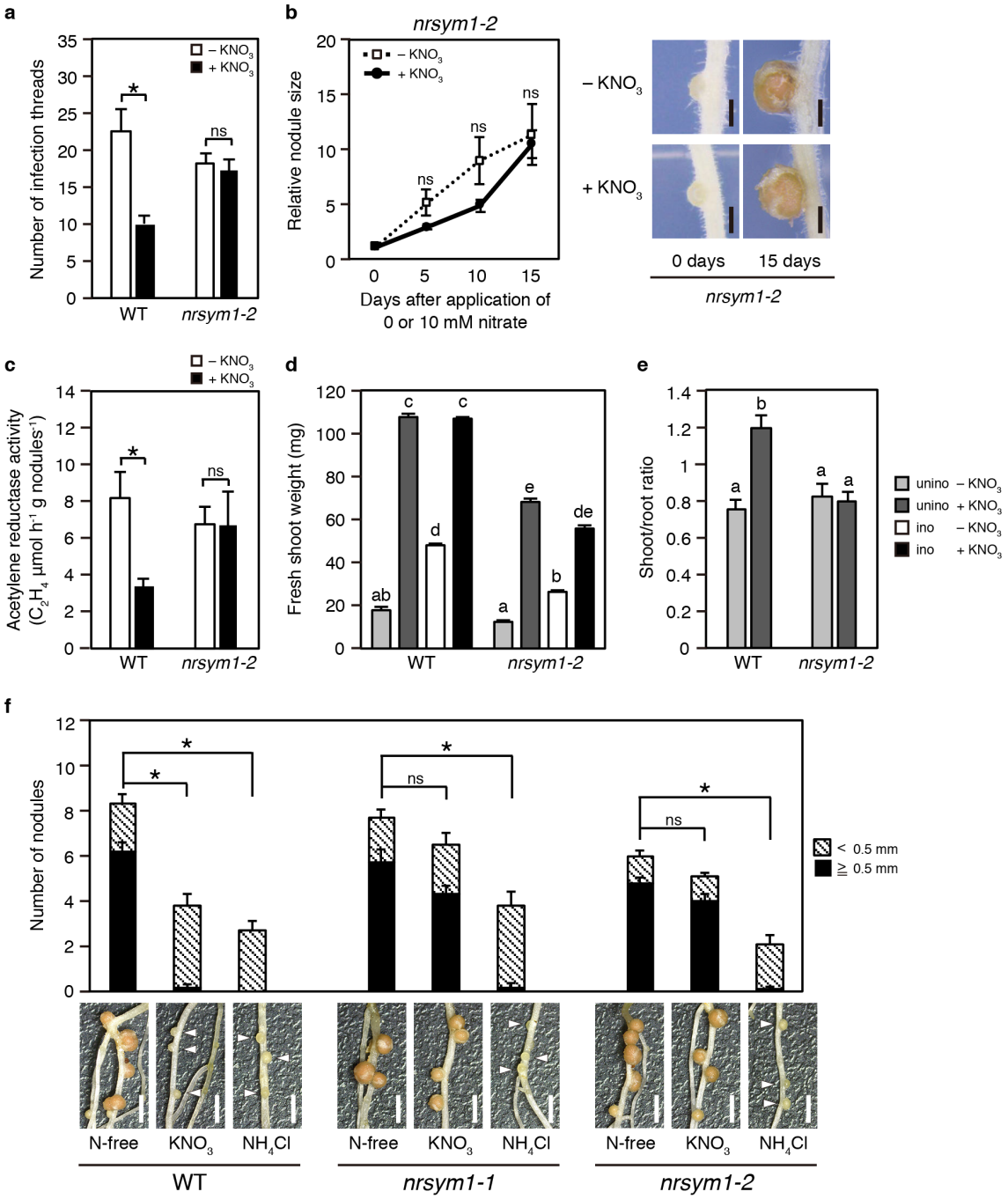

Figure 2-2. Nodulation and plant growth phenotype of the *nrsym1-2* mutant and effect of ammonium on nodulation.

For figure legend, see next page.

Figure 2-2. Nodulation and plant growth phenotype of the *nrsym1-2* mutant and effect of ammonium on nodulation.

(a) The number of infection threads in WT and the *nrsym1-2* mutants with 0 or 10 mM KNO_3 at 7 dai with rhizobia that constitutively express *DsRED* (n = 14–16 plants). (b) Relative nodule size (daily nodule size/nodule size at day 0) of the *nrsym1-2* mutants (n = 10–18 nodules). Individual nodule size was measured at 0, 5, 10 and 15 days after the transfer to agar plates with 0 or 10 mM KNO_3. **P* < 0.05 (Student's *t*-test compared 0 mM KNO_3-treated nodules with 10 mM KNO_3-treated nodules on the same day). ns, not significant. Scale bars: 0.5 mm. (c) Acetylene reduction activity (ARA) (μmol h^{-1} g $nodules^{-1}$) of nodules formed on WT and the *nrsym1-2* mutants (n = 4 plants). Twenty-one dai plants without KNO_3 were supplied with 0 or 10 mM KNO_3, and after 3 days the ARA of nodules from each plant was measured. (d) Fresh shoot weight and (e) shoot to root fresh weight ratio of WT and the *nrsym1-2* mutants grown in 0 or 10 mM KNO_3 at 21 dai (ino) or without rhizobia (unino) (n = 10–12 plants). (f) Nodulation and nodule numbers of WT, the *nrsym1-1* mutant and the *nrsym1-2* mutant treated with 0, 10 mM KNO_3 or 10 mM NH_4Cl at 21 dai (n = 10–12 plants). Arrowheads indicate small and premature nodules. Scale bars: 2 mm. Error bars indicate SE. **P* < 0.05 by Student's *t*-test. ns, not significant (a-c,f). Columns with the same lower-case letter indicate no significant difference (Tukey's test, *P* < 0.05) (d,e).

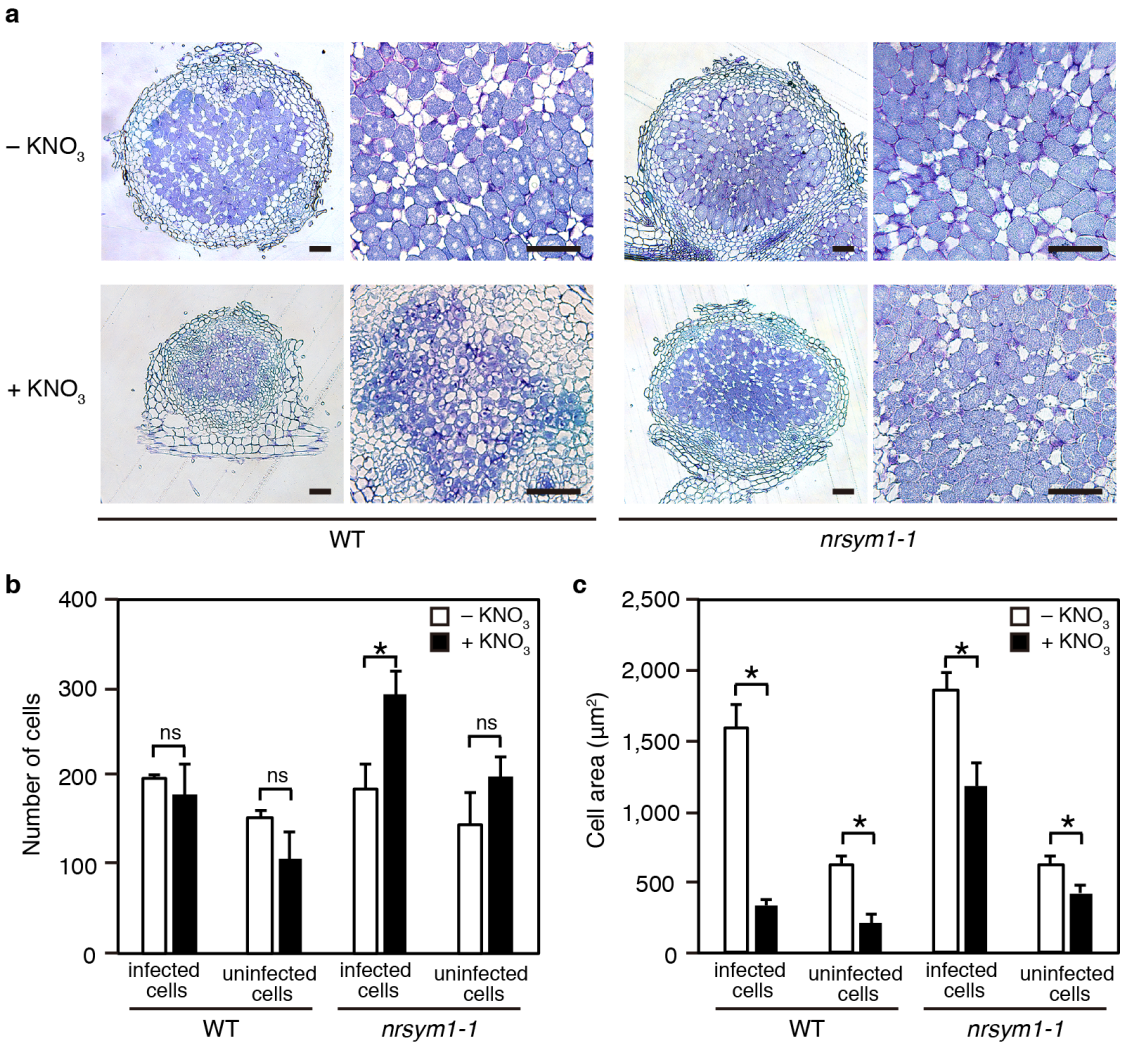

Figure 2-3. The effect of nitrate on nodule growth.

(a) Sections through 21 dai nodules of WT and the *nrsym1-1* mutants grown in the presence of 0 or 10 mM KNO_3. Sections were stained with toluidine blue. Scale bars: 100 µm. (b) The number of cells and (c) the cell area (μm^2) in the inner region of nodule sections. After images of individual nodule sections of maximum diameter had been collected, cell number and cell area were measured using ImageJ software (http://imagej.nih.gov/ij/) (n = 4–5 nodules section). Infected and uninfected cells located in the inner region of nodule parenchyma were scored for the presence or absence of cell staining, respectively. To calculate cell area, the area of all infected and uninfected cells was measured and averaged (170–637 cells per nodule section). Using the obtained average cell area in respective nodule sections, the average cell area per nodule section was calculated. *$P < 0.05$ by Student's *t*-test. ns, not significant. Error bars indicate SE.

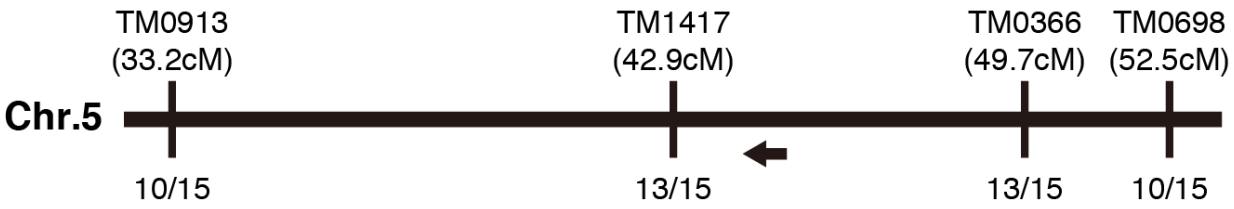

Figure 2-4. Map-based cloning of *NRSYM1*.

The *nrsym1* locus was mapped using an F_2 population derived from a cross between *nrsym1-1* and Gifu B-129 plants. Fifteen F_2 plants that exhibited the nitrate-tolerant phenotype were used for this analysis. The arrow indicates the relative location of the *NRSYM1* candidate gene (chr5.CM0148.170.r2.a (*LjNLP4*)) found in the *L. japonicus* genomic sequence database. The primers used for PCR are listed in Table 2-3.

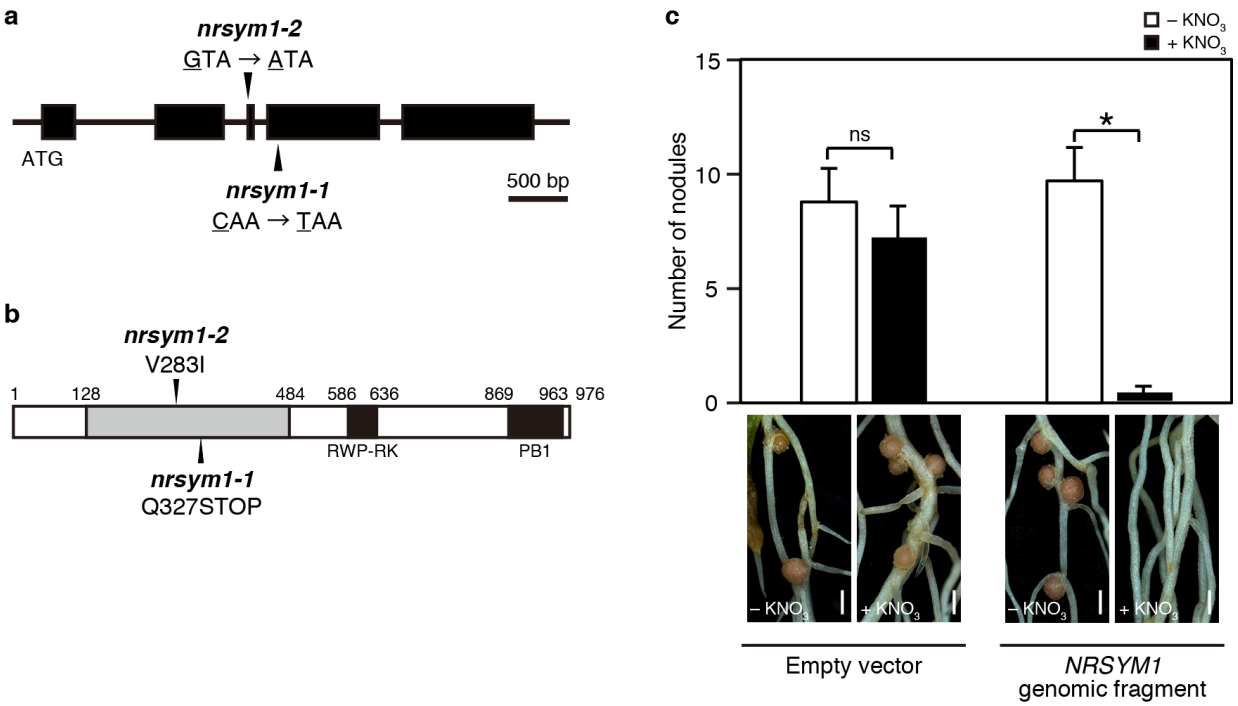

Figure 2-5. Structure of the *NRSYM1* gene.

(a) Exon-intron structure of the *NRSYM1* gene. Black boxes indicate exons. Arrowheads indicate locations of the *nrsym1* mutations. (b) Structure of the deduced NRSYM1 protein. An N-terminal conserved region is indicated by the gray box. C-terminal regions containing an RWP-RK DNA-binding domain (RWP-RK) and a conserved domain (PB1) are shown as black boxes. Arrowheads indicate locations of the *nrsym1* mutations. (c) Complementation of the *nrsym1* nodulation phenotype. Representative transgenic hairy roots of *L. japonicus* carrying a control empty vector or a 7.5-kb genomic fragment encompassing the entire *NRSYM1* locus. Transgenic roots were identified by GFP fluorescence. The number of nodules was counted in the transgenic roots of *nrsym1-1* mutants containing either an empty vector or a genomic fragment of *NRSYM1* in the presence of 0 or 10 mM KNO_3 at 21 dai (n = 8–10 plants). *$P < 0.05$ by Student's *t*-test. ns, not significant. Error bars indicate SE. Scale bars: 1 mm.

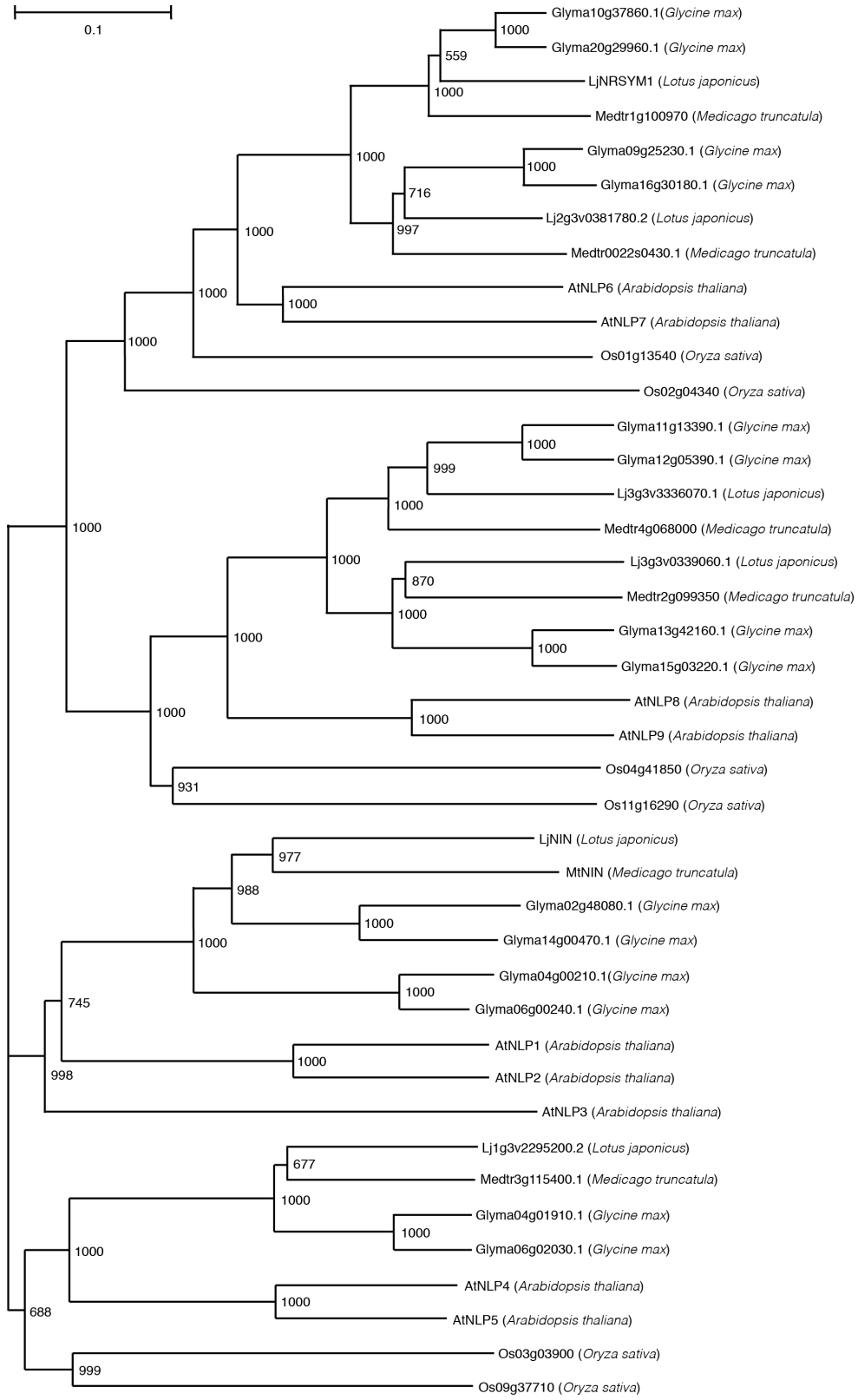

Figure 2-6. A phylogenetic tree of the NLP family.

For figure legend, see next page.

Figure 2-6. A phylogenetic tree of the NLP family.

Full-length amino acid sequences were compared and the tree was constructed by the neighbor-joining method. The numbers are bootstrap values from 1000 replicates. Accession numbers of the amino acid sequences of related proteins are as follows: LjNRSYM1 (Lj5g3v1999250.2), LjNIN (Lj2g3v3373110.1), MtNIN (Medtr5g099060), AtNLP1 (AT2G17150.1), AtNLP2 (AT4G35270.1), AtNLP3 (AT4G38340.1), AtNLP4 (AT1G20640.1), AtNLP5 (AT1G76350.1), AtNLP6 (AT1G64530.1), AtNLP7 (AT4G24020.1), AtNLP8 (AT2G43500.1) and AtNLP9 (AT3G59580.1).

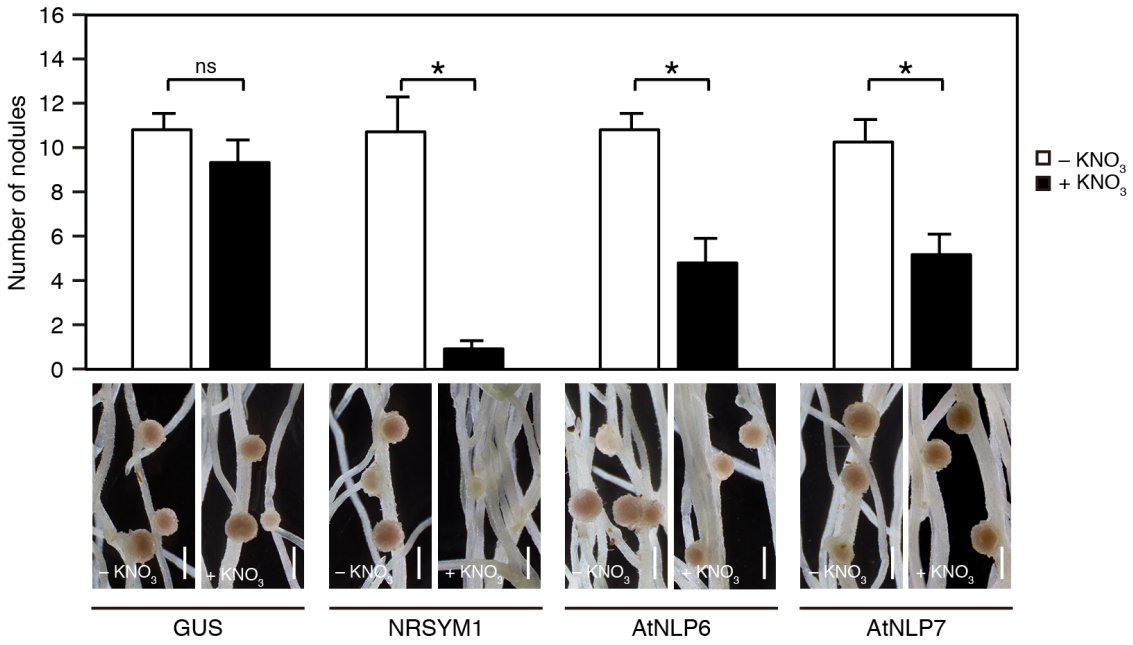

Figure 2-7. Complementation of the *nrsym1* nodulation phenotype by the expression of *AtNLP6* or *AtNLP7*.

Nodulation and the number of nodules in transgenic hairy roots produced from the *nrsym1-1* mutants containing *pLjUBQ::GUS*, *pLjUBQ::NRSYM1*, *pLjUBQ::AtNLP6*, or *pLjUBQ::AtNLP7* constructs grown in the presence of 0 or 10 mM KNO_3 at 21 dai (n = 10–12 plants). Transgenic roots were identified by GFP fluorescence. **P* < 0.05 by Student's *t*-test. ns, not significant. Error bars indicate SE. Scale bars: 1 mm.

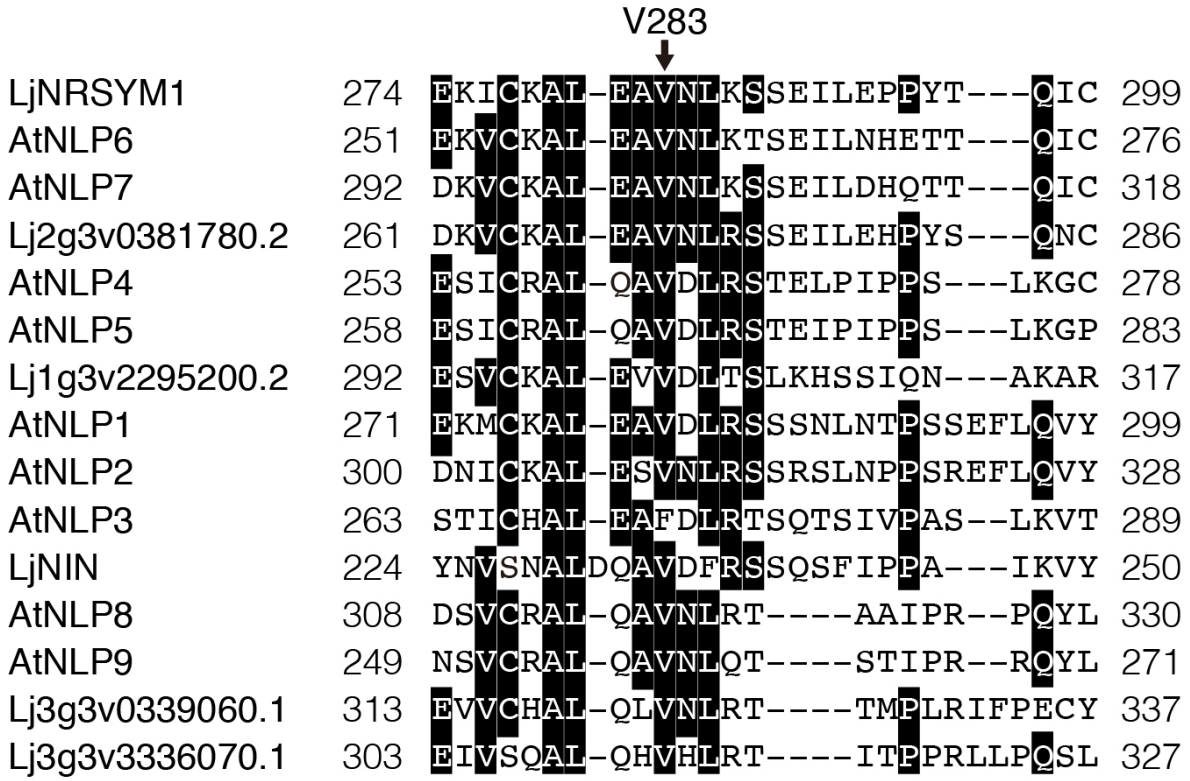

Figure 2-8. Alignment of the amino acid sequences of *L. japonicus* and Arabidopsis NLPs.
Amino acid sequence alignment of a partial N-terminal conserved region containing the *nrsym1-2* mutation (V283) is shown. Amino acid residues that are conserved in more than half of the amino acid sequences are shaded in black. Accession numbers of the amino acid sequences of related proteins are as follows: LjNRSYM1 (Lj5g3v1999250.2), LjNIN (Lj2g3v3373110.1), AtNLP1 (AT2G17150.1), AtNLP2 (AT4G35270.1), AtNLP3 (AT4G38340.1), AtNLP4 (AT1G20640.1), AtNLP5 (AT1G76350.1), AtNLP6 (AT1G64530.1), AtNLP7 (AT4G24020.1), AtNLP8 (AT2G43500.1), and AtNLP9 (AT3G59580.1).

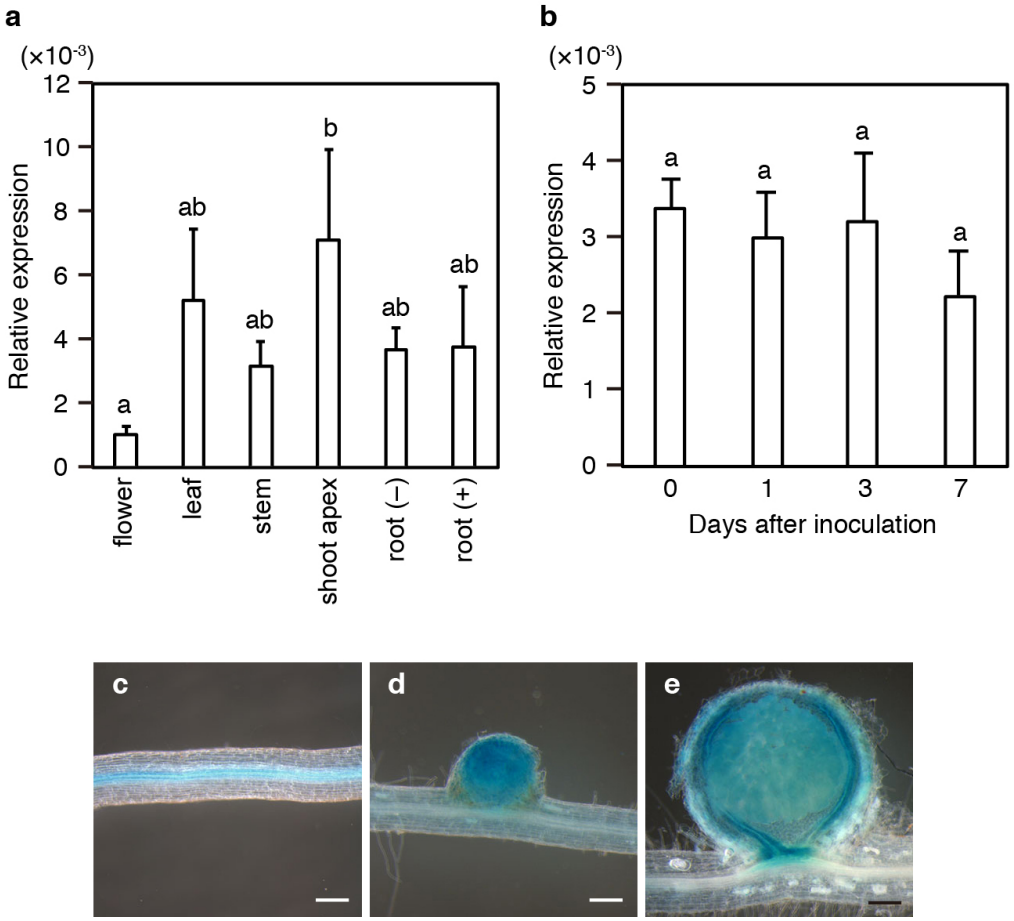

Figure 2-9. The *NRSYM1* expression pattern.

(a) Real-time RT-PCR analysis of *NRSYM1* expression in WT. Each cDNA sample was prepared from total RNA derived from flowers, leaves, stems, shoot apices, or roots incubated with 0 (–) or 10 mM (+) KNO_3 for 24 h (n = 3 independent pools of roots). (b) Real-time RT-PCR analysis of *NRSYM1* expression in WT non-inoculated (0) and inoculated roots at 1, 3, and 7 dai under nitrate-free conditions (n = 4 independent pools of roots). Each cDNA sample was prepared from total RNA derived from a whorl of roots. The expression of *LjUBQ* was used as a reference. Error bars indicate SE. Columns with the same lower-case letter indicate no significant difference (Tukey's test, $P < 0.05$). (c-e) Spatial expression patterns of *NRSYM1*. Blue staining indicates GUS activity under the control of the *NRSYM1* promoter in the (c) root, (d) nodule primordia and (e) a mature nodule of WT. GUS activity was observed at 10 dai (c,d) or 14 dai (e). Scale bars: 200 μm.

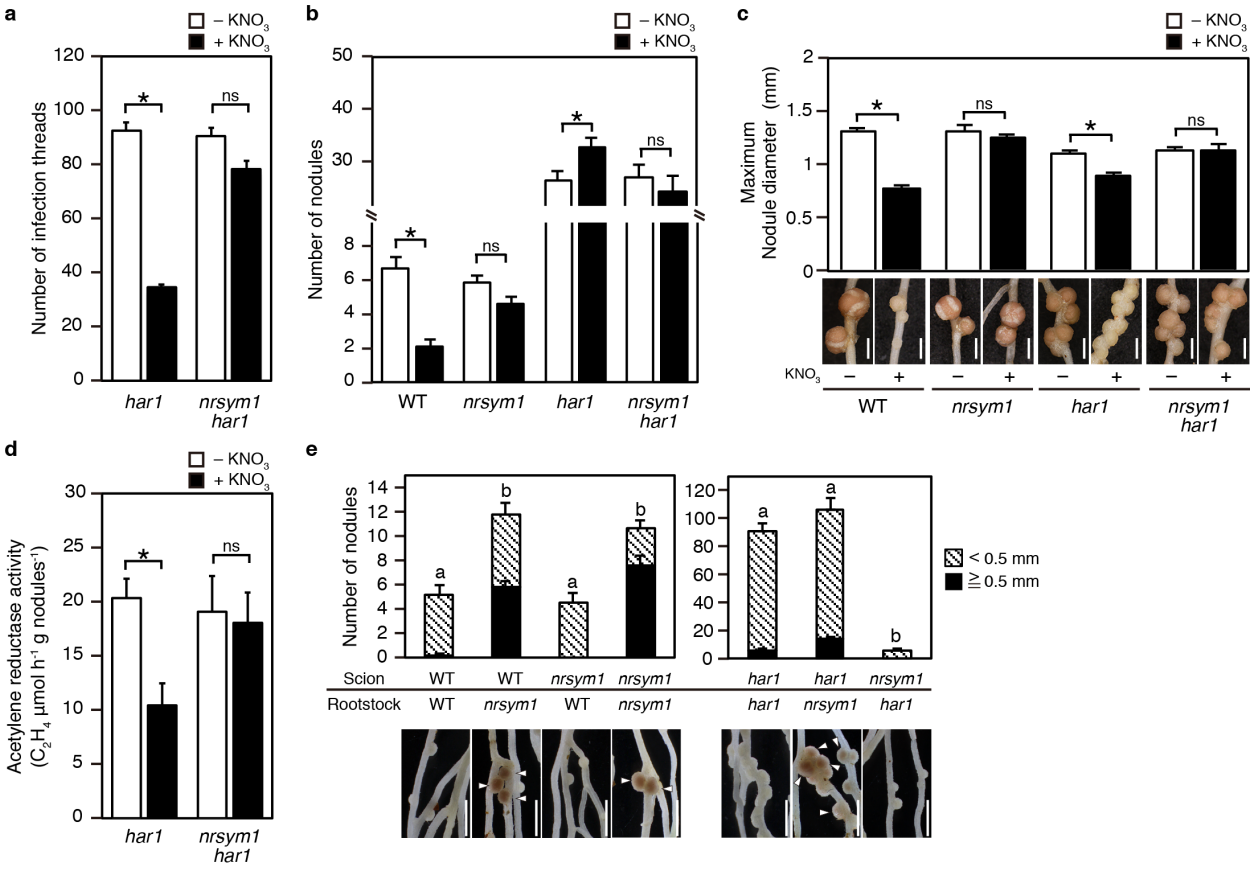

Figure 2-10. Effects of nitrate on nodulation in the *nrsym1 har1* double mutants.

(a) The number of infection threads in the *har1-7* mutants and the *nrsym1-1 har1-7* double mutants (n = 11–12 plants). Plant growth conditions were the same as those shown in Fig. 2-1c. (b) The number of nodules and (c) maximum nodule diameter (mm) in WT, the *nrsym1-1* mutants, the *har1-7* mutants, and the *nrsym1-1 har1-7* double mutants grown in the presence of 0 or 10 mM KNO_3 at 21 dai (n = 9–12 plants). (d) Acetylene reduction activity (ARA) (µmol /h g nodule) of nodules formed on the *har1-7* mutants and the *nrsym1-1 har1-7* double mutants (n = 4 plants). Plant growth conditions were the same as those shown in Fig. 2-1e. (e) Nodulation and nodule numbers of plants derived from shoot-root grafts having WT, *nrsym1-1,* and *har1-7* genotypes. Plants were grown in the presence of 10 mM KNO_3 for 21 dai (n = 13 plants). Arrowheads indicate mature nodules. *$P < 0.05$ by Student's *t*-test. ns, not significant (a-d). Columns with the same lower-case letter indicate no significant difference (Tukey's test, $P < 0.05$) (e). Error bars indicate SE. Scale bars: 1 mm (c); 2 mm (e).

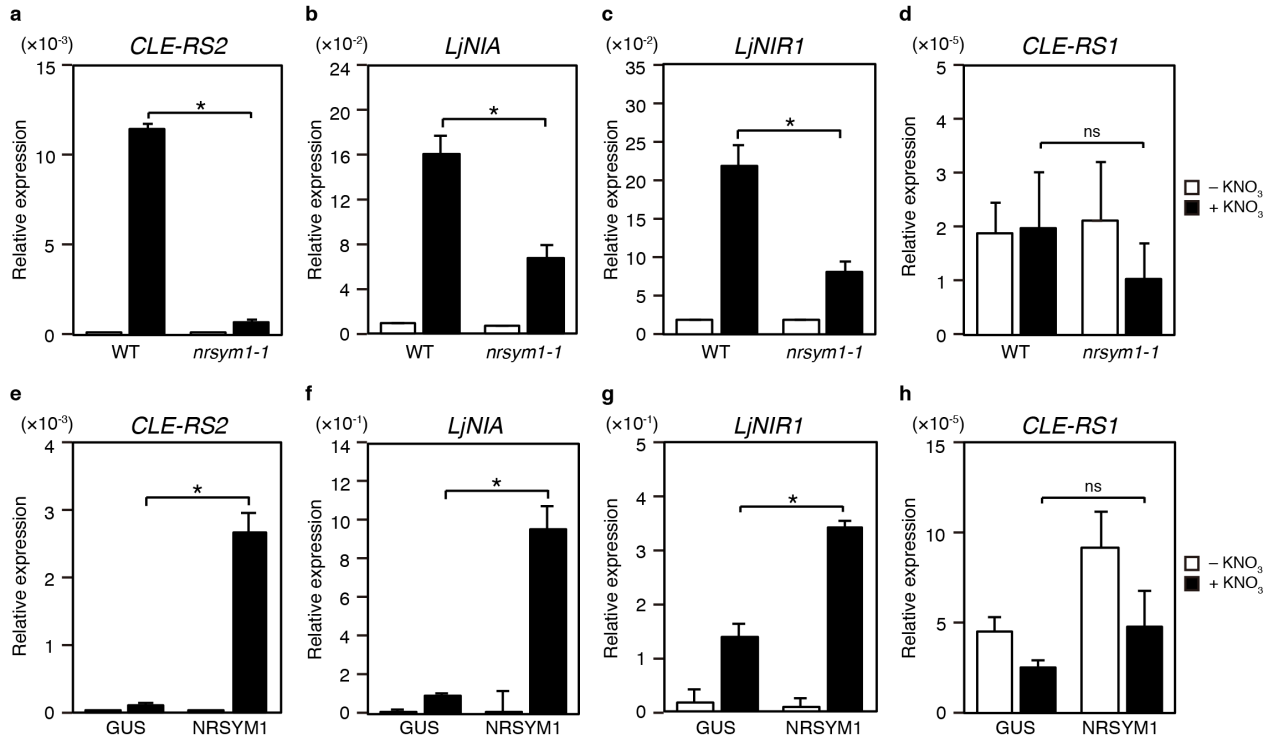

Figure 2-11. The effect of the *nrsym1* mutation or *NRSYM1* constitutive expression on gene expression.

(a-d) Real-time RT-PCR analysis of (a) *CLE-RS2*, (b) *LjNIA*, (c) *LjNIR1,* and (d) *CLE-RS1* expression in roots of WT and the *nrsym1-1* mutants. (e-h) Real-time RT-PCR analysis of (e) *CLE-RS2*, (f) *LjNIA*, (g) *LjNIR1,* and (h) *CLE-RS1* expression in transgenic hairy roots produced from WT containing the *pLjUBQ::GUS* or *pLjUBQ::NRSYM1* constructs. Each cDNA sample was prepared from total RNA derived from an uninoculated whorl of roots grown in the presence of 0 or 10 mM KNO_3 for 24 h. The expression of *LjUBQ* was used as the reference. Error bars indicate SE. (n = 3 independent pools of roots). **P* < 0.05 by Student's *t*-test. ns, not significant.

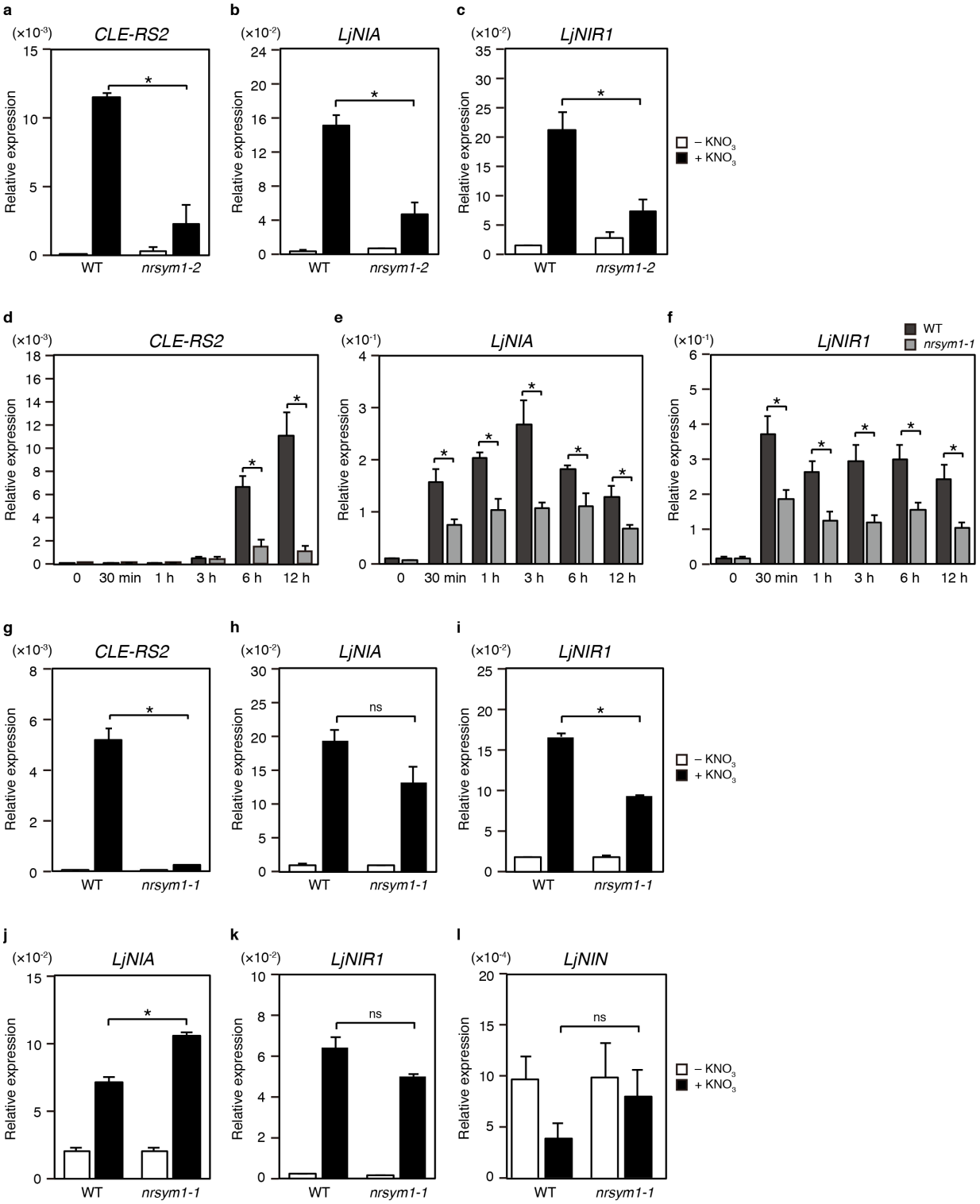

Figure 2-12. The effect of the *nrsym1* mutation on gene expression.

For figure legend, see next page.

Figure 2-12. The effect of the *nrsym1* mutation on gene expression.

(a-c) Real-time RT-PCR analysis of (a) *CLE-RS2*, (b) *LjNIA* and (c) *LjNIR1* expression in uninoculated roots of WT and the *nrsym1-2* mutants grown in the presence of 0 or 10 mM KNO_3 for 24 h. (d-i) Real-time RT-PCR analysis of (d,g) *CLE-RS2*, (e,h) *LjNIA*, and (f,i) *LjNIR1* in uninoculated roots of WT and the *nrsym1-1* mutants grown in N-free medium (0, $–KNO_3$) or in the presence of 10 mM KNO_3 for 30 min, 1, 3, 6, or 12 h (d-f) or 200 μM KNO_3 for 24 h (g-i). (j,k) Real-time RT-PCR analysis of (j) *LjNIA* and (k) *LjNIR1* in WT or *nrsym1-1* mutant leaves grown in the presence of 0 or 10 mM KNO_3 for 24 h. (l) Real-time RT-PCR analysis of *LjNIN* in 1 dai roots of WT and the *nrsym1-1* mutants grown in the presence of 0 or 10 mM KNO_3 for 24 h. Each cDNA sample was prepared from total RNA derived from (a-i,l) a whorl of roots or (j,k) leaves. The expression of *LjUBQ* was used as the reference. Error bars indicate SE. (n = 3 independent pools of roots or leaves). $*P < 0.05$ by Student's *t*-test. ns, not significant.

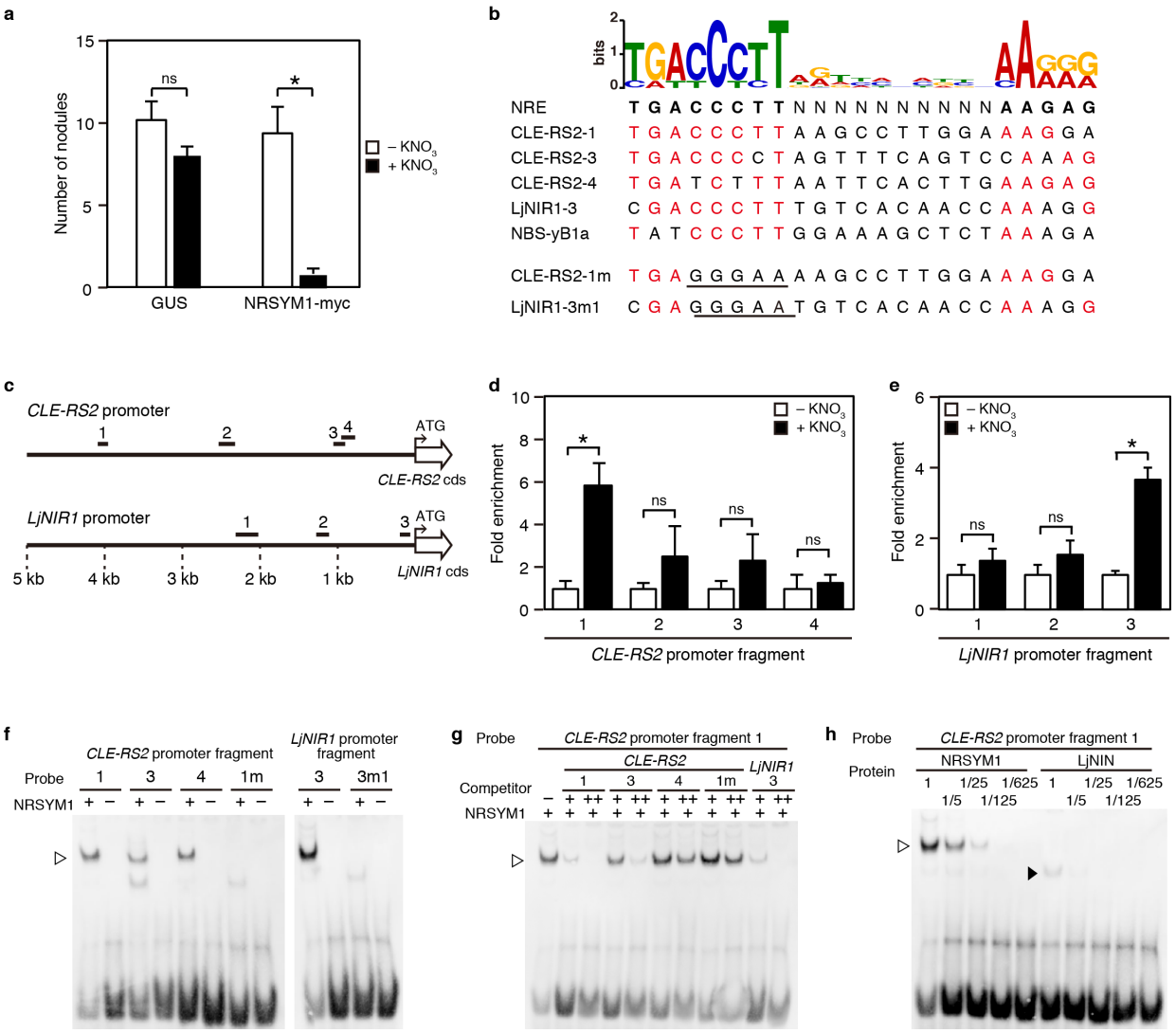

Figure 2-13. Interaction of NRSYM1 with *CLE-RS2* and *LjNIR1* promoters.

For figure legend, see next page.

Figure 2-13. Interaction of NRSYM1 with *CLE-RS2* and *LjNIR1* promoters.

(a) The number of nodules in transgenic hairy roots produced from the *nrsym1-1* mutants containing either *pLjUBQ::GUS* or *pLjUBQ::NRSYM1-myc* constructs grown in the presence of 0 or 10 mM KNO_3 at 21 dai. Transgenic roots were identified by GFP fluorescence. Error bars indicate SE. (n = 10–15 plants) (b) Nucleotide sequences of the consensus sequence of NRE (Konishi and Yanagisawa, 2011), NBS-yB1a (Soyano et al., 2013) and NRE/NBS sequences that were identified in the *CLE-RS2* and *LjNIR1* promoter regions. Frequencies of nucleotide distributions among these sequences are shown with the MEME algorithm (http://meme-suite.org/index.html) (Bailey et al., 2009). Conserved nucleotide sequences among respective NRE/NBSs are shown in red letters. The mutated nucleotide sequences in CLE-RS2-1m and LjNIR1-3m1 are underlined. (c) A schematic diagram of the location of DNA fragments used for ChIP-qPCR analyses and electrophoretic mobility shift assay (EMSA) in the 5-kb promoter regions of *CLE-RS2* and *LjNIR1*. The numbering of fragments within each promoter region corresponds to those referenced in (d-g). (d,e) qPCR analysis to examine NRSYM1 binding with the (d) *CLE-RS2* and (e) *LjNIR1* promoter regions after ChIP. DNA fragments were co-immunoprecipitated with polyclonal anti-myc antibody from chromatin suspensions prepared from *pLjUBQ::NRSYM1-myc* roots that were incubated with 0 or 10 mM KNO_3 for 24 h without rhizobia. The PCR products were quantified by comparison with products amplified using primers specific to *LjUBQ*. The fold enrichment of nitrate-induced NRSYM1 binding was calculated as the ratio between $+KNO_3$ and $-KNO_3$-immunoprecipitated amplification signals. Error bars indicate SE. (n = 3 independent pools of roots). $*P < 0.05$ by Student's *t*-test. ns, not significant. (f,g) EMSA showing NRSYM1-binding with the NRE/NBS of the *CLE-RS2* and *LjNIR1* promoter (b). Biotin-labeled probes were incubated with NRSYM1(531–976)-myc (+) or *in vitro* translation products without template (−). The *CLE-RS2* promoter 1m and *LjNIR1* promoter 3m1, contain mutations in the NRE/NBS of *CLE-RS2* promoter 1 and *LjNIR1* promoter 3, respectively (b; Table 2-2). (g) NRSYM1 (531-976)-myc and a labeled *CLE-RS2* promoter 1 probe were incubated with their respective competitors. Non-labelled probes were used as competitor DNA at an excess molar ratio (–, 1:0; +, 1:20; ++, 1:100). Arrowheads indicate locations of the band shift. (h) EMSA showing NRSYM1 or LjNIN-binding with the *CLE-RS2* promoter 1. White and black arrowheads respectively indicate the position of shifted bands when the NRSYM1(531–976)-myc or LjNIN(520–878)-myc protein was incubated with the biotin-labeled probe. A dilution series of NRSYM1(531–976)-myc and LjNIN(520–878)-myc proteins were used for EMSA after adjusting for equal protein amounts by western blotting.

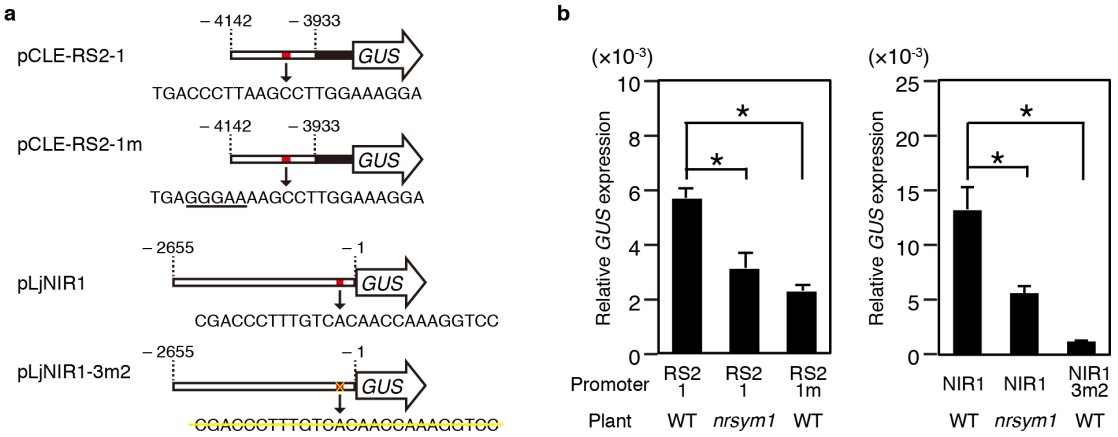

Figure 2-14. Activation of *GUS* gene by *CLE-RS2* and *LjNIR1* promoters.

(a) A schematic diagram of the promoter-*GUS* constructs used in (b). Promoter fragments containing NRE/NBS (red bars) from the *CLE-RS2* and *LjNIR1* promoter regions were inserted upstream of the *GUS* gene. Black bars indicate the CaMV35S minimal promoter. The mutated nucleotide sequence in pCLE-RS2-1m is underlined. The entire NRE/NBS region is deleted in pLjNIR1-3m2. (b) Real-time RT-PCR analysis of *GUS* expression in WT and *nrsym1-1* transgenic hairy roots expressing each GUS construct (a). Each cDNA sample was prepared from total RNA derived from an uninoculated whorl of roots grown in the presence of 10 mM KNO_3 for 24 h. Transgenic roots were identified by GFP fluorescence. The expression of *GFP* was used as the reference. Error bars indicate SE. (n = 5 independent pools of roots). **P* < 0.05 by Student's *t*-test.

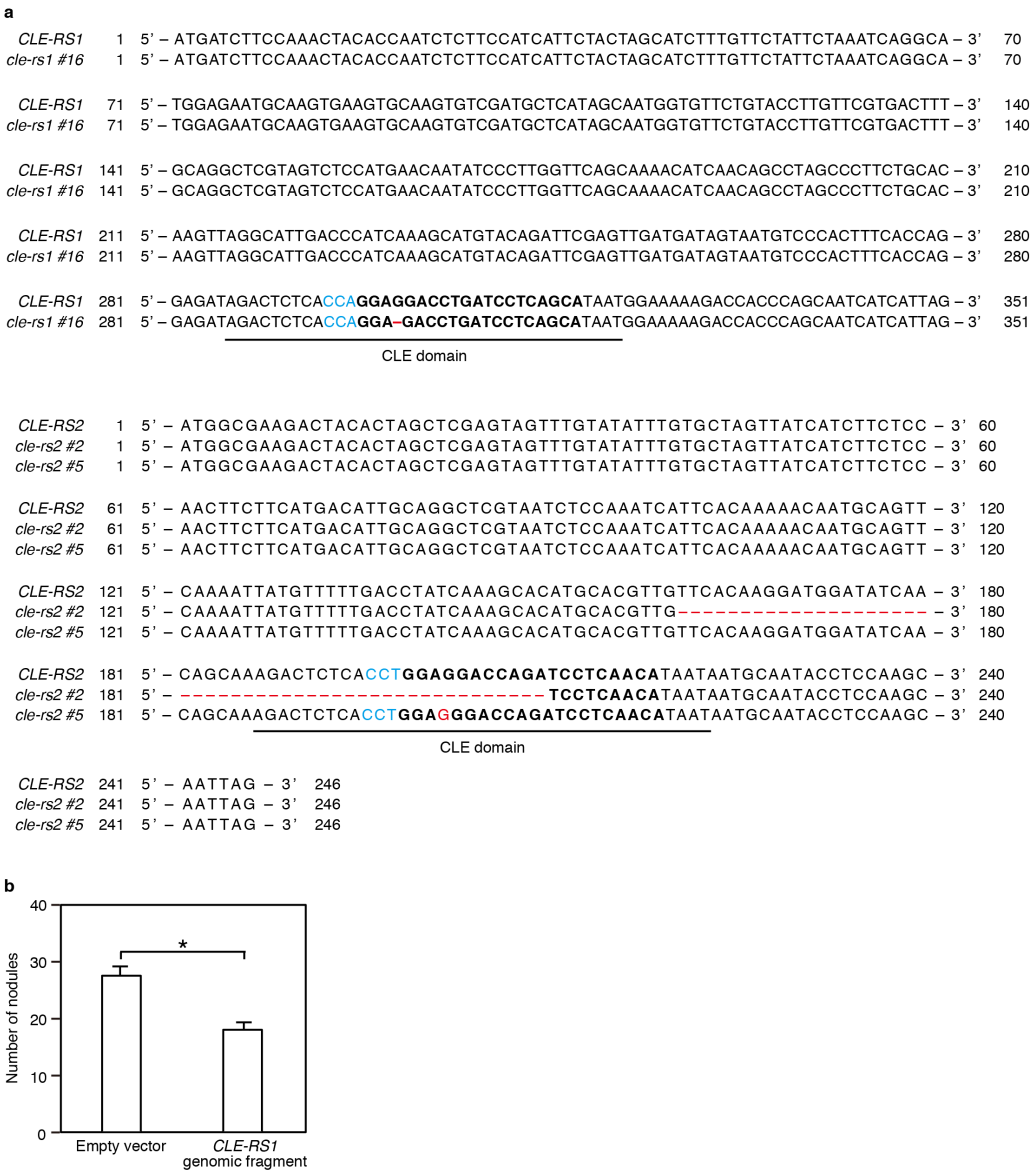

Figure 2-15. The position of mutations in *cle-rs1* and *cle-rs2* plants created by the CRISPR/Cas9 genome editing system and complementation of the *cle-rs1 cle-rs2* double mutant nodulation phenotype.

(a) Nucleotide alignment of *CLE-RS1* and *CLE-RS2* genes. The indel mutations near the protospacer adjacent motif (PAM) site (blue letters) of *CLE-RS1* and *CLE-RS2* are shown in red. The sgRNA target is indicated in bold letters. The nucleotides sequences that encode amino acids of the CLE domains are underlined. (b) The number of nodules in transgenic hairy roots produced from the *cle-rs1 cle-rs2* double mutants carrying either a control empty vector or a 7.4-kb genomic fragment encompassing the entire *CLE-RS1* locus at 21 dai (n = 26 plants). Transgenic roots were identified by GFP fluorescence. **P* < 0.05 by Student's *t*-test. Error bars indicate SE.

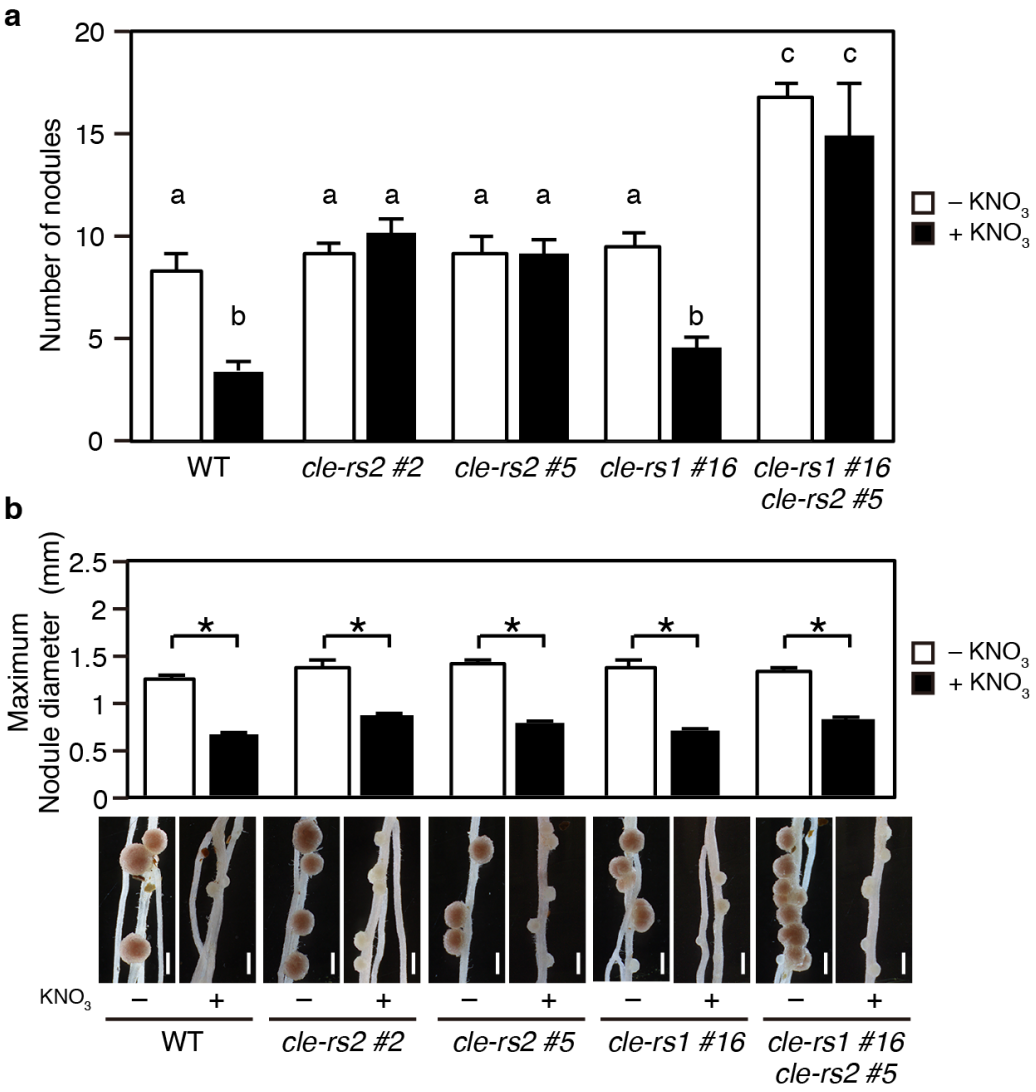

Figure 2-16. Effects of loss-of-function mutations in *CLE-RS1/2* on nodulation.

(a) The number of nodules and (b) maximum nodule diameter (mm) in WT, the *cle-rs1* mutants (T2), the *cle-rs2* mutants (T2) and the *cle-rs1 cle-rs2* double mutants grown in the presence of 0 or 10 mM KNO_3 (n = 7–14 plants). The *cle-rs1 cle-rs2* double mutants were obtained by crossing the single mutants. The *cle-rs1* and *cle-rs2* mutants were obtained by the CRISPR/Cas9 genome editing system (Fig. 2-15a). Error bars indicate SE. Columns with the same lower-case letter indicate no significant difference (Tukey's test, $P < 0.05$) (a). *$P < 0.05$ by Student's *t*-test. Scale bars: 1 mm (b).

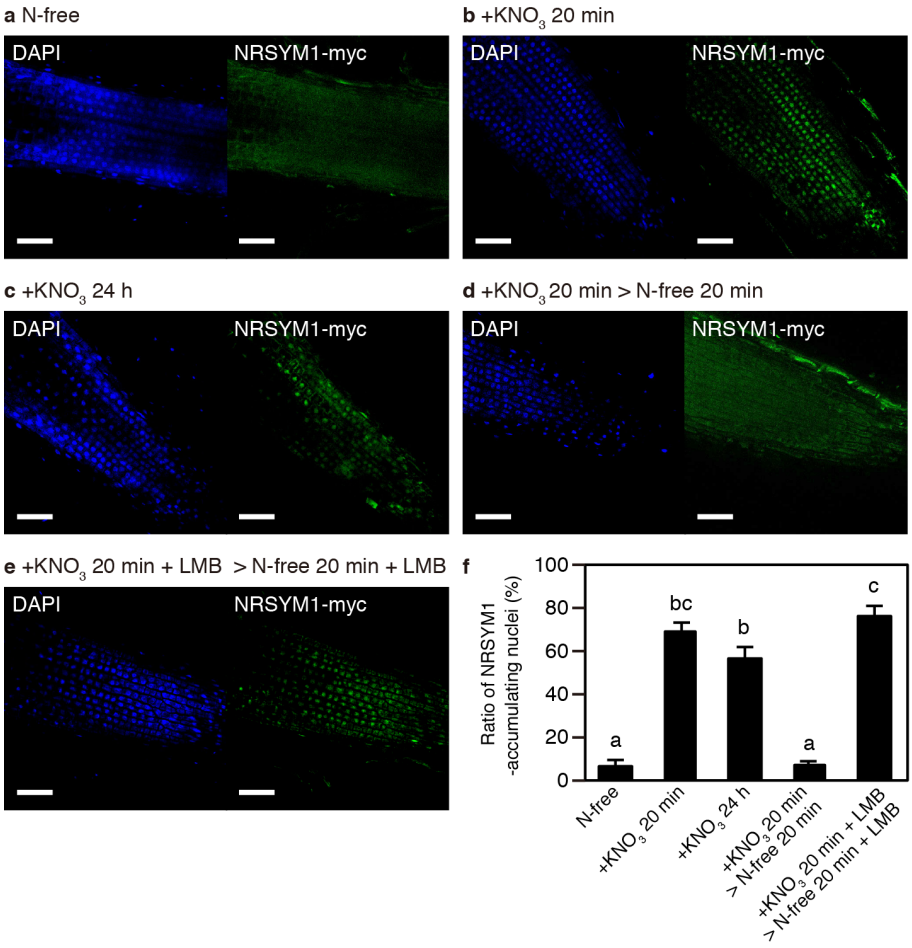

Figure 2-17. Subcellular localization of NRSYM1.

(a-e) Immunohistochemistry of the NRSYM1-myc protein in root apical cells. A polyclonal anti-myc antibody and an antibody conjugated to Alexa Fluor 488 (green signal) were used as primary and secondary antibodies. Nuclei were visualized with DAPI (blue signal). Plants with transgenic hairy roots carrying the *pLjUBQ::NRSYM1-myc* construct were grown in the absence of nitrate for 3 days. N-starved plants were transferred to (a) N-free or (b) 10 mM KNO_3 medium for 20 min or (c) 24 h. (d) N-starved plants were transferred to 10 mM KNO_3 medium for 20 min, and then to N-free medium for 20 min. (e) N-starved plants were first incubated with leptomycin B (LMB) in a N-free medium for 3 h, and then transferred to 10 mM KNO_3 medium with LMB for 20 min and to N-free medium with LMB for 20 min. Scale bars: 50 μm. (f) The ratio of NRSYM1-accumulating nuclei. Using respective fluorescent images, the percentages of nuclei having green signals among all DAPI-stained nuclei were calculated. Error bars indicate SE. (n = 5 roots). Columns with the same lower-case letter indicate no significant difference (Tukey's test, $P < 0.05$).

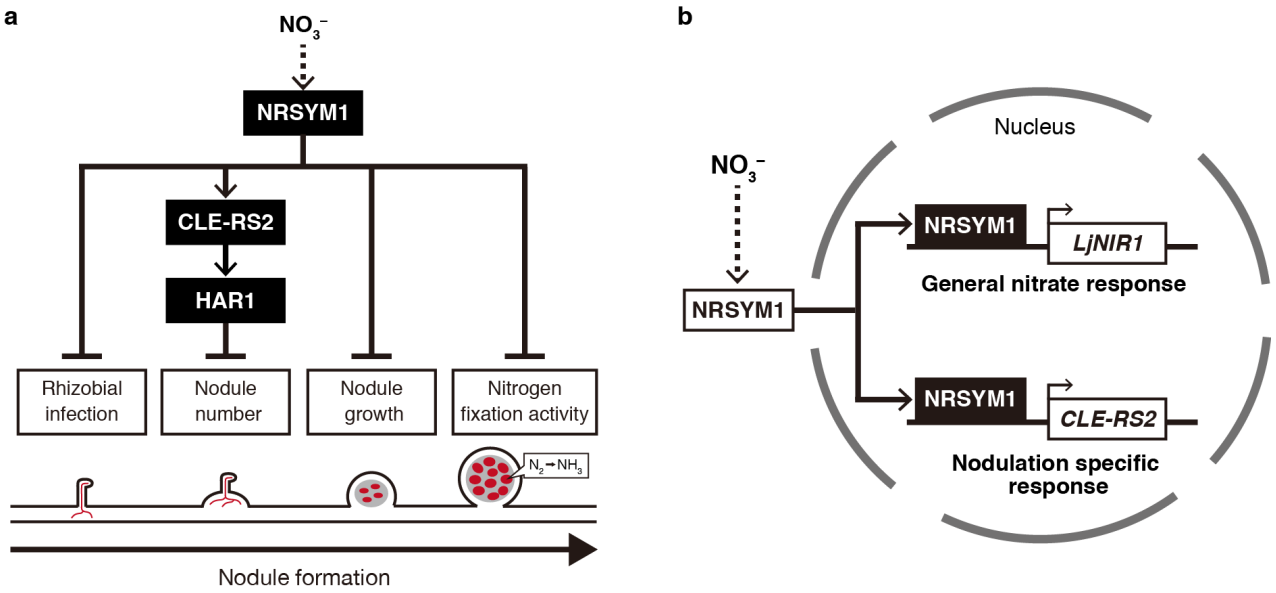

Figure 2-18. Model for the control of root nodule symbiosis in response to nitrate.

(a) Sequential progress of nodulation is shown. In response to nitrate, NRSYM1 regulates pleiotropic phases of root nodule symbiosis, including rhizobial infection, nodule number, nodule growth, and nitrogen fixation activity. Whereas NRSYM1 activates the CLE-RS2>HAR1 signaling pathway leading to the negative regulation of nodule number, NRSYM1 is likely to use different downstream targets to achieve the regulation of other nitrate-affected processes. Red lines and red cells, respectively, indicate the infection threads and rhizobia-colonized cells. (b) A model for cellular-level NRSYM1 function. Nuclear localization of NRSYM1 is controlled by nitrate. In the nucleus, NRSYM1 regulates both the general nitrate response and root nodule symbiosis by directly regulating related genes such as *LjNIR1* and *CLE-RS2*.

Table 2-1. SNP filtering in the nrsym1 mutants

	WT (MG20)	***nrsym1-1***	***nrsym1-2***
Total raw reads	125,479,432	178,108,716	102,628,550
Total nucleotides (Mb)	12,673	17,988	10,365
Coverage	27.0x	38.3x	22.1x
Total SNP / genome	378,841	403,934	366,454
Number of homo-type SNP candidates / genome	85,519	93,569	82,360
Comparison of SNP candidates of MG20 / genome	-	22,509	17,167
C to T, G to A / genome	-	4,320	3,541
SNPs in the exon and intron acceptor and donor site / genome	-	350	304
F2 plants used for rough mapping	-	15	15
Mapped region	-	6.0 Mb	6.0 Mb
Gene number annotated / mapped region	-	561	561
SNPs in the exon and intron acceptor/donor site / mapped region	-	3	1
Shared SNPs in same genes	-	chr5.CM0148.170.r2.a	

Table 2-2. EMSA probes

EMSA-RS2-1-F	5'–ggtgTGTGAGTTCTGACCCTTAAGCCTTGGAAAGGACAGTCATGCAA–3'
EMSA-RS2-1-R	5'–ggtgTTGCATGACTGTCCTTTCCAAGGCTTAAGGGTCAGAACTCACA–3'
EMSA-RS2-2-F	5'–ggtgGGTTTACGACCTAACTCATTGAGGCATGATGTGACTTGACTTGT–3'
EMSA-RS2-2-R	5'–ggtgACAAGTCAAGTCACATCATGCCTCAATGAGTTAGGTCGTAAACC–3'
EMSA-RS2-3-F	5'–ggtgGTATCAAACTGACCCCTAGTTTCAGTCCAAAGCCACCTTGATTG–3'
EMSA-RS2-3-R	5'–ggtgCAATCAAGGTGGCTTTGGACTGAAACTAGGGGTCAGTTTGATAC–3'
EMSA-RS2-4-F	5'–ggtgATATATTCATGATCTTTAATTCACTTGAAGAGTTAGTGATTGAT–3'
EMSA-RS2-4-R	5'–ggtgATCAATCACTAACTCTTCAAGTGAATTAAAGATCATGAATATAT–3'
EMSA-RS2-1m-F	5'–ggtgTGTGAGTTCTGAGGGAAAAGCCTTGGAAAGGACAGTCATGCAA–3'
EMSA-RS2-1m-R	5'–ggtgTTGCATGACTGTCCTTTCCAAGGCTTTTCCCTCAGAACTCACA–3'
EMSA-LjNIR1-2-F	5'–ggtgTCATGTACCCCCCTTCCCAAAGTAGGAAGAGGTCGTCCCTCAAC–3'
EMSA-LjNIR1-2-R	5'–ggtgGTTGAGGGACGACCTCTTCCTACTTTGGGAAGGGGGGTACATGA–3'
EMSA-LjNIR1-3-F	5'–ggtgACACAAACACGACCCTTTGTCACAACCAAAGGTCCATTGTAGCA–3'
EMSA-LjNIR1-3-R	5'–ggtgTGCTACAATGGACCTTTGGTTGTGACAAAGGGTCGTGTTTGTGT–3'
EMSA-LjNIR1-3m1-F	5'–ggtgACACAAACACGAGGGAATGTCACAACCAAAGGTCCATTGTAGCA–3'
EMSA-LjNIR1-3m1-R	5'–ggtgTGCTACAATGGACCTTTGGTTGTGACATTCCCTCGTGTTTGTGT–3'

Table 2-3. Primers used in chapter 2

Map-based cloning of *NRSYM1*			
	TM0913-F	5'–ATGAAGGTACTGCATTCCAC–3'	
	TM0913-R	5'–TTTGCCATGGTTCAATTCTG–3'	
	TM1417-F	5'–GGCTTTTGAAAGAGATCCAG–3'	
	TM1417-R	5'–GGAGGTATATTTAGTGCAGGG–3'	
	TM0366-F	5'–CAGGGGATTTTATCATGGGG–3'	
	TM0366-R	5'–CATCCGGGTCTCTGACCCTC–3'	
	TM0698-F	5'–CGCATCCATCACCTCTTTTC–3'	
	TM0698-R	5'–GTGACCTGTTCACAGTTTCG–3'	
Sequencing of *NRSYM1*			
	NRSYM1-F1	5'–TGAGTTGCCTTGAAGGTTTG–3'	
	NRSYM1-R1	5'–GGTAGTTGATGCCACAACAAGA–3'	
	NRSYM1-F2	5'–AAGTGTATCCACAGGTCGCT–3'	
	NRSYM1-R2	5'–TGAAGTTCATCCTGTGGTTA–3'	
	NRSYM1-F3	5'–GTATTTCCAGCTAGCAGAAG–3'	
	NRSYM1-F4	5'–CACATAATCATCATCTCCTG–3'	
	NRSYM1-F5	5'–GGTACACATCAAACATAAGC–3'	
Complementation of *nrsym1*			
	NRSYM1-F6	5'–CAAGTCGACCATACGCACCGCTCAGAAATCG–3'	SalI site is added
	NRSYM1-R3	5'–ACCGTCGACGGAGTGTTAGGTTGCTACCTGG–3'	SalI site is added
Cloning of *NRSYM1* cds			
	NRSYM1-F8	5'–CACCATGTCAGAATCTGATGAAGA–3'	
	NRSYM1-R5	5'–TCACTCCCCTGAGCTCTCAC–3'	
Cloning of *AtNLP6* cds			
	NLP6-F1	5'–CACCATGGAACTTGACGACTTGGA–3'	
	NLP6-R1	5'–TCACAAGCACATCATAGTTT–3'	
Cloning of *AtNLP7* cds			
	NLP7-F1	5'–CACCATGTGCGAGCCCGATGATAA–3'	
	NLP7-R1	5'–TCACAATTCTCCAGTGCTCT–3'	

Table 2-3. (continued)

NRSYM1 RT-PCR			
	NRSYM1-RT-PCR-F	5'–GCATCACTTACAACAAGGTCAAGG–3'	
	NRSYM1-RT-PCR-R	5'–TGGGTAATGTTTGGGCAGAAG–3'	
Cloning of *NRSYM1* promoter			
	NRSYM1-F7	5'–CAAGAGCTCGGAGTGTTAGGTTGCTACCTGG–3'	SacI site is added
	NRSYM1-R4	5'–CAAGGTACCTTTTCTCTCTCAGGGTGCTAAC–3'	KpnI site is added
LjUBQ RT-PCR			
	UBQ-RT-PCR-F	5'–ATGCAGATCTTCGTCAAGACCTTG–3'	
	UBQRT-PCR-R	5'–ACCTCCCCTCAGACGAAG–3'	
CLE-RS1 RT-PCR			
	RS1-RT-PCR-F	5'–TGCAAGTGTCGATGCTCATAGC–3'	
	RS1RT-PCR-R	5'–GATGTTTTGCTGAACCAAGGGATA–3'	
CLE-RS2 RT-PCR			
	RS2-RT-PCR-F	5'–GCTCGTAATCTCCAAATCATTCACA–3'	
	RS2-RT-PCR-R	5'–GGTGAGAGTCTTTGCTGTTGATATCC–3'	
LjNIA RT-PCR			
	LjNIA1-RT-PCR-F	5'–GAAGGACCCAGAGGATCACA–3'	
	LjNIA1-RT-PCR-R	5'–CGGTCTTCGTACTTCTTCGC–3'	
LjNIR1 RT-PCR			
	LjNIR1-RT-PCR-F	5'–GCAAGTGCAGGTTGCTGATA–3'	
	LjNIR1-RT-PCR-R	5'–CTTCCTATCCTCCCTCCCAG–3'	
LjNIN RT-PCR			
	LjNIN-RT-PCR-F	5'–CAATGCTCTTGATCAGGCTGTTGA–3'	
	LjNIN-RT-PCR-R	5'–GAGTGCTAATGGCAAATTGTGTGTC–3'	
Cloning of *NRSYM1* cds without a stop codon			
	NRSYM1-F8	5'–CACCATGTCAGAATCTGATGAAGA–3'	
	NRSYM1-R6	5'–CTCCCCTGAGCTCTCACATG–3'	
Cloning of *NRSYM1-myc*			
	NRSYM1-F8	5'–CACCATGTCAGAATCTGATGAAGA–3'	
	NRSYM1-R7	5'–TGAACGATCGGGGAAATTCG–3'	

Table 2-3. (continued)

CLE-RS2 ChIP-qPCR			
	ChIP-RS2-1-F	5'–CTTCATATCAATCTTGAGGCTG–3'	
	ChIP-RS2-1-R	5'–GGCTTAAGAAAACTCTTTGGC–3'	
	ChIP-RS2-2-F	5'–GCTACGAGGCAGCTGTTAGG–3'	
	ChIP-RS2-2-R	5'–TAATATTACATGAACAAGTTAGTTTATCAAGCA–3'	
	ChIP-RS2-3-F	5'–AGACCTTATCCTATCAAGCCTAATG–3'	
	ChIP-RS2-3-R	5'–CTAACGTATGTATGTGGACAAATAGG–3'	
	ChIP-RS2-4-F	5'–CACCTTGATTGGGCAGTACTTC–3'	
	ChIP-RS2-4-R	5'–GTTAGAAGGATCCGAAGTGAAAATG–3'	
LjNIR1 ChIP-qPCR			
	ChIP-LjNIR1-1-F	5'–CCCTAAAATCGGTCATAAACCC–3'	
	ChIP-LjNIR1-1-R	5'–GGTTTAGGGTTTAGGGATAGGG–3'	
	ChIP-LjNIR1-2-F	5'–TTGTGCTCTCATCCACCTCA–3'	
	ChIP-LjNIR1-2-R	5'–CGGTTTGGCTAAGGATGCTA–3'	
	ChIPLjNIR-1-3-F	5'–CCTCCATTTTGACTAACCATGTGC–3'	
	ChIP-LjNIR1-3-R	5'–GGAGTGGAACCTTCCGTGAAG–3'	
Cloning of *NRSYM1-myc* for EMSA			
	NRSYM1-F9	5'–ATTGTCGACATGGAGGAAGTGCCAAAGGATC–3'	SalI site is added
	NRSYM1-R8	5'–ATTGCGGCCGCTCACTCCCCTGAGCTCTCAC–3'	NotI site is added
	Myc-F1	5'–ATTGCGATCGCGGAACCAATTCAGTCGAGAT–3'	SgfI site is added
	NRSYM1-R9	5'–ATTGTTTAAACTCACTCCCCTGAGCTCTCAC–3'	PmeI site is added
GUS RT-PCR			
	GUS-RT-PCR-F	5'–TAACGATCAGTTCGCCGATG–3'	
	GUS-RT-PCR-R	5'–TTTGCCGTAATGAGTGACCG–3'	
GFP RT-PCR			
	GFP-RT-PCR-F	5'–TATATCATGGCCGACAAGCA–3'	
	GFP-RT-PCR-R	5'–TGTTCTGCTGGTAGTGGTCG–3'	

Table 2-3. (continued)

Cloning of *LjNIR1* promoter			
	LjNIR1-F1	5'–ATTGAGCTCGCCACATATGCGATGACTGG–3'	SacI site is added
	LjNIR1-R1	5'–ATTCCCGGGGGTGAGGTGAGGGAGTGTGG–3'	SmaI site is added
	LjNIR1-F2	5'–ATTGGTACCATTGTAGCAACAAAGAACCTC–3'	KpnI site is added
	LjNIR1-R2	5'–ATTGGTACCTGTTTGTGTTTGATTCAACTGG–3'	KpnI site is added
sgRNA of CLE-RS1			
	RS1-F1	5'–ATTGTGCTGAGGATCAGGTCCTCC–3'	
	RS1-R1	5'–AAACGGAGGACCTGATCCTCAGCA–3'	
sgRNA of CLE-RS2			
	RS2-F1	5'–ATTGTGTTGAGGATCTGGTCCTCC–3'	
	RS2-R1	5'–AAACGGAGGACCAGATCCTCAACA–3'	
Complementation of *cle-rs1*			
	RS1-F2	5'–ATTGGTACCGTCTTCCTAGAAGTGGGCTAGG–3'	KpnI site is added
	RS1-R2	5'–ATTGGATCCTGACATTAGGGCGTCGCAGTAG–3'	BamHI site is added
Sequencing of *CLE-RS1*			
	RS1-RT-PCR-F	5'–TGCAAGTGTCGATGCTCATAGC–3'	
	RS1-R3	5'–AAAGAGGAGTGCAGACGGAA–3'	
Sequencing of *CLE-RS2*			
	RS2-F2	5'–GCAGGCTCGTAATCTCCAAA–3'	
	RS2-R2	5'–GGCTCTTCATTGCTTTCCAG–3'	
Sequencing of *LjCLE49*			
	CLE49-F1	5'–CCTCTGAACCCAACAGTGGT–3'	
	CLE49-R1	5'–CCCACCATGCTGTGATTTTA–3'	
Sequencing of *CLE-RS3*			
	RS3-F1	5'–GGGGTTCCACCTTATGGAGT–3'	
	RS3-R1	5'–TCACACCGCAGAGAAGAGAA–3'	

Chapter 3

Expression of the *CLE-RS3* gene suppresses root nodulation in *Lotus japonicus*

3.1 Introduction

In plants, cell-to-cell communication has important roles not only for development but also for responses to environmental stimuli. There are diverse kinds of mobile signals that may include phytohormones, small RNAs, transcription factors, or small peptides. Among these signaling molecules, recent genetic and biochemical studies have focused on the roles of small peptides (Djordjevic et al., 2015; Endo et al., 2014). The CLE family is one of the best characterized small peptide family in plants, and in most cases LRR- RLKs function as the receptors that transmit signals to the downstream pathway (Cock and McCormick, 2001; Miyawaki et al., 2013). In plant development, the currently available data indicate that a significant feature of the signal transduction events mediated by CLE-LRR-RLK modules are associated with controlling the balance between cell proliferation and differentiation in stem cells. First, Arabidopsis *CLV3* is expressed in the stem cell region located at the tip of the shoot apical meristem (SAM). AtCLV3 non-cell autonomously represses the expression of *WUSCHEL* (*WUS*), which encodes a WUS-related homeobox (WOX) transcription factor (Brand et al., 2000; Fletcher et al., 1999; Haecker et al., 2004; Mayer et al., 1998; Schoof et al., 2000). AtCLV3 physically interacts with an LRR-RLK, AtCLV1, that is located in cells beneath the stem cell region that overlaps with *WUS*-expressing cells (Clark et al., 1997; Ogawa et al., 2008). WUS also acts as a mobile signal and can move to the stem cell region, thereby directly activating *AtCLV3* expression (Daum et al., 2014; Yadav et al., 2011). The CLV-WUS negative feedback loop is crucial for the maintenance of stem cell homeostasis in the SAM. Second, in the Arabidopsis root apical meristem (RAM), *AtCLE40* is expressed in differentiated columella cells, and the encoded peptide is transferred to the columella stem cell region, where it controls stem cell fate (Stahl et al., 2009). Genetic data suggest that ARABIDOPSIS CRINKLY 4 (ACR4), which is not an LRR-RLK but another type of RLK, is required for AtCLE40 action. In addition, AtCLV1 is expressed in the RAM and physically interacts with ACR4 (Stahl et al., 2013). The CLE40/ACR4-CLV1 signaling pathway appears to be involved in the down-regulation of *AtWOX5*, a key regulator of quiescent center specification. Finally, in Arabidopsis vascular stem cells, proliferation is controlled by an interaction between a AtCLE peptide, TRACHEARY ELEMENT DIFFERENTIATION INHIBITORY FACTOR (TDIF), and an LRR-RLK, TDIF RECEPTOR (TDR)/PHLOEM INTERCALATED WITH XYLEM (PXY) (Fisher and Turner, 2007; Hirakawa et al., 2008; Ito

et al., 2006). AtWOX4 is identified as a key target of the TDIF–TDR/PXY signaling pathway (Hirakawa et al., 2010).

The signaling pathways mediated by the above-mentioned CLE peptides can be characterized as types of short-range cell-to-cell communication, in which the peptides move within a local region such as between adjacent cells or in the most distant cases across several cell layers. In contrast, long-distance action of Arabidopsis *CLE6* has been shown; the root-specific expression of *AtCLE6* rescues the shoot phenotype caused by gibberellin deficiency (Bidadi et al., 2014). Recently, the production of several small peptides that belong to the C-terminally encoded peptide (AtCEP) family were reported to be induced in the root in response to nitrogen deficiency (Tabata et al., 2014). Subsequently, these AtCEP family peptides are translocated to the shoot and recognized by two LRR-LRKs (Tabata et al., 2014). In addition, using soybean xylem sap, several small peptides were identified as long-distance mobile signals that belong to the CLE and CEP families (Okamoto et al., 2015). Although the emerging roles for CLE peptides indicate their use as long-distance mobile signals and other key peptides have been identified, there is little known of the molecular function of long-distance signals in comparison with short-range signals.

AON is a conserved mechanism observed among diverse leguminous species by which plants restrict the number of root nodules, the symbiotic organs containing nitrogen-fixing rhizobia, to conserve energy related to nodulation (Caetano-Anolles and Gresshoff, 1991; Oka-Kira and Kawaguchi, 2006; Suzaki et al., 2015). The basic concept of AON is as follows. Rhizobial infection not only initiates a signaling pathway resulting in nodule formation but also induces the production of mobile negative factors for nodulation called root-derived signals that are translocated to the shoot through the xylem. When the signal is perceived in the shoot, the second signals, referred to as SDIs, are generated. The SDIs are then transferred to the root through the phloem and block further nodule development. Among the 39 *LjCLE* genes identified from *L. japonicus*, the expression of 2 *LjCLE* genes, *CLE-RS1* and *CLE-RS2*, is induced immediately in response to rhizobial inoculation after direct activation by an RWP-RK type transcription factor LjNIN (Okamoto et al., 2009; Schauser et al., 1999; Soyano et al., 2014). In addition, in *M, truncatula*, exogenous application of cytokinin to roots induces the expression of *MtCLE13*, a functional counterpart of the *CLE-RS1*/*2* genes (Mortier et al., 2010; Mortier et al., 2012), suggesting that activation of the nodulation-related *CLE* genes occur at the downstream part of cytokinin signaling in roots, of which finding was recently confirmed in *L. japonicus* (Soyano et al., 2014). There is direct evidence that CLE-RS2 meets at least one criterion for a

root-derived signal because mature CLE glycopeptides derived from the CLE domain of CLE-RS2 are detected in xylem sap of plants that express *CLE-RS2* (Okamoto et al., 2013). The mature CLE-RS2 peptide can physically interact with HAR1, an LRR-RLK that is orthologous to AtCLV1 (Krusell et al., 2002; Nishimura et al., 2002; Okamoto et al., 2013). The constitutive expression of either *CLE-RS1* or *CLE-RS2* almost completely abolishes nodulation, and functional *HAR1* is required for CLE-RS1/2 action (Okamoto et al., 2009). Moreover, a loss-of function mutation in the *HAR*1 gene significantly increases nodule numbers, and reciprocal grafting experiments between roots and shoots indicate that shoot-acting *HAR1* is involved in the control of nodule number (Krusell et al., 2002; Nishimura et al., 2002; Wopereis et al., 2000). Hence, the CLE-RS1/2–HAR1 module is hypothesized to play a pivotal role in the negative regulation of nodulation in AON. KLV, another shoot-acting LRR-RLK, seems to be involved in CLE-RS1/2-mediated negative regulation of nodulation (Miyazawa et al., 2010; Oka-Kira et al., 2005). Recently cytokinin production was reported to be induced in the shoot by the downstream part of the CLE-RS1/2–HAR1 signaling pathway (Sasaki et al., 2014). In addition, shoot-applied cytokinin is able to move to roots and inhibit nodulation. These results suggest that shoot-derived cytokinin is an SDI candidate. There may be a proteasome-mediated degradation process for an unidentified protein in the most downstream part of AON in roots because the negative effect of shoot-applied cytokinin is masked by a mutation in the F-box protein TML (Magori et al., 2009; Sasaki et al., 2014; Takahara et al., 2013). In soybean, microRNA (miR) 172c appears to control nodule number by repressing its target gene, *NODULE NUMBER CONTROL 1* encoding an AP2-type transcription factor, and a mutation in the *NARK* gene, which encodes an LRR-RLK that is orthologous to HAR1, increases the expression level of *miR172c* in roots (Searle et al., 2003; Wang et al., 2014). These results suggest that in soybean SDIs play a role in the miRNA-mediated transcriptional control of genes involved in the regulation of nodulation. Although our knowledge of AON has been furthered, identification of additional components of AON will be undoubtedly essential for a deeper understanding of the mechanism.

In this study, five new *CLE* genes were identified from the *L. japonicus* genome by an *in silico* search. Expression analyses of the *LjCLE* genes suggested that it is likely that two of them are involved in nodulation. In addition, it was revealed that nodulation-related *CLE* genes had diverse expression patterns. Constitutive expression of *CLE-RS3* in the root significantly suppressed nodulation possibly through long-distance communication between roots and shoots. Functional *HAR1* was required for *CLE-RS3* action. These results place CLE-RS3 as the third CLE peptide involved in AON in *L. japonicus*.

3.2 Results

Identification of five new *CLE* genes in *L. japonicus*

A previous *in silico* search of the *L. japonicus* genome sequence database for genes containing a CLE domain resulted in the identification of 39 *LjCLE* genes (Okamoto et al., 2009). The ratio of the coverage of the gene space in the database, however, was estimated at 91.3 % (Sato et al., 2008). Hence, it was possible that this search was insufficient to fully cover the *L. japonicus CLE* genes. In this new study, I used another database (http://mycorrhiza.nibb.ac.jp) that has a reference sequence data set containing the *L. japonicus* genome assembly Lj2.5 and the unique de novo assembled contigs derived from *L. japonicus* (Handa et al., 2015). A BLAST search using the amino acid sequence of a CLE domain from CLE-RS1 as a query found five new small proteins that show some similarity with CLE-RS1. The five genes encode small proteins with a conserved CLE domain at their C-termini; thus, they were named CLE-RS3, LjCLE39, LjCLE40, LjCLE41 and LjCLE42 (Fig. 3-1; Tables 3-1,2). For reasons described below, one of the genes was named CLE-RS3 because it is more likely to be involved in nodulation (see below). Of note, three *CLE* genes, *CLE-RS2*, *CLE-RS3* and *LjCLE40*, are located in tandem within the limits of about 33-kb on chromosome 3 (Fig. 3-2; Table 3-1).

Expression of *CLE-RS3* and *LjCLE40* is induced during nodulation

I first monitored the expression patterns of the *LjCLE* genes identified above in some vegetative and reproductive organs. *CLE-RS3* and *LjCLE40* were expressed most specifically in roots, whereas the expression of *LjCLE39*, *LjCLE41* and *LjCLE42* were widely observed in the organs examined (Fig. 3-3). The strong expressions of *CLE-RS3* and *LjCLE40* are similar to those of *CLE-RS1* and *CLE-RS2*, which were expressed specifically in inoculated roots (Fig. 3-3). To gain insights into the role of the *CLE* genes during root nodule symbiosis, I examined their time-course expression patterns after inoculation of rhizobia. The known expression pattern of *LjNIN*, which is strongly induced in response to rhizobia (Schauser et al., 1999), served as a reference standard for the cDNA prepared for this real-time RT-PCR analysis (Fig. 3-4h). I found that the induction of *CLE-RS3* was detectable at 3 dai (Fig. 3-4a). Subsequently, the expression continued increasing until 14 dai. I also found upregulation of *LjCLE40* at 7 dai with expression becoming stronger as a function of time after inoculation (Fig. 3-4b). In contrast, the expression of the other *LjCLE* genes, *LjCLE39*, *LjCLE41*, and *LjCLE42*, was largely unaffected by rhizobial inoculation (Fig. 3-4e-g). Although it is known that the *CLE-RS1* and *CLE-RS2* genes are rapidly upregulated by rhizobial inoculation (Okamoto et al., 2009), their expression patterns at later nodulation stages

were unknown. Therefore, I determined the expression patterns of *CLE-RS1*/*2* along a longer time course; expression levels were highest at 3 or 5 dai and then gradually decreased with time after inoculation (Fig. 3-4c,d). Previous studies have shown that *LjCLE3* and *LjCLE16* expression is upregulated in nodulated roots, although their detailed expression patterns remain unknown (Okamoto et al., 2009; Handa et al., 2015). In summary, *L. japonicus* has at least 6 *LjCLE* genes, *CLE-RS1*/*2*/*3*, *LjCLE3*, *LjCLE16* and *LjCLE40*, whose expression patterns are differentially regulated during nodulation. The spatial expression patterns of *CLE-RS3* and *LjCLE40* were next determined using transgenic hairy roots that were transformed with either the *ProCLE-RS3::GUS* or *ProLjCLE40::GUS* constructs, in which a 3.0- or 1.1-kb fragment of the promoter region of the respective gene was inserted upstream of the *GUS* reporter gene. The *M. loti* strain, which constitutively expresses *DsRED*, was used to visualize rhizobia enabling me to find infection foci. In *ProCLE-RS3::GUS* roots, GUS activity was observable at the site of presumptive incipient nodule primordia beneath root hairs with infection threads, where the bulges of nodule primordia were not yet visible (Fig. 3-5a). In contrast, at the corresponding site in *ProLjCLE40::GUS* roots, GUS activity was undetectable (Fig. 3-5d). After the formation of nodule primordial bulges into which rhizobia start to colonize, GUS activity in both *ProCLE-RS3::GUS* and *ProLjCLE40::GUS* roots was observed within nodule primordia (Fig. 3-5b,c,e,f). These results suggest that *CLE-RS3* and *LjCLE40* are primarily expressed along the nodulation cell lineage, but the timing of expression seems to be different between the two genes. The relatively delayed induction of *LjCLE40* expression in comparison with *CLE-RS3* as determined by GUS activity in hairy roots agrees with the results of real-time RT-PCR (see above).

Constitutive expression of *CLE-RS3* suppresses nodulation

On the basis of the relatively earlier induction of *CLE-RS3* expression compared with *LjCLE40*, *CLE-RS3* may have a role during an earlier nodulation stage. Because the negative regulation of nodulation mediated by AON is known to occur during the early nodulation stages (Suzuki et al., 2008), I hereafter examined the potential involvement of *CLE-RS3* in AON. The effect of constitutive expression of *CLE-RS3* on nodulation was examined using transgenic hairy roots transformed with the *35S::CLE-RS3* construct. Nodule number was significantly reduced by the constitutive expression of *CLE-RS3* (Fig. 3-6a-e). Since these inhibitory effects on nodulation were observed not only in transformed but also in untransformed roots (Fig. 3-6a, b), it is likely that *CLE-RS3* expression has a systemic effect possibly through long-distance communication between roots and shoots. To confirm these effects, stable *L. japonicus* transgenic plants in which

CLE-RS3 was constitutively expressed were generated. (Fig. 3-7). The phenotype of reduced nodule number was observed in two independent transgenic plants that constitutively expressed *CLE-RS3* (Fig. 3-8). This result concluded that CLE-RS3 acts as a negative factor in nodulation.

As previously shown, constitutive expression of either *CLE-RS1* or *CLE-RS2* attenuates nodulation (Miyazawa et al., 2010; Okamoto et al., 2009; Sasaki et al., 2014; Suzaki et al., 2012; Takahara et al., 2013). In my experimental conditions, the effect of constitutive expression of *CLE-RS3* was significantly weaker in comparison with those of *CLE-RS1* or *CLE-RS2*. Nodule development was almost completely compromised in plants that constitutively expressed the *CLE-RS1* or *CLE-RS2* genes, whereas a few nodules were formed in plants that expressed *CLE-RS3* (Fig. 3-6a-g). The negative CLE-RS1/2 effect on nodulation is required for shoot-acting *HAR1* and root-acting *TML*, which, respectively, encode an LRR-RLK that acts as a putative receptor for the CLE peptides and a putative F-box protein. Thus, the CLE-RS1/2-mediated suppression of nodulation activity was masked in the *har1* or *tml* mutants (Okamoto et al., 2009). In order to elucidate the *HAR1*- or *TML*-dependency of CLE-RS3 action, I next constitutively expressed *CLE-RS3* in the corresponding mutants. The hypernodulating phenotype of the *har1* and *tml* plants was unaffected by the constitutive expression of *CLE-RS3* (Fig. 3-6h-l), suggesting that HAR1 and TML is required for the suppression of nodulation mediated by CLE-RS3.

***CLE-RS3* and *LjCLE40* expression is responsive to nitrate**

Nodulation is known to be inhibited in the presence of high nitrate concentrations, and some data suggest that the nitrate-mediated inhibition of nodulation share a partly conserved mechanism with AON; the mutants involved in AON are partially tolerant to high nitrate (Magori et al., 2009). Furthermore, the expression of *CLE-RS2* is induced by exogenous application of nitrate (Okamoto et al., 2009). In addition to the known induction of *CLE-RS2*, the expression of *CLE-RS3* and *LjCLE40* was induced 24 h after nitrate application (Fig. 3-9a). On the other hand, the expression of *LjCLE39*, *LjCLE41*, and *LjCLE42* genes was unaffected by nitrate (Fig. 3-9a). Given that the *CLE-RS2*, *CLE-RS3* and *LjCLE40* loci are located in tandem (Table 3-1) and the three genes are induced both by rhizobial infection and nitrate (Figs. 3-4a,b,d, 9a), it is possible that the genes may have duplicated from a common gene.

Cytokinin is another known factor involved in the activation of nodulation-related *CLE* genes (Mortier et al., 2012; Soyano et al., 2014). *CLE-RS1* and *CLE-RS2* expressions are activated in response to exogenous cytokinin treatment as previously shown (Fig. 3-9b; Soyano

et al., 2014). In contrast, the expression of other five *LjCLE* genes was unaffected by cytokinin (Fig. 3-9b).

3.3 Discussion

Prior to this investigation, only two nodulation-related *LjCLE* genes in *L.japonicus*, *CLE-RS1* and *CLE-RS2*, were well characterized. Additionally, *LjCLE3* and *LjCLE16* may have roles related to nodulation because their expression is upregulated in nodulated roots (Handa et al., 2015; Okamoto et al., 2009). A previous split-root experiment using *L. japonicus* indicates that the negative effect on nodulation by AON starts to be observed at 3 dai, and full inhibition of nodulation is accomplished at 5 dai (Suzuki et al., 2008). This observation implies that production of root-derived signals should occur at a much earlier timing than 3 dai. Following the initiation of *LjNIN* expression at 3 h after inoculation, the expression of *CLE-RS1*/*2*, direct targets of LjNIN, is detected at the latest at 6 h after inoculation (Okamoto et al., 2009; Soyano et al., 2014). These immediate responses of *CLE-RS1*/*2* by rhizobial inoculation correspond to the expected behavior for root-derived signals. Here, another *L. japonicus* nodulation-related *CLE* gene was newly identified, designated as *CLE-RS3*, of which expression is induced by rhizobial inoculation and constitutive expression of the gene results in a reduction in nodule number. In my experimental conditions, the activation of *CLE-RS3* expression starts to be detected at 3 dai, although the level is much less than the expression of *CLE-RS1*/*2*. *CLE-RS3* expression continues to increase with time after inoculation. In contrast, after 5 dai, when nodulation seems fully inhibited, *CLE-RS1*/*2* expression levels gradually decrease as the nodulation process proceeds. The seemingly transient, high expression of *CLE-RS1*/*2* before 5 dai suggests that upregulation of the genes play a major role in the AON in order to establish immediate control of nodulation in response to rhizobial infection. On the other hand, we never observed an exponential increase in the number of nodules, even if the plants were grown for an extremely long time. Therefore, I hypothesize that there is a mechanism enabling long-term control of nodule numbers. One possibility is that in the downstream part of the CLE-RS1/2–HAR1 signaling module, there may be a mechanism to memorize the activation of the signal transduction to continuously produce SDI. Alternatively, other LjCLE peptides can be replaced with CLE-RS1/2 at a later stage to predominantly interact with HAR1, resulting in the production of SDI. The prolonged, higher expression of *CLE-RS3* may account for the latter case. I, however, cannot rule out the possibility that the *CLE-RS3* expression at the later stages may be related to different aspects of root nodule symbiosis other than AON, such as nitrogen fixation and utilization processes. If the *CLE* gene has a role

related to innate nitrogen control, it is notable that its expression is induced by nitrate application. The expression of *LjCLE40*, another newly identified, was not detected in infection foci and started to be specifically expressed after the formation of nodule primordia bulges, suggesting that it has a role during nodulation. Nevertheless, I currently cannot reach the convincing conclusion regarding the effect of *LjCLE40* overexpression on nodulation due to the probable instability of *LjCLE40* overexpression. *LjCLE40* expression responds to nitrate application as well. The nitrate responsiveness of some nodulation-related *CLE* genes is thought to be conserved in leguminous plants because in soybean the expression of the *NITRATE-INDUCED CLE 1* gene also responds to nitrate (Reid et al., 2011). Further functional analyses focusing on the role of CLE-RS3 and LjCLE40 at the later nodulation stages may provide new insights into the role of CLE peptides in the control of root nodule symbiosis. Although rhizobial infection or nitrate treatment commonly activates the *CLE-RS2*, *CLE-RS3,* and *LjCLE40* expression, cytokinin treatment can induce only *CLE-RS2* expression. Thus, there may be both common and context-dependent mechanisms with respect to the activation of these genes.

Like *CLE-RS1*/*2*, constitutive expression of *CLE-RS3* suppresses nodulation. On the other hand, the effect of *p35::CLE-RS3* on nodulation is weaker than those of *p35::CLE-RS1* or *p35::CLE-RS2*. It is unlikely that different expression levels of the respective genes are attributable to the differences in response because the same promoter was used in this assay. Generally, *CLE* genes encode a small protein with a conserved CLE domain at the C-terminus. In the case of CLE-RS2, the 12 amino acid peptide derived from the CLE domain can function similarly to the mature active form. In soybean, RHIZOBIA-INDUCED CLE 1 (RIC1), which has a CLE domain that is considerably conserved with those of CLE-RS1/2, has a negative effect on nodulation (Reid et al., 2011). A site-directed mutagenesis study of the CLE domain of RIC1 showed that the Arg1, Ala3, Pro4, Gly6, Pro7, Asp8, His11, and Asn12 residues are critical for its nodulation suppression activity (Reid et al., 2013). Alignment of CLE domain sequences of CLE-RS1, CLE-RS2, CLE-RS3 and RIC1 showed that the Arg1 residue is not conserved in CLE-RS3, whereas the other potentially important amino acid residues are mostly conserved among the CLE peptides (Fig. 3-1). The small difference in the CLE domain may determine the relatively weaker suppression activity of CLE-RS3. Root-specific constitutive expression of *CLE-RS3* suppressed nodulation of both transformed and untransformed roots. The result indirectly suggests that CLE-RS3 can act as a long-distance signal between roots and shoots, of which conclusion needs to be confirmed by more rigid assay such as split-root experiments. The suppression effects were masked in the *har1* mutants; therefore, HAR1 may be required for CLE-

RS3 action. CLE-RS1 and -RS2 also have negative effects on nodulation in a HAR1-dependent manner (Okamoto et al., 2009). Currently, there is direct evidence that CLE-RS2 physically interacts with HAR1 (Okamoto et al., 2013). On the basis that the CLE domain of CLE-RS1 is completely identical to that of CLE-RS2 (Fig. 3-1), it seems reasonable to propose that HAR1 can also recognize CLE-RS1. Although 3 of 12 residues in the CLE domain of CLE-RS3 are different from those of CLE-RS1/2 (Fig. 3-1), is it possible for CLE-RS3 to interact with HAR1? In Arabidopsis, AtCLV1 can bind to AtCLE2 or AtCLE9, both of which belong to phylogenetically different clades from AtCLV3 (Ogawa et al., 2008). AtCLV1 was recently shown to be required for AtCLE3-mediated control of root architecture in response to nitrogen-deficiency (Araya et al., 2014). The genetic data suggest that AtCLE3, which also belongs to a phylogenetically different clade than AtCLV3, can be recognized by AtCLV1. In addition, the expression of rice *FLORAL ORGAN NUMBER 2* (*FON2*), which encodes a CLE protein, can rescue the *Atclv3* mutant phenotype, although 3 of 12 residues of the FON2 CLE domain are different from those of AtCLV3 (Suzaki et al., 2006). These observations suggest that, in addition to AtCLV3, AtCLV1 can recognize other CLE peptides with some affinity within a permissible range. It is therefore possible that CLE-RS3 acts as a negative regulator of nodulation through interaction with HAR1.

With respect to the genetic relationship between *CLE-RS3* and known components of AON, in addition to HAR1, TML may be required for the CLE-RS3 action, because the *tml* mutation suppresses the effect of *CLE-RS3* overexpression. Given that *klv* nodulation phenotype is almost identical to *har1* and KLV can physically interact with HAR1 (Miyazawa et al., 2010), I can presume that KLV can be required for the CLE-RS3 action.

3.4 Methods

Plant materials and growth conditions

The Miyakojima MG-20 ecotype of *L. japonicus* (Kawaguchi, 2000) was used as the WT plant in this study. A description of *har1-7* and *tml-4* plants was published previously (Takahara et al., 2013). Plants were grown with or without Mesorhizobium loti MAFF 303099 as previously described (Suzaki et al., 2013).

Identification of new *CLE* genes in *L. japonicus*

Five new *LjCLE* genes were identified using the deduced amino acid sequence of a CLE domain from CLE-RS1 as a query for a BLAST search of a database (http://mycorrhiza.nibb.ac.jp) that

contains the reference sequence data set for the *L. japonicus* genome assembly Lj2.5 and the unique de novo assembled contigs derived from *L. japonicu*s (Handa et al., 2015). The cDNA sequences of the genes were determined by rapid amplification of cDNA ends (RACE) methods using a SMARTer RACE cDNA Amplification Kit (Clontech) according to the manufacturer's protocol. The putative signal sequence cleavage sites were predicted by SignalP 3.0 (http://www.cbs.dtu.dk/services/SignalP-3.0/).

Expression analyses

The method was the same as in Chapter 2 (2.4 Methods). The primers used for PCR are listed in Table 3-3.

Constructs and hairy root transformation of *L.japonicus*

The primers used for PCR are listed in Table 3-3. The 3.0- or 1.1-kb fragments of the promoter region of *CLE-RS3* or *LjCLE40* were, respectively, amplified by PCR from WT genomic DNA, and inserted between the *Sac*I and *Sma*I sites of pCAMBIA1300-GUS-GFP-LjLTI6b that are located upstream of the *GUS* gene. The coding sequence of *CLE-RS3* was amplified by PCR from template cDNA prepared from WT *L. japonicus* and cloned into the pENTR/D-TOPO vector (Invitrogen). The insert was transferred into pH7WG2D,1 (Karimi et al., 2002) by the LR recombination reaction to make the *p35S::CLE-RS3* construct. The plasmids used for the constitutive expression of *CLE-RS1*, *CLE-RS2* or *GUS* were previously described (Okamoto et al., 2009). The resulting constructs were introduced into *L. japonicus* plants by *Agrobacterium rhizogenes*-mediated hairy root transformation as in Chapter 2 (2.4 Methods).

Stable transformation of *L. japonicus*

The *p35S::CLE-RS3* described above or *p35S::GUS* (Okamoto et al., 2009) plasmids were introduced into *L. japonicus* plants by *A. tumefaciens*-mediated transformation as in Chapter 2 (2.4 Methods). Transformed plants were identified by amplifying the *HPT* gene. The primers used for PCR are listed in Table 3-3.

Accession numbers

Sequence data from this article can be found in the Gen-Bank/EMBL data libraries under the following accession numbers: CLE-RS1, AP010912; CLE-RS2, AP010911; CLE-RS3,

LC120808; LjCLE39, LC120809; LjCLE40, LC120810; LjCLE41, LC120811; LjCLE42, LC120812.

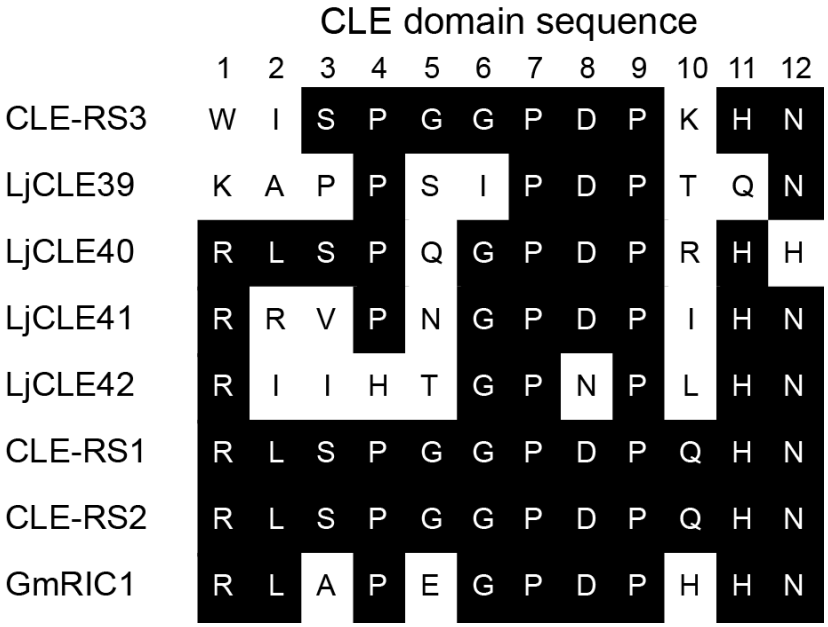

Figure 3-1. Amino acid alignment of the CLE domains of related proteins.

Amino acid alignment of the CLE domains of CLE-RS3, LjCLE39, LjCLE40, LjCLE41, LjCLE42, CLE-RS1, CLE-RS2, and GmRIC1. Conserved amino acid residues are highlighted.

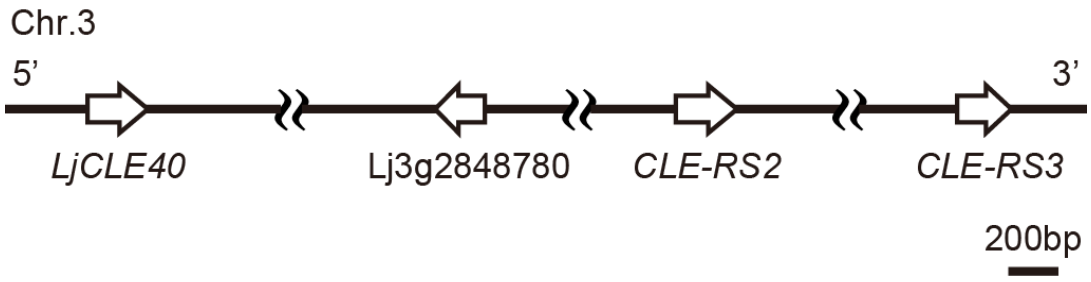

Figure 3-2. Schematic structure of the genomic region harboring *CLE-RS2*, *CLE-RS3* and *LjCLE40*.

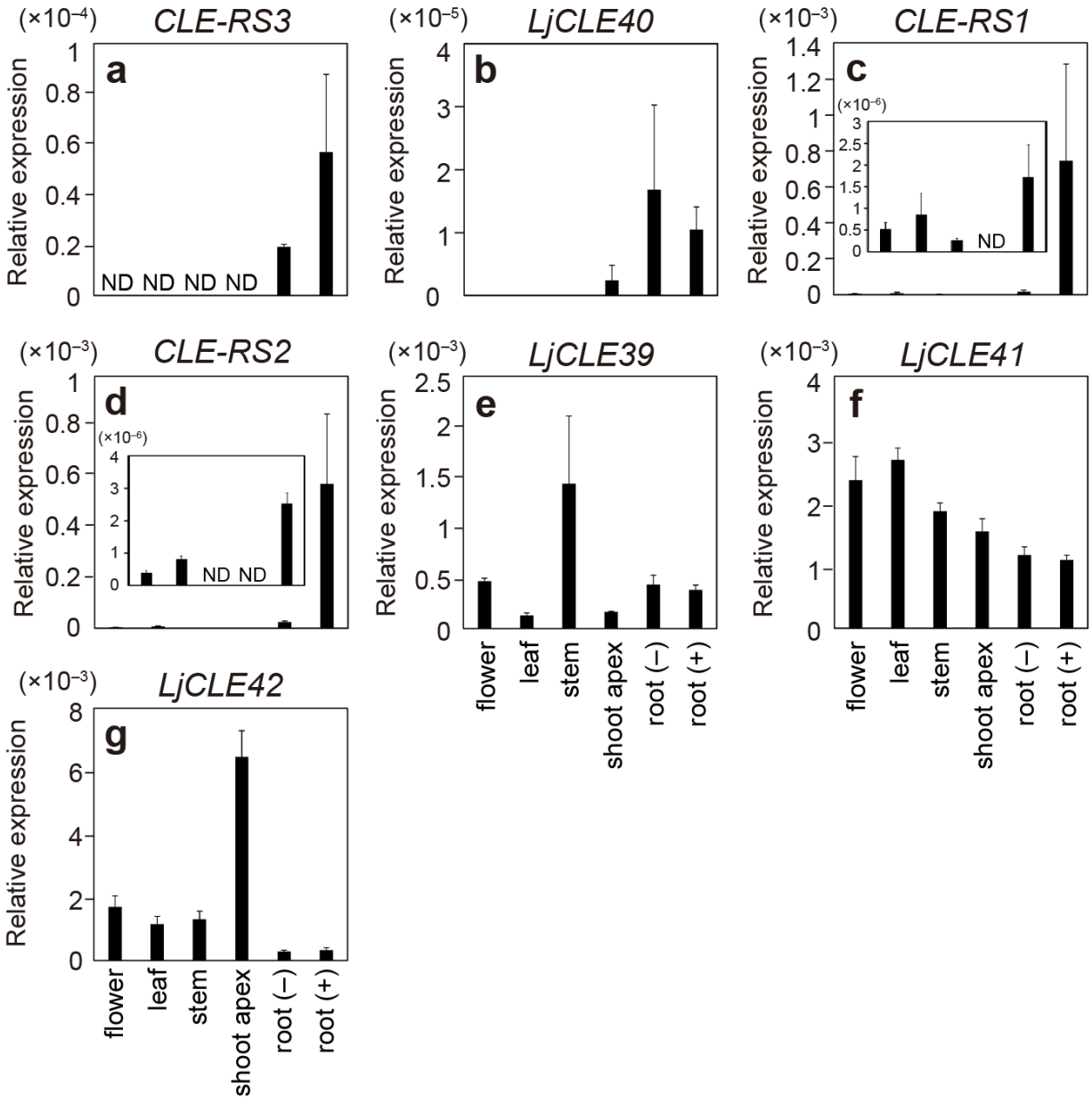

Figure 3-3. The *CLE* genes expression pattern.

Real-time RT-PCR analysis of (a) *CLE-RS3*, (b) *LjCLE40*, (c) *CLE-RS1*, (d) *CLE-RS2*, (e) *LjCLE39*, (f) *LjCLE41* and (g) *LjCLE42* expression in WT. Each cDNA sample was prepared from total RNA derived from the flower, leaf, stem, shoot apex, non-inoculated (–) and 1 dai (+) roots. The expression patterns of *CLE-RS1* and *CLE-RS2* in the organs other than inoculated roots are shown as inset (c, d). *LjUBQ* was used to assess the relative expression of each gene. Error bars indicate SE (n = 3 independent pools of respective organs).

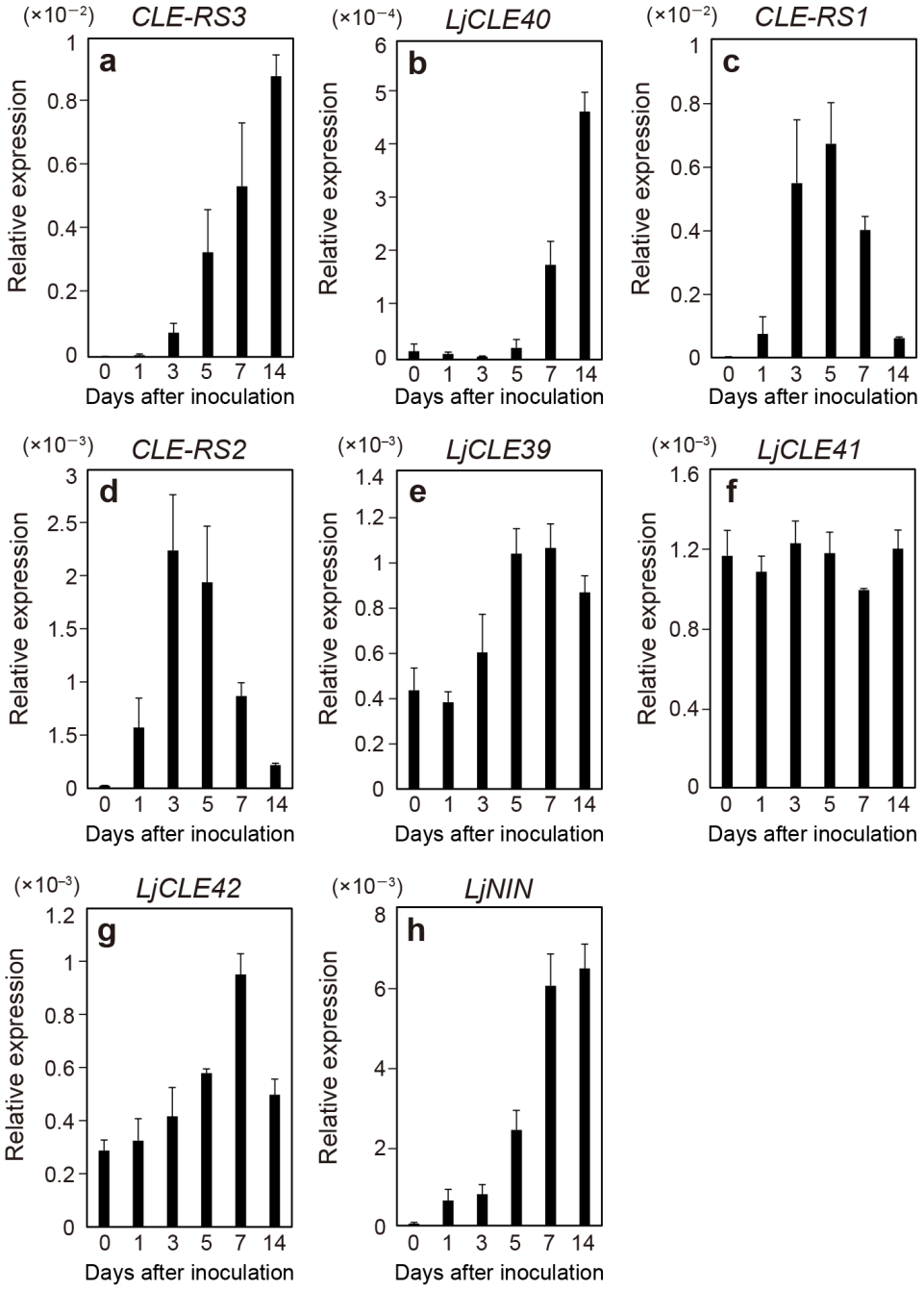

Figure 3-4. Time-course expression patterns of *CLE* genes and *LjNIN* gene after inoculation. Real-time RT-PCR analysis of (a) *CLE-RS3*, (b) *LjCLE40*, (c) *CLE-RS1*, (d) *CLE-RS2*, (e) *LjCLE39*, (f) *LjCLE41*, (g) *LjCLE42*, and (h) *LjNIN* expression in WT non-inoculated roots (0) and 1, 3, 5, 7 and 14 dai. Each cDNA sample was prepared from total RNA derived from the entire root. *LjUBQ* was used to assess the relative expression of each gene. Error bars indicate SE (n = 3–4 independent pools of roots).

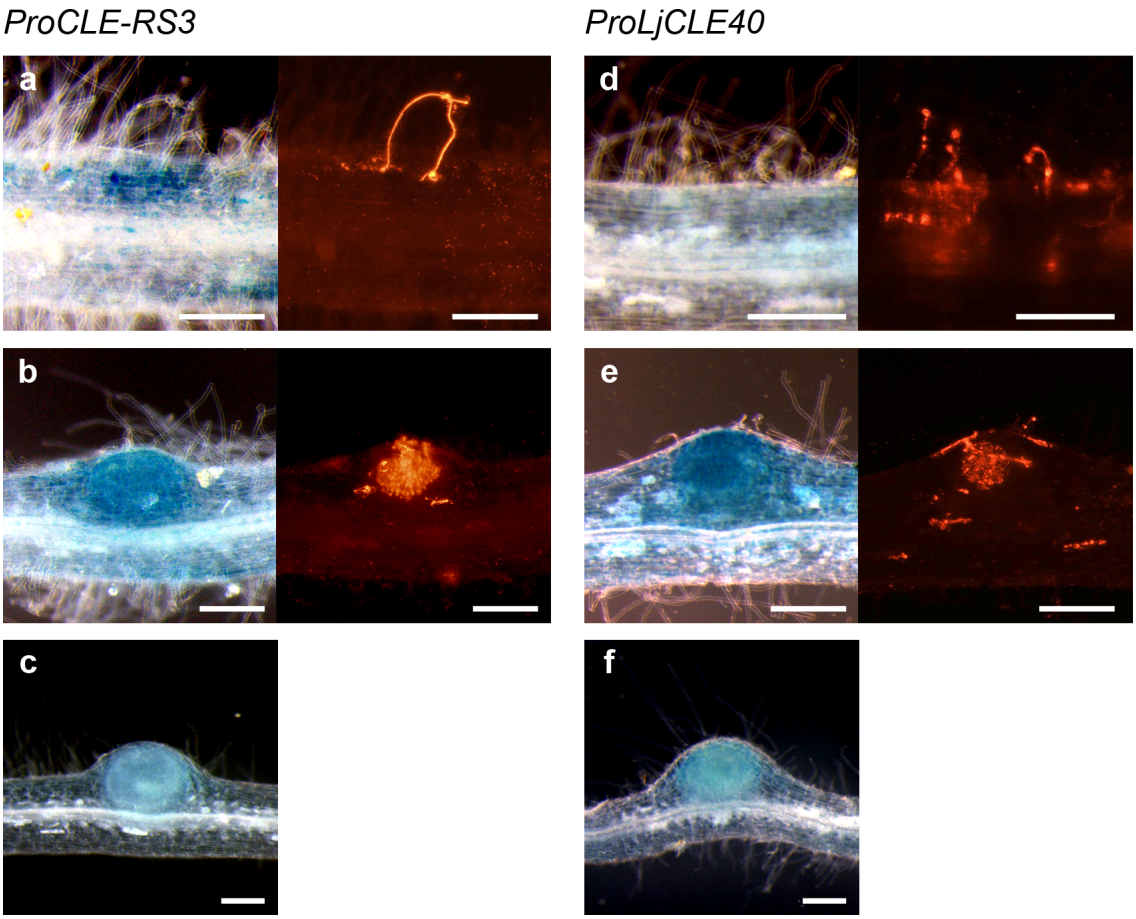

Figure 3-5. Spatial expression patterns of the *CLE-RS3* and *LjCLE40* genes.

Blue staining indicates GUS activity under the control of the (a-c) *CLE-RS3* and (d-f) *LjCLE40* promoters at the site of presumptive incipient nodule primordia (a, d) and nodule primordia (b, c, e, f) of WT plants. GUS activity was observed at 7 dai (a, b, d, e) or 10 dai (c, f). The *M. loti* strain that constitutively expresses *DsRED* was used for these experiments. *DsRED* fluorescence shown on the right panels represents infection foci. Scale bars: 200 μm.

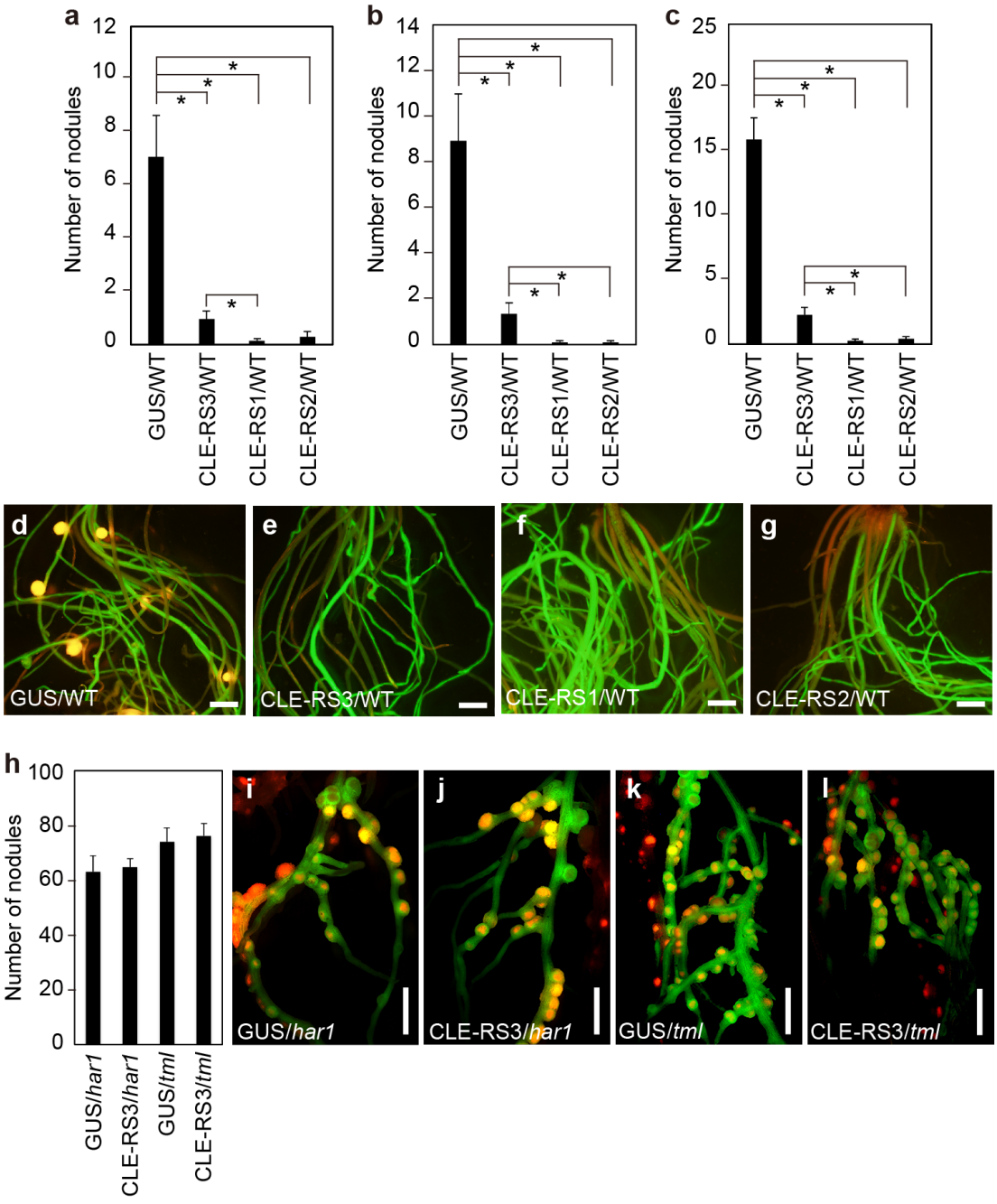

Figure 3-6. Effect of constitutive expression of *CLE-RS3*, *CLE-RS1*, *CLE-RS2* on nodulation.

For figure legend, see next page.

Figure 3-6. Effect of constitutive expression of *CLE-RS3*, *CLE-RS1*, *CLE-RS2* on nodulation. (a-c) The number of nodules formed on (a) transformed, (b) untransformed and (c) total roots of the WT plants that have transgenic hairy roots constitutively expressing the respective genes (n = 14–20 plants). The nodulation phenotype of the plants that have transgenic hairy roots constitutively expressing (d) *GUS*, (e) *CLE-RS3*, (f) *CLE-RS1* and (g) *CLE-RS2*. (h) The number of nodules formed on all the roots of the *har1-7* and *tml-4* plants that have transgenic hairy roots constitutively expressing the *GUS* or *CLE-RS3* genes (n = 11–20 plants). The nodulation phenotype of the plants that have transgenic hairy roots constitutively expressing (i,k) *GUS* or (j,l) *CLE-RS3* in the respective mutants. Transgenic roots were identified by GFP fluorescence. The nodulation phenotype was observed at 21 dai. The *M. loti* strain that constitutively expresses *DsRED* was used in these experiments. Error bars indicate SE. Scale bars: 2 mm. **P* = 0.05 by Student's *t* test.

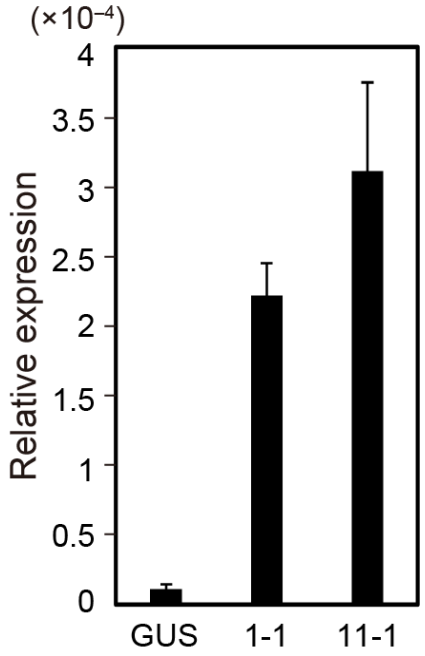

Figure 3-7. *CLE-RS3* expression in stable transgenic plants that were constitutively expressing *CLE-RS3*.

Real-time RT-PCR analysis of *CLE-RS3* expression in stably transformed *L. japonicus* transgenic plants that were constitutively expressing *CLE-RS3* or *GUS*. Each cDNA was prepared from total RNA derived from the entire root. *LjUBQ* was used to assess the relative expression of each gene. Error bars indicate SE (n = 3 independent pools of roots).

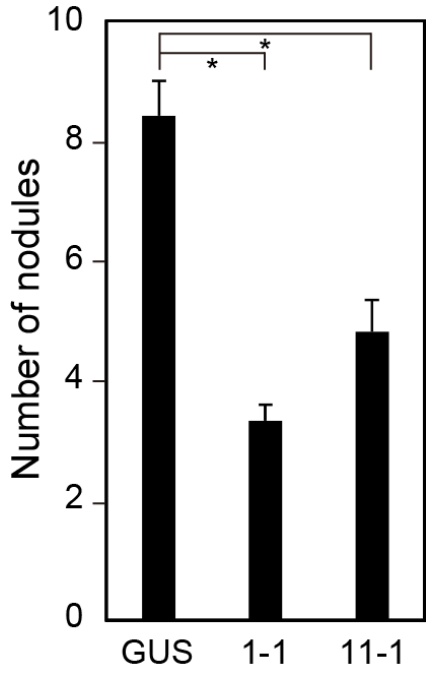

Figure 3-8. Nodulation phenotype of stable transgenic plants that were constitutively expressing *CLE-RS3*.

Number of nodules in stably transformed *L. japonicus* transgenic plants that were constitutively expressing *CLE-RS3* or *GUS*. The nodulation phenotype was observed at 21 dai (n = 11–12 plants). Error bars indicate SE. **P* = 0.05 by Student's *t* test.

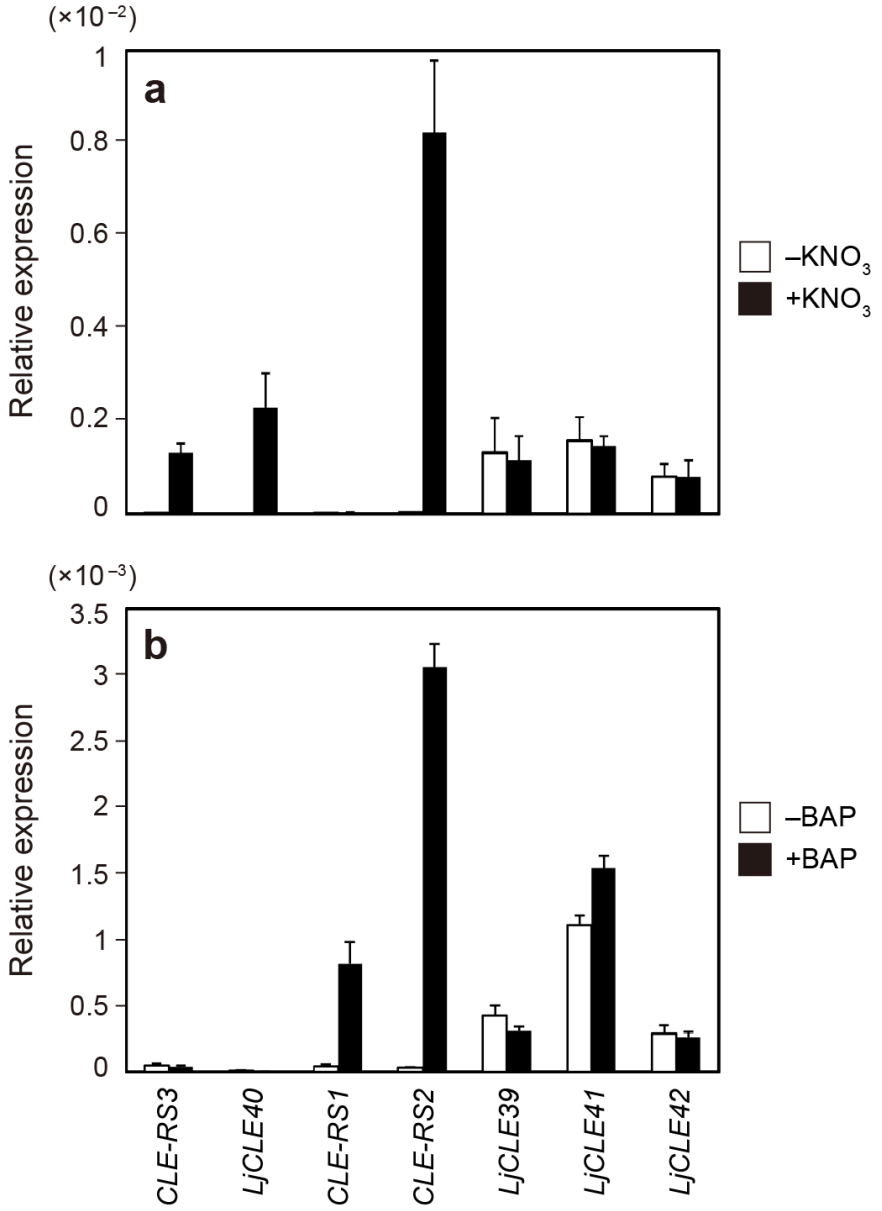

Figure 3-9. Effect of nitrate and cytokinin on *CLE* genes expression.

(a) WT plants were grown with 10 mM (black bars) or without (white bars) KNO_3 for 24 h. (b) WT plants were grown with 50 nM (black bars) or without (white bars) benzylaminopurine (BAP) for 24 h. Expression of each gene was determined by real-time RT-PCR. Each cDNA was prepared from total RNA derived from the entire root. *LjUBQ* was used to assess the relative expression of each gene. Error bars indicate SE (n = 3 independent pools of roots).

Table 3-1. Features of the CLE genes identified in this study

Name	Chromosome location	Orientation	Number of amino acid residues	Predicted intron	SP cleavage site
LjCLE-RS3	Chr3:35048895-35049113	Forward	72	N	29
LjCLE39	Chr1:50801117-50801398	Reverse	93	N	28
LjCLE40	Chr3:35016355-35016597	Forward	80	N	23
LjCLE41	Chr2:21357987-21360256	Forward	98	Y	37
LjCLE42	Chr4:10320058-10320393	Forward	111	N	42
LjCLE-RS1	unknown	Reverse	116	N	24
LjCLE-RS2	Chr3:35039780-35040025	Forward	81	N	29

The genetic location, number of amino acid residues of the encoded protein, presence of intron and putative signal peptide (SP) cleavage site of the encoded protein, are shown. The genetic location is based on pseudomolecule data obtained from miyakogusa.jp (http://www.kazusa.or.jp/lotus/index.html). Putative SP cleavage sites were predicted by SignalP 3.0 server (http://www.cbs.dtu.dk/services/SignalP-3.0/).

Table 3-2. Amino acid sequences of the CLE proteins identified in this study

Name	Amino acid sequence
LjCLE-RS3	MANASRIMRVFIVMLMMSTLFIMSLVQARSLERRVDSQHLLQMMKHKHPRRALED**WISPGGPDPKHN**KQGHG
LjCLE39	MKITSCRVLAAILALVLVHFLLFSSFCLHHRQSFSRETSLPVSRKLLSSSSTSSASFFTRFGKISGSRNQNRKTVEPSLR**KAPPSIPDPTQN**K
LjCLE40	MANSKQVTCLVLLMLLISKMESRSLEASMETKKISAKGGSQELIQKSQLLKASFAKGGNIFPNLYDTN**RLSPQGPDPRHH**
LjCLE41	MGTSSSSFLPRFFFRVLVVVWLVCVLVLGSLGSGGATRELATQWSSEGLKHEQVVGRDMPVNHAELDFNYMSK**RRVPNGPDPIHN**RRAGNSGRPPGQT
LjCLE42	MIGFSFSREKERTSSRSSETITRLSLARAAIFSLWVMLVFALISLLFSINNHDQIQTTHSTPRRVLNKKHSFSTTLFHPPSSSSAQNIAENTALYGDDK**RIIHTGPNPLHN**

Underline indicates the putative signal sequence as predicted by SignalP 3.0 (http://www.cbs.dtu.dk/services/SignalP-3.0). Amino acid sequences of the CLE domains are shown in bold.

Table 3-3. Primers used in chapter 3

LjUBQ RT-PCR			
	UBQ-F	5'-ATGCAGATCTTCGTCAAGACCTTG-3'	
	UBQ-R	5'-ACCTCCCCTCAGACGAAG-3'	
CLE-RS1 RT-PCR			
	RS1-F	5'-TGCAAGTGTCGATGCTCATAGC-3'	
	RS1-R	5'-GATGTTTTGCTGAACCAAGGGATA-3'	
CLE-RS2 RT-PCR			
	RS2-F	5'-GCTCGTAATCTCCAAATCATTCACA-3'	
	RS2-R	5'-GGTGAGAGTCTTTGCTGTTGATATCC-3'	
CLE-RS3 RT-PCR			
	RS3-F	5'-GCAGGCTCGAAGTCTAGAGAGAC-3'	
	RS3-R	5'-GTGAGATCCAATCTTCCAAAGCT-3'	
LjCLE39 RT-PCR			
	CLE39-F	5'-AGTGGAAGCAGGAATCAGAACAGGA-3'	
	CLE39-R	5'-CTACTTGTTCTGGGTAGGATCTGGGATG-3'	
LjCLE40 RT-PCR			
	CLE40-F	5'-ATCACAGTTACTGAAGGCAAG-3'	
	CLE40-R	5'-GTCTATTCGTATCGTAGAGATTTGGA-3'	
LjCLE41 RT-PCR			
	CLE41-F	5'-GCCTGTGAACCATGCAGAATTGGA-3'	
	CLE41-R	5'-CTAAGTCTGGCCAGGAGGTCTACCAGA-3'	
LjCLE42 RT-PCR			
	CLE42-F	5'-CCTTCTTCTTCAAGTGCTCAGA-3'	
	CLE42-R	5'-CTAGTTGTGCAGAGGATTTGGACCGGTGTG-3'	
LjNIN RT-PCR			
	LjNIN-F	5'-CAATGCTCTTGATCAGGCTGTTGA-3'	
	LjNIN-R	5'-GAGTGCTAATGGCAAATTGTGTGTC-3'	
Cloning of *CLE-RS3* promoter			
	proRS3-F	5'-CAAGAGCTCCTCTCTCTCATTCTCATTCT-3'	*SacI* site is added
	proRS3-R	5'-CAACCCGGGTCTATATCCCAAGGGCGCAT-3'	*SmaI* site is added

Table 3-3. (continued)

Cloning of *LjCLE40* promoter		
proCLE40-F	5'-CAAGAGCTCCCACCTCTCCACACCTCATT-3'	*SacI* site is added
proCLE40-R	5'-CAACCCGGGGCATGCAATGGAAGTTTAAA-3'	*SmaI* site is added
Cloning of *CLE-RS3* CDS		
RS3 CDS-F	5'-CACCATGGCGAATGCAAGTAGAATAATGCG-3'	
RS3 CDS-R	5'-TCAACCATGACCCTGCTTATTATGCTTA-3'	
HPT PCR		
HPT-F	5'-CTATTCCTTTGCCCTCGGAC-3'	
HPT-R	5'-ATGAAAAAGCCTGAACTCAC-3'	

Chapter 4
GENERAL DISCUSSION

Root nodule symbiosis is advantageous for the study of nitrate responses in plants

Because plants are sessile organisms, the ability to sense and to adapt to fluctuating nutritional environments is directly linked to their survival. To date, nitrate signaling in plants has been predominantly studied in Arabidopsis (Guan, 2017; Sun et al., 2017). A recent report has revealed that AtCPKs act as master regulators that orchestrate the primary nitrate response, and this has greatly contributed to our understanding of the molecular framework for nitrate signaling pathway (Liu et al., 2017). Nitrate sensing by AtNRT1.1 induces a transient increase in Ca^{2+} concentration in plant cells. The Ca^{2+} signal is decoded by AtCPKs, which triggers the phosphorylation of AtNLP7. Phosphorylated AtNLP7 can be retained in the nucleus and activate many nitrate-responsive genes (Ho et al., 2009; Konishi and Yanagisawa, 2013; Marchive et al., 2013; Liu et al., 2017; Krouk, 2017). Considering accumulating knowledge and established genetic resources, Arabidopsis may be a useful plant for the study of nitrate signaling. However, in Arabidopsis, the effects of nitrate on plant development are not clear, because of an inherent feature of this species, apparent phenotypes of Arabidopsis mutants related to nitrate transport or signaling are generally weak (Castaings et al., 2009, Sato et al., 2017). Therefore, it is almost impossible to screen mutants based on a certain nitrate-related phenotype. In fact, to the best of my knowledge, there are currently no examples of forward genetics studies that have successfully discovered Arabidopsis mutants relevant to the nitrate response. Moreover, complete loss of nitrate strongly affects germination and survival of Arabidopsis, whereas high concentrations of nitrate strongly impair plant growth. The narrow ranging nitrate response may make it difficult to analyze the effects of nitrate deficiency or sufficiency on plant development. In contrast, *L. japonicus* can germinate and survive for at least 2–3 weeks under a complete nitrate-deficient condition, and plant can grow under high concentrations of nitrate such as 50 mM KNO_3. In addition, as shown in this dissertation, the effect of nitrate is clearly detectable during root nodule symbiosis. Nodulation is a unique plant developmental process, where *de novo* organogenesis occurs in response to infection by symbiotic bacteria, and several key processes required for the establishment of the symbiosis, including bacterial infection, and initiation, growth, and function of symbiotic organ, are controlled by nitrate. Indeed, as a result of mutant screening using *L. japonicus*, I successfully identified *nrsym* mutants, which are involved in the nitrate response during the symbiosis (Nishida et al., 2018). The clear nitrate-affected phenotypes enabled me to

dissect the role of a *NRSYM* gene, *NRSYM1*. Because the function of NRSYM1 is not restricted to root nodule symbiosis, further analysis of NRSYM1 may contribute to our understanding of general plant development in varying nitrate environments. In addition, the identification of genes responsible for other *nrsym* mutants such as *nrsym2* and *nrsym3* would further contribute to our understanding of nitrate responses.

The significance of nitrate-induced pleiotropic control of root nodule symbiosis

In this study, NRSYM1 is likely to regulate pleiotropic nodulation processes, such as rhizobial infection, nodule initiation, nodule growth, and nitrogen fixation activity through the use of different downstream target genes in response to nitrate. Nitrate concentrations sufficient to inhibit nodulation processes differed depending on the process. Nodule growth and nitrogen fixation are more sensitive to nitrate than processes involved in the initiation of nodulation (Streeter and Wong, 1988). Mutants in which the positive regulation of nodulation is defective are roughly classified into three phenotypic categories, Nod$^-$, Hist$^-$, and Fix$^-$ mutants (Kawaguchi et al., 2002). Nod$^-$ mutants exhibit a complete loss of nodulation, phenotypes lacking infection thread development and nodule organogenesis. In most cases, loss-of-function mutations in genes involved in the early nodulation signaling pathway cause Nod$^-$ phenotypes (Kouchi et al., 2010; Suzaki et al., 2015). In the Fix$^-$ mutants, although mature nodules are produced, they are functionally deficient in terms of nitrogen fixation activity (Hakoyama et al., 2009, Krusell et al., 2005, Kumagai et al., 2007). Hist$^-$ mutants form immature nodules and subsequent nodule developmental processes involving endosymbiosis are arrested. Thus, the site of action of the Hist$^-$ mutation can be located between those affected by Nod$^-$ and Fix$^-$ mutations (Kawaguchi et al., 2002; Yano et al., 2006). In the presence of rhizobia, the growth of Fix$^-$ mutant plants is commonly more restricted than that of Hist$^-$ and Nod$^-$ mutants. Thus, the process of nodule growth is thought to consume more energy than nodule initiation. In order to optimize energy consumption relevant to root nodule symbiosis, plants may finely regulate the nodulation process in response to nitrate concentrations. In *L. japonicus*, it takes about 10 days for rhizobial infection to results in the formation of mature nodules with nitrogen fixation activity (Hayashi et al., 2005). This implies that, if once plants stop the early stages of nodulation in response to nitrate, in afterward nitrate-deficient conditions plants may restart nodule development but need to wait in order to acquire a nitrogen source owing to the formation of functional nodules. In contrast, nitrate-induced inhibition of nodule growth and nitrogen fixation activity is reported to be a quickly reversible processes (Fujikake et al., 2002). For example, the inhibition of nodule growth

due to high nitrate treatment could be reversed 2 days after transferring to nitrogen-free conditions (Fujikake et al., 2003). Therefore, the pleiotropic control of root nodule symbiosis by nitrate may be a reasonable strategy allowing plants to adapt to fluctuating nitrate concentrations in soil.

The impact of NRSYM1-mediated symbiotic balance on plant growth.

To balance the benefits and costs associated with root nodule symbiosis, plants have developed at least two negative regulatory systems. One strategy involves the regulation of nodule number in response to rhizobial infection through AON, which is currently understood as a systemic long-range signaling process between roots and shoots (Caetano-Anolles and Gresshoff, 1991; Oka-Kira and Kawaguchi, 2006; Suzaki et al., 2015). Here, it was shown that CLE-RS3 is a new component of AON in *L. japonicus*, which may act as a potential root-derived signal through interaction with HAR1 (Nishida et al., 2016). Another strategy involves the regulation of root nodule symbiosis in response to nitrate. In this study, the NRSYM1 transcription factor was identified as a key regulator involved in the pleiotropic control of root nodule symbiosis by nitrate (Nishida et al. 2018). In addition, it was demonstrated that NRSYM1 directly regulates *CLE-RS2* expression in response to nitrate. The NRSYM1>CLE-RS2 signaling pathway is thought to control the number of nodules via downstream signaling, similar to that of AON (Fig. 4-1). Thus, CLE peptides>HAR1 signaling pathway is shared between rhizobial infection and nitrate responses. In the former case, LjNIN activates *CLE-RS1/2* (Soyano et al., 2014), and in the latter, NRSYM1 activates *CLE-RS2*. Activated LjCLE peptides are translocated to the shoot, where they bind to their receptor, HAR1. This then induces cytokinin production, which is a potential candidate of SDIs, to negatively regulate nodulation (Okamoto et al., 2013; Sasaki et al., 2014). Expression of *LjNIN* is down-regulated by nitrate application (Barbulova et al., 2007). Moreover, constitutive expression of *LjNIN* in hairy roots systemically downregulates endogenous *LjNIN* expression in untransformed roots of the same plant (Soyano et al., 2014). In both cases, HAR1 is required for the downregulation of *LjNIN*. I also showed that the downregulation of *LjNIN* by nitrate occurred in an NRSYM1-dependent manner. Thus, based on these results, an inhibition of LjNIN playing a positive role in nodulation may be a final step of nitrate- or rhizobia-mediated negative regulation of nodule number. Since *CLE-RS3* expression is induced by rhizobial infection and by nitrate application, it may work downstream of both NRSYM1 and LjNIN.

WT legumes can suitably control the energy associated with root nodule symbiosis using two methods of negative regulation. NRSYM1 is likely to adjust the balance between nitrogen availability from the soil and carbon sources consumed during symbiosis under nitrate-

sufficient conditions. In this control, inclining the balance to benefit external nitrogen rather than maintaining the equilibrium can be meaningful (Fig. 4-2). The *nrsym1* mutants, which cannot change the inclination, form mature nodules under nitrate-sufficient conditions. Hence, the *nrsym1* plants seem to be unable to save the cost associated with nodulation. In fact, their growth is worse than that of the WT (Fig. 4-3). The AON system provides another balance to maintain nitrogen sources obtained owing to symbiosis and carbon sources consumed in symbiosis (Oka-Kira and Kawaguchi, 2006; Kouchi et al., 2010). In this case, it may be important to maintain the equilibrium. AON mutants such as *har1*, show limited plant growth due to hypernodulation, where negative regulation of nodulation in response to rhizobial infection is ineffective (Wopereis et al., 2000; Oka-Kira et al., 2005; Magori et al., 2009). Because AON is additionally and partially involved in the inhibition of nodule number by nitrate, under nitrate-sufficient conditions the *har1* mutation causes excessive immature nodule formation, thereby reducing plant growth (Fig. 4-3). The *nrsym1 har1* double mutants, in which the two negative regulations were concurrently disrupted, display excessive formation of mature nodule, and show more severe defects compared with each single mutant (Fig. 4-3). This observation demonstrates the significance of the regulation of the two balances to optimize symbiosis and plant growth in nitrate-sufficient environments.

In nitrate-sufficient environments, plants may use more energy on shoot development than on root system development (Sun et al., 2017; Nacry et al., 2013). Given that both roots and nodules are organs for obtaining a nitrogen source, nitrate-induced control of both root development and nodulation can be interpreted as a strategy for balancing plant growth and nitrogen availability. The shoot-root fresh weight ratio is lower in *nrsym1* mutants compared with WT under nitrate-sufficient conditions. This indicates that NRSYM1 regulates the balance of nitrogen availability and carbon sources consumed during root development, as well as in nodules. Therefore, the findings obtained from the NRSYM1 analysis may help us to the understand the mechanisms controlling root nodule symbiosis and plant development in response to nitrogen nutrition.

Potential implication of NRSYM1 in a signaling in response to nitrate starvation

Nitrate is usually distributed unevenly in the soil. Thus, plants have developed a systemic long-range signaling mechanism, through which nitrogen starvation in part of the root leads to increased nitrate uptake in nitrate-rich zones of the root (Gansel et al., 2001; Ruffel et al., 2011; Ruffel et al., 2008). Root-to-shoot mobile peptides belonging to the AtCEP family are induced in

nitrogen-starved roots, and they are received by two LRR-RLKs, CEPR1 and CEPR2, in the shoot (Tabata et al., 2014). Then, the production of phloem-specific polypeptides, CEP DOWNSTREAM 1 (CEPD1) and CEPD2, is induced in leaves, and they are transported from the shoot to root through the phloem, leading to the induction of *AtNRT2.1* expression in nitrate-rich zones to uptake nitrate (Ohkubo et al., 2017). Although the relationship between CEP signaling and nitrate acquisition is largely unknown in legumes, *M. truncatula COMPACT ROOT ARCHITECTURE 2* (*CRA2*), which encodes an LRR-RLK orthologous to CEPR1, has been reported to act as a positive regulator in nodulation (Huault et al., 2014). Reciprocal grafting experiments using WT and *cra2* mutants showed that the low nodulation phenotype only occurred when *cra2* plants were used as the scion (Huault et al., 2014). In addition, the MtCEP1 peptide can promote nodulation in a CRA2-dependent manner (Mohd-Radzman et al., 2016). In this study, I focused on signaling pathways induced under nitrate-sufficient conditions. While root nodule symbiosis is promoted in nitrogen-deficient environments, it is not known how signaling associated with nitrate deficiency activates root nodule symbiosis. Recently, AtNLP6/7 was shown to physically interact with TEOSINTE BRANCHED1/CYCLOIDEA/PROLIFERATING CELL FACTOR1-20 (AtTCP20) via PB1 domains and TCP20-NLP6/7 heterodimers, to down-regulate the expression of the cell cycle gene *AtCYCB1;1* and control root meristem growth under nitrogen-deficient conditions (Guan et al., 2017). This suggests that AtNLP6/7 function under both nitrate-sufficient and -deficient conditions. In addition, LjNIN, which belong to the same NLP family as NRSYM1, has dual roles in the regulation of nodulation; LjNIN acts as a positive regulator for nodule organogenesis and as a negative regulator that suppresses nodulation by inducing *CLE-RS1/2* expression (Schauser et al., 1999; Marsh et al., 2007; Soyano et al., 2013; Soyano et al., 2014). Therefore, it may be worth investigating the possibility that NRSYM1 positively regulates root nodule symbiosis under certain conditions, such as nitrogen deficient environment. Studies on the implication of NRSYM1 during nitrate deficiency will involve the investigation of a potential interaction between NRSYM1 and CEP signaling.

Possibility of applying root nodule symbiosis and knowledge of NRSYM1 to sustainable agriculture

Discovery of the so-called Haber-Bosch process in 1909 enabled the production of inorganic nitrogen fertilizer from atmospheric nitrogen, which dramatically improved crop productivity. In modern agriculture, large amounts of nitrogen fertilizer are applied to fields to maintain high crop productivity. However, the Haber-Bosch process requires the extensive use of nonrenewable

fossil fuel resources (Galloway et al., 1995; Vance, 2001). In addition, plants take up only 25–50% of the nitrogen fertilizer applied to fields every year. Fertilizer nitrogen that is not used by the plants leaches into water streams, and causes serious problems, such as hypoxic zones and eutrophication (Hirel et al., 2011; Undurraga et al., 2017). Hence, excessive application of nitrogen fertilizers has environmental costs, in addition to the economic costs associated with fertilizer production. The importance of root nodule symbiosis is reaffirmed in sustainable agriculture. However, plants grown solely in symbiotic association with rhizobia under nitrogen-free conditions are inferior to those grown under high nitrate. Thus, nitrogen derived from symbiotic nitrogen fixation seems to be insufficient to fully improve plant growth. Nitrate-induced control of root nodule symbiosis may need to be understood in terms of the compatibility between symbiosis and nitrogen fertilizer application. Further study on NRSYM1 may provide useful basic knowledge for the future realization of sustainable agriculture. In addition, utilization of legumes as green manure is a time-honored and well-known way of agriculture. It is estimated that properly managed alfalfa-corn rotations could reduce fertilizer inputs by up to 25% without loss of production (Vance, 2001). The induction level of nitrate assimilation-related genes in *nrsym1* roots was lower than that of WT, implying that nitrate is not assimilated in the mutants. Therefore, the use of *nrsym1* mutation in useful legumes may have the potential to exert a higher capacity than green manure, due to the lower effect on nitrate consumption.

Future subjects

In this study, NRSYM1 was shown to regulate pleiotropic phases of root nodule symbiosis in response to nitrate. While NRSYM1 was shown to regulate the nitrate-induced control of nodule number through the CLE-RS2>HAR1 signaling module, the genes directly targeted by NRSYM1 in other nitrate-induced regulatory processes, such as rhizobial infection, nodule growth, and nitrogen fixation, remain unknown. Thus, in order to understand the nitrate-induced pleiotropic control of root nodule symbiosis, future studies should aim to identify NRSYM1 target genes other than *CLE-RS2* during the control of such processes. To this end, comprehensive approaches in combination with the *nrsym1* mutants may be useful, which involve spatiotemporal RNA-seq and ChIP-seq analysis. The split-root experiment using *L. japonicus* suggested that systemic AON signaling takes about 3 days after inoculation to inhibit nodule formation (Suzuki et al., 2008). Conversely, sufficient inhibition of nodule growth and nitrogen fixation activity is observed within 1 day of nitrate treatment (Saito et al., 2014; Cabeza et al., 2014). On the basis of this quick response, the latter two processes may be regulated locally in the root. In soybean, the results of

split-root and two-layered pot experiments suggest that both systemic and local mechanisms control each aspect of root nodule symbiosis controlled by nitrate (Cho and Harper, 1991; Yashima et al., 2003). For example, nodule growth and nitrogen fixation activity are both systemically and locally controlled by nitrate, although the local action has stronger effects than the systemic action. To verify these, split-root experiments using *L. japonicus* in combination with nitrate are essential, and these will contribute to a more detailed understanding of the molecular framework for systemic and/or local regulation of root nodule symbiosis in response to nitrate.

In the current model of AON, although expression of *CLE-RS1/2* is rapidly and transiently induced in response to rhizobial infection. AON appears to maintain nodule number following the repression of *CLE-RS1/2*. It is probable that unidentified factors contribute to the control of nodule number during later nodulation stages. Indeed, a historic surgical excision experiment of mature nodules indicated that the inhibition of nodulation can occur during the later nodulation stages (Nutman, 1952). Furthermore, some Fix$^-$ mutants, such as *sst1, sen1*, and *amsh1*, in *L. japonicus* tend to form increased numbers of nodules (Krusell et al., 2005; Suganuma et al., 2003; Małolepszy et al., 2015). These observations imply that a mechanism may be involved in the control of nodule number during the later nodulation stage, which may be associated with the monitoring of nitrogen-fixing activity in nodules. Elucidation of this point may provide a new insight into the research of AON. I found that the timing of *CLE-RS3* and *LjCLE40* induction after rhizobia inoculation was slower than that of *CLE-RS1/2* (Fig. 4-4). Thus, it may be hypothesized that the newly-identified *LjCLE* genes play a role in AON at later nodulation stages. Conversely, unlike *CLE-RS1/2/3*, constitutive expression of *LjCLE40* by hairy root transformation did not have definitive effects on nodule number (Nishida et al., unpublished data). Thus, it is possible that *LjCLE40* is not important for AON, and may be involved in the control of nodule growth and nitrogen fixation activity. To verify this, future studies should aim to clarify the detailed function of *LjCLE40*, whereby determining the loss-of-function effects of this gene on nodulation will be essential. Additionally, *CLE-RS3* and *LjCLE40* may be possible downstream factors of NRSYM1, because their expression is induced by nitrate application. The elucidation of direct protein-DNA interactions between NRSYM1-*CLE-RS3/LjCLE40* will be another important task.

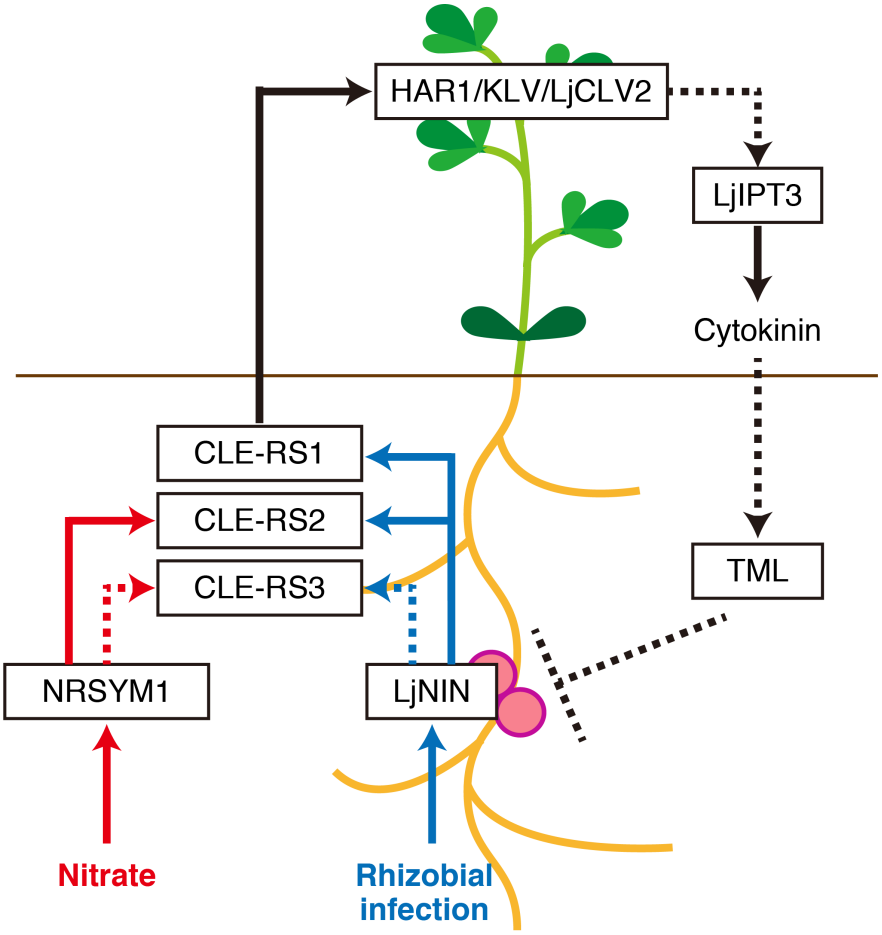

Figure 4-1. Model of systemic long-range signaling that negatively regulates nodule number in response to either rhizobial infection or nitrate.

LjNIN activates *CLE-RS1/2* in response to rhizobial infection, while NRSYM1 activates *CLE-RS2* in response to nitrate. Although different RWP-RK type transcription factors regulate the transcription of *CLE* under each condition, a downstream signaling pathway is likely to be shared between the two different inputs. Cytokinin, a potential candidate of SDIs, inhibits nodulation probably by down-regulating *LjNIN* expression. CLE-RS3 may act downstream of both LjNIN and NRSYM1 as a potential root-derived signal.

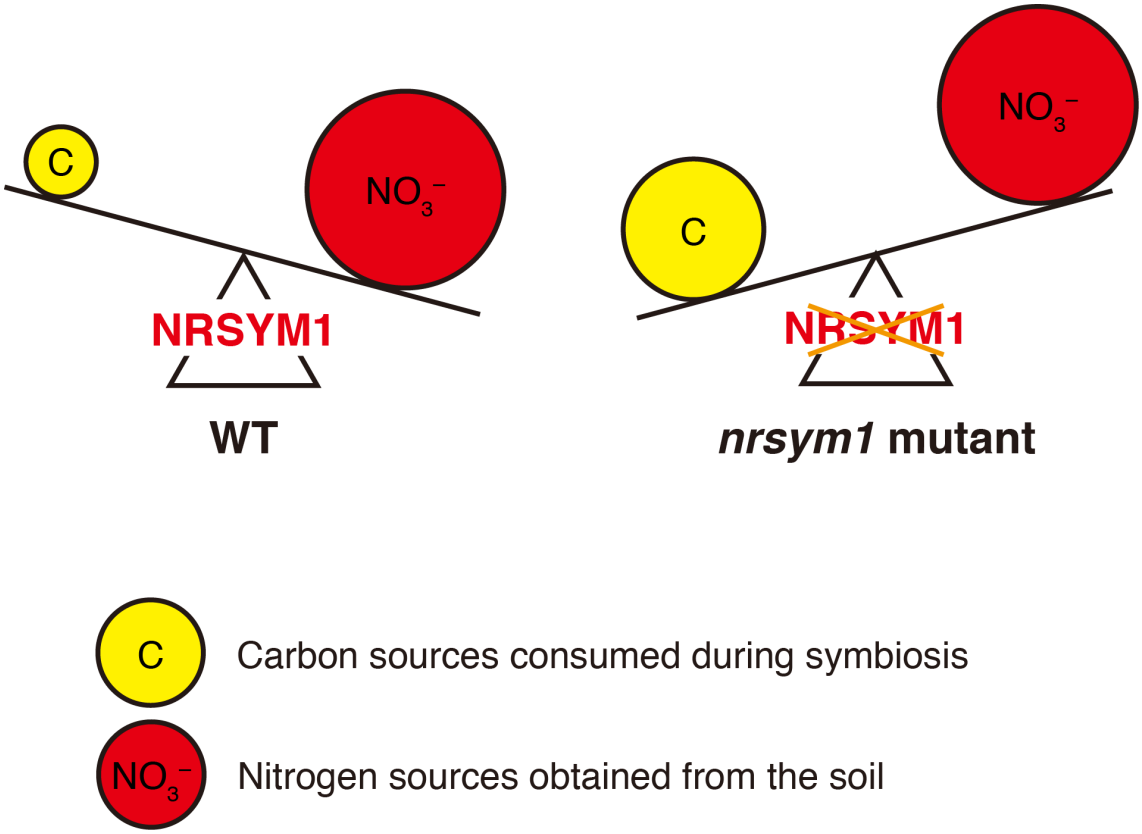

Figure 4-2. Model of NRSYM1-mediated balancing nutritional benefit and cost relevant to root nodule symbiosis

Under nitrate-sufficient conditions, NRSYM1 favors a balance towards obtaining external nitrogen and reducing carbon sources consumed during symbiosis, by ceasing the symbiosis. Loss-of-function of NRSYM1 cannot change the inclination, and is unable to prevent the cost associated with nodulation. Nitrogen sources obtained by symbiosis are not incorporated into this model.

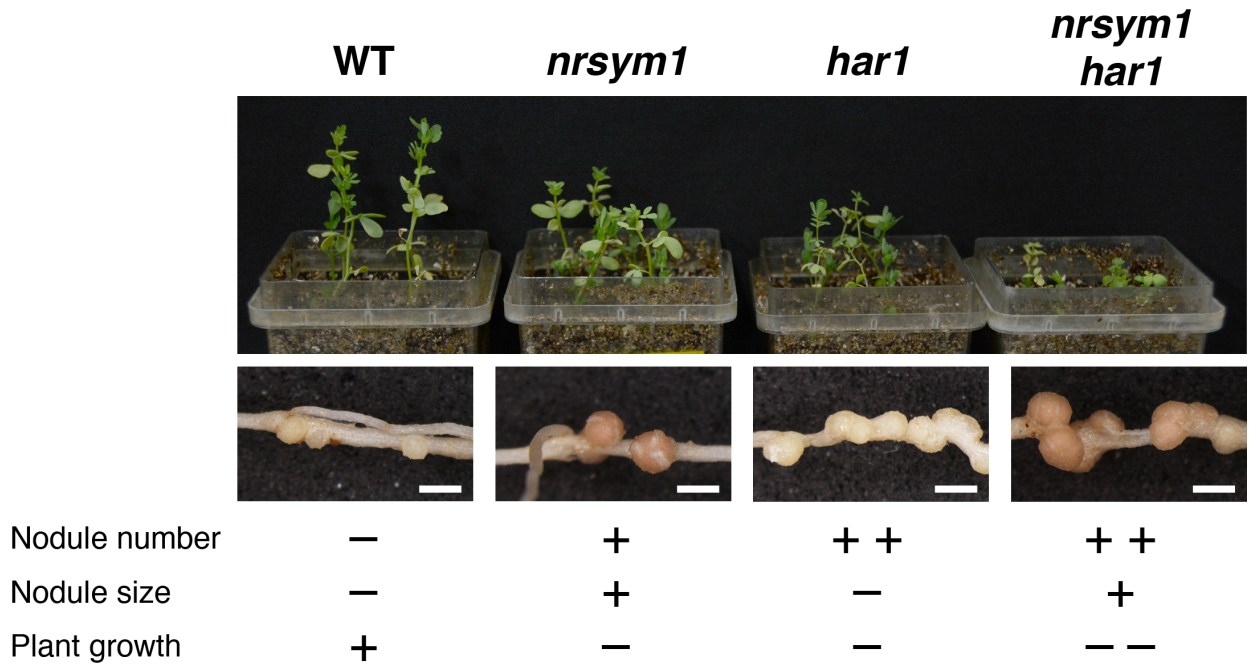

Figure 4-3. The effect of NRSYM1-mediated symbiotic balance on plant growth and nodulation.

Shoots (42 dai) and nodules (21 dai) of WT, *nrsym1-1* mutants, *har1-7* mutants, and the *nrsym1-1 har1-7* double mutants are shown. Plants were grown in the presence of 10 mM KNO_3 and inoculated with rhizobia. Scale bars: 1 mm. – –, further reduction; –, reduction; +, normal; ++, excess.

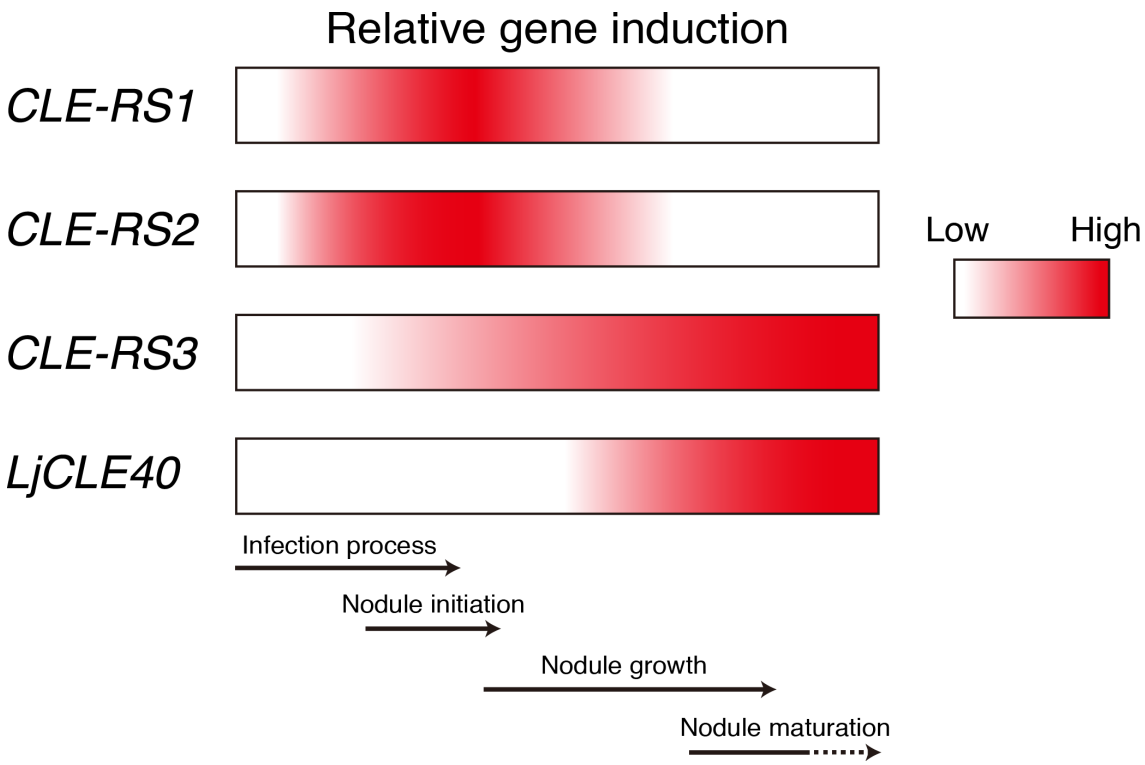

Figure 4-4. Schematic representation showing the timing of nodulation-related *LjCLE* gene induction after rhizobial infection

Timing of *CLE-RS1*, *CLE-RS2*, *CLE-RS3*, and *LjCLE40* induction by rhizobial infection is schematically shown. Deeper color indicates a higher level of relative induction.

ACKNOWLEDGEMENTS

I deeply appreciate the generous guidance of my supervisor, Dr. Masayoshi Kawaguchi and the kind advice offered by Dr. Takuya Suzaki. Without their support, completion of my Ph.D. would not have been possible.

I also thank my advisory committee members, Dr. Mitsuyasu Hasebe, Dr. Shuji Shigenobu, and Dr. Takuji Ohyama for their valuable comments. In addition, I thank the rest of my advisors of NIBB, Dr. Ryutaro Tokutsu, and Dr. Yoshiaki Kamada.

Additionally, I was supported by many collaborators. I especially thank Dr. Sachihiro Matsunaga, Dr. Shigeyuki Betsuyaku, and Dr. Yuki Sakamoto for their technical assistance and advice with microscope observation, Dr. Yoshihiro Handa for analyzing data from the genome-resequencing approach, and Dr. Kenji Miura, Dr. Momoyo Ito, Ms. Sachiko Tanaka, and Dr. Takashi Soyano, for their technical support and useful advice.

I am grateful to the current and former lab members for their suggestions and discussion, because of whom I was able to spend a fruitful five years. Finally, I express my sincere gratitude to my family for watching over me.

REFERENCES

Alboresi A, Gestin C, Leydecker MT, Bedu M, Meyer C, Truong HN: **Nitrate, a signal relieving seed dormancy in *Arabidopsis***. *Plant Cell Environ.* 2005, **28**:500-512.

Araya T, Miyamoto M, Wibowo J, Suzuki A, Kojima S, Tsuchiya YN, Sawa S, Fukuda H, von Wirén N, Takahashi H: **CLE-CLAVATA1 peptide-receptor signaling module regulates the expansion of plant root systems in a nitrogen-dependent manner**. *Proc. Natl. Acad. Sci. USA* 2014, **111**:2029-2034.

Bagchi R, Salehin M, Adeyemo OS, Salazar C, Shulaev V, Sherrier DJ, Dickstein R: **Functional assessment of the *Medicago truncatula* NIP/LATD protein demonstrates that it is a high-affinity nitrate transporter**. *Plant Physiol.* 2012, **160**:906-916.

Bailey TL, Boden M, Buske FA, Frith M, Grant CE, Clementi L, Ren J, Li WW, Noble WS: **MEME Suite: tools for motif discovery and searching**. *Nucleic Acids Res.* 2009, **37**:W202-W208.

Barbulova A, Rogato A, D'Apuzzo E, Omrane S, Chiurazzi M: **Differential effects of combined N sources on early steps of the nod factor–dependent transduction pathway in *Lotus japonicus***. *Mol. Plant Microbe Interact.* 2007, **20**:994-1003.

Becker A, Bergès H, Krol E, Bruand C, Rüberg S, Capela D, Lauber E, Meilhoc E, Ampe F, de Bruijn FJ, et al.: **Global changes in gene expression in *Sinorhizobium meliloti* 1021 under microoxic and symbiotic conditions**. *Mol. Plant Microbe Interact.* 2004, **17**:292-303.

Bhuvaneswari TV, Bhagwat AA, Bauer WD: **Transient susceptibility of root cells in four common legumes to nodulation by Rhizobia**. *Plant Physiol.* 1981, **68**:1144-1149.

Bhuvaneswari TV, Turgeon BG, Bauer WD: **Early events in the infection of soybean (*Glycine max* L. Merr) by *Rhizobium japonicum***. *Plant Physiol.* 1980, **66**:1027-1031.

Bidadi H, Matsuoka K, Sage-Ono K, Fukushima J, Pitaksaringkarn W, Asahina M, Yamaguchi S, Sawa S, Fukuda H, Matsubayashi Y, et al.: ***CLE6* expression recovers gibberellin deficiency to promote shoot growth in Arabidopsis**. *Plant J.* 2014, **78**:241-252.

Brand U, Fletcher JC, Hobe M, Meyerowitz EM, Simon R: **Dependence of stem cell fate in *Arabidopsis* on a feedback loop regulated by *CLV3* activity**. *Science* 2000, **289**:617-619.

Broughton WJ, Dilworth MJ: **Control of leghaemoglobin synthesis in snake beans**. *Biochem. J.* 1971, **125**:1075-1080.

Caba JM, Centeno ML, Fernández B, Gresshoff PM, Ligero F: **Inoculation and nitrate alter phytohormone levels in soybean roots: differences between a supernodulating mutant and the wild type**. *Planta* 2000, **211**:98-104.

Caba JM, Recalde L, Ligero F: **Nitrate-induced ethylene biosynthesis and the control of nodulation in alfalfa**. *Plant Cell Environ.* 1998, **21**:87-93.

Cabeza R, Koester B, Liese R, Lingner A, Baumgarten V, Dirks J, Salinas-Riester G, Pommerenke C, Dittert K, Schulze J: **An RNA sequencing transcriptome analysis reveals novel insights into molecular aspects of the nitrate impact on the nodule activity of *Medicago truncatula***. *Plant Physiol.* 2014, **164**:400-411.

Caetano-Anolles G, Gresshoff PM: **Plant genetic control of nodulation**. *Annu. Rev. Microbiol.* 1991, **45**:345-382.

Carroll BJ, Mathews A: **Nitrate inhibition of nodulation in legumes**. *Molecular Biology of Symbiotic Nitrogen Fixation* 1990, 159-180.

Carroll BJ, McNeil DL, Gresshoff PM: **Isolation and properties of soybean [*Glycine max* (L.) Merr.] mutants that nodulate in the presence of high nitrate concentrations**. *Proc. Natl. Acad. Sci. USA* 1985, **82**:4162-4166.

Castaings L, Camargo A, Pocholle D, Gaudon V, Texier Y, Boutet-Mercey S, Taconnat L, Renou J-P, Daniel-Vedele F, Fernandez E, et al.: **The nodule inception-like protein 7 modulates nitrate sensing and metabolism in Arabidopsis**. *Plant J.* 2009, **57**:426-435.

Castro Marín I, Loef I, Bartetzko L, Searle I, Coupland G, Stitt M, Osuna D: **Nitrate regulates floral induction in Arabidopsis, acting independently of light, gibberellin and autonomous pathways**. *Planta* 2011, **233**:539-552.

Cho M-J, Harper JE: **Effect of localized nitrate application on isoflavonoid concentration and nodulation in split-root systems of wild-type and nodulation-mutant soybean plants**. *Plant Physiol.* 1991, **95**:1106-1112.

Clark SE, Williams RW, Meyerowitz EM: **The *CLAVATA1* gene encodes a putative receptor kinase that controls shoot and floral meristem size in Arabidopsis**. *Cell* 1997, **89**:575-585.

Cock JM, McCormick S: **A large family of genes that share homology with *CLAVATA3***. *Plant Physiol.* 2001, **126**:939-942.

Coronado C, Zuanazzi JAS, Sallaud C, Quirion JC, Esnault R, Husson HP, Kondorosi A, Ratet P: **Alfalfa root flavonoid production is nitrogen regulated**. *Plant Physiol.* 1995, **108**:533-542.

Crawford NM, Forde BG: **Molecular and developmental biology of inorganic nitrogen nutrition**. *Arabidopsis Book* 2002, **1**:e0011.

Crawford NM, Glass ADM: **Molecular and physiological aspects of nitrate uptake in plants**. *Trends Plant Sci.* 1998, **3**:389-395.

Daum G, Medzihradszky A, Suzaki T, Lohmann JU: **A mechanistic framework for noncell autonomous stem cell induction in *Arabidopsis***. *Proc. Natl. Acad. Sci. USA* 2014, **111**:14619-14624.

Delves AC, Mathews A, Day DA, Carter AS, Carroll BJ, Gresshoff PM: **Regulation of the soybean-*Rhizobium* nodule symbiosis by shoot and root factors**. *Plant Physiol.* 1986, **82**:588-590.

Djordjevic MA, Mohd-Radzman NA, Imin N: **Small-peptide signals that control root nodule number, development, and symbiosis**. *J. Exp. Bot.* 2015, **66**:5171-5181.

Drew MC, Saker LR: **Nutrient supply and the growth of the seminal root system in Barley.** *J. Exp. Bot.* 1975, **26**:79-90.

Ehrhardt DW, Wais R, Long SR: **Calcium spiking in plant root hairs responding to Rhizobium nodulation signals**. *Cell* 1996, **85**:673-681.

Endo S, Betsuyaku S, Fukuda H: **Endogenous peptide ligand–receptor systems for diverse signaling networks in plants**. *Curr. Opin. Plant Biol.* 2014, **21**:140-146.

Esseling JJ, Lhuissier FGP, Emons AMC: **Nod factor-induced root hair curling: continuous polar growth towards the point of nod factor application.** *Plant Physiol.* 2003, **132**:1982-1988.

Ferguson BJ, Indrasumunar A, Hayashi S, Lin M-H, Lin Y-H, Reid DE, Gresshoff PM: **Molecular analysis of legume nodule development and autoregulation**. *J. Integr. Plant Biol.* 2010, **52**:61-76.

Fisher K, Turner S: **PXY, a receptor-like kinase essential for maintaining polarity during plant vascular-tissue development**. *Curr. Biol.* 2007, **17**:1061-1066.

Fletcher JC, Brand U, Running MP, Simon R, Meyerowitz EM: **Signaling of cell fate decisions by *CLAVATA3* in *Arabidopsis* shoot meristems**. *Science* 1999, **283**:1911-1914.

Force A, Lynch M, Pickett FB, Amores A, Yan Y-l, Postlethwait J: **Preservation of duplicate genes by complementary, degenerative mutations**. *Genetics* 1999, **151**:1531-1545.

Fournier J, Timmers ACJ, Sieberer BJ, Jauneau A, Chabaud M, Barker DG: **Mechanism of infection thread elongation in root hairs of *Medicago truncatula* and dynamic interplay with associated rhizobial colonization**. *Plant Physiol.* 2008, **148**:1985-1995.

Frank B: **Ueber die Pilzsymbiose der Leguminosen**. *Berichte der Deutschen Botanischen Gesellschaft* 1889, **7**:332-346.

Fred EB, Graul EJ: **The effect of soluble nitrogenous salts on nodule formation.** *J. Am. Soc. Agron*. 1916, **8**:316.

Frink CR, Waggoner PE, Ausubel JH: **Nitrogen fertilizer: Retrospect and prospect**. *Proc. Natl. Acad. Sci. USA* 1999, **96**:1175-1180.

Fujikake H, Yamazaki A, Ohtake N, Sueyoshi K, Matsuhashi S, Ito T, Mizuniwa C, Kume T, Hashimoto S, Ishioka NS, et al.: **Quick and reversible inhibition of soybean root nodule growth by nitrate involves a decrease in sucrose supply to nodules**. *J. Exp. Bot.* 2003, **54**:1379-1388.

Fujikake H, Yashima H, Sato T, Ohtake N, Sueyoshi K, Ohyama T: **Rapid and reversible nitrate inhibition of nodule growth and N_2 fixation activity in soybean (*Glycine max* (L.) Merr.)**. *Soil Sci. Plant Nutr.* 2002, **48**:211-217.

Galloway JN, Schlesinger WH, Levy H, Michaels A, Schnoor JL: **Nitrogen fixation: Anthropogenic enhancement-environmental response**. *Global Biogeochemical Cycles* 1995, **9**:235-252.

Gansel X, Muños S, Tillard P, Gojon A: **Differential regulation of the NO_3^- and NH_4^+ transporter genes AtNrt2.1 and AtAmt1.1 in Arabidopsis: relation with long-distance and local controls by N status of the plant**. *Plant J.* 2001, **26**:143-155.

Gruber BD, Giehl RFH, Friedel S, von Wirén N: **Plasticity of the Arabidopsis root system under nutrient deficiencies**. *Plant Physiol.* 2013, **163**:161.

Guan P: **Dancing with Hormones: A Current Perspective of Nitrate Signaling and Regulation in Arabidopsis**. *Front Plant Sci.* 2017, **8**.

Guan P, Ripoll J-J, Wang R, Vuong L, Bailey-Steinitz LJ, Ye D, Crawford NM: **Interacting TCP and NLP transcription factors control plant responses to nitrate availability**. *Proc. Natl. Acad. Sci. USA* 2017, **114**:2419-2424.

Guo F-Q, Young J, Crawford NM: **The nitrate transporter AtNRT1.1 (CHL1) functions in stomatal opening and contributes to drought susceptibility in Arabidopsis**. *Plant Cell* 2003, **15**:107.

Haasen D, Köhler C, Neuhaus G, Merkle T: **Nuclear export of proteins in plants: AtXPO1 is the export receptor for leucine-rich nuclear export signals in *Arabidopsis thaliana***. *Plant J.* 1999, **20**:695-705.

Haecker A, Groß-Hardt R, Geiges B, Sarkar A, Breuninger H, Herrmann M, Laux T: **Expression dynamics of *WOX* genes mark cell fate decisions during early embryonic patterning in *Arabidopsis thaliana***. *Development* 2004, **131**:657-668.

Hakoyama T, Niimi K, Watanabe H, Tabata R, Matsubara J, Sato S, Nakamura Y, Tabata S, Jichun L, Matsumoto T, et al.: **Host plant genome overcomes the lack of a bacterial gene for symbiotic nitrogen fixation**. *Nature* 2009, **462**:514.

Hakoyama T, Oi R, Hazuma K, Suga E, Adachi Y, Kobayashi M, Akai R, Sato S, Fukai E, Tabata S, et al.: **The SNARE protein SYP71 expressed in vascular tissues is involved in symbiotic nitrogen fixation in *Lotus japonicus* nodules**. *Plant Physiol.* 2012, **160**:897-905.

Handa Y, Nishide H, Takeda N, Suzuki Y, Kawaguchi M, Saito K: **RNA-seq transcriptional profiling of an arbuscular mycorrhiza provides insights into regulated and coordinated gene expression in *Lotus japonicus* and *Rhizophagus irregularis***. *Plant Cell Physiol.* 2015, **56**:1490-1511.

Handberg K, Stougaard J: ***Lotus japonicus*, an autogamous, diploid legume species for classical and molecular genetics**. *Plant J.* 1992, **2**:487-496.

Hastwell AH, de Bang TC, Gresshoff PM, Ferguson BJ: **CLE peptide-encoding gene families in *Medicago truncatula* and *Lotus japonicus*, compared with those of soybean, common bean and Arabidopsis**. *Sci. Rep.* 2017, **7**:9384.

Hayashi M, Tansengco ML, Suganuma N, Szczyglowski K, Krusell L, Ott T, Udvardi M: **Methods for studying nodule development and function.** *Lotus japonicus Handbook*, *Springer. Printed in the Netherlands.* 2005, 53-82.

Hellriegel H, Wilfarth, H: **Untersuchungen uber die Stickstoff-Nahrung der gramineen und leguminosen.** *Zeitschrift fur der verschiedige Rubenzucker des Deutsches Reichs* 1888

Hirakawa Y, Kondo Y, Fukuda H: **TDIF peptide signaling regulates vascular stem cell proliferation via the *WOX4* homeobox gene in *Arabidopsis***. *Plant Cell* 2010, **22**:2618-2629.

Hirakawa Y, Shinohara H, Kondo Y, Inoue A, Nakanomyo I, Ogawa M, Sawa S, Ohashi-Ito K, Matsubayashi Y, Fukuda H: **Non-cell-autonomous control of vascular stem cell fate by a CLE peptide/receptor system**. *Proc. Natl. Acad. Sci. USA* 2008, **105**:15208-15213.

Hirel B, Tétu T, Lea P, Dubois F: **Improving nitrogen use efficiency in crops for sustainable agriculture**. *Sustainability* 2011, **3**:1452-1485.

Ho C-H, Lin S-H, Hu H-C, Tsay Y-F: **CHL1 functions as a nitrate sensor in plants**. *Cell* 2009, **138**:1184-1194.

Horváth B, Domonkos Á, Kereszt A, Szűcs A, Ábrahám E, Ayaydin F, Bóka K, Chen Y, Chen R, Murray JD, et al.: **Loss of the nodule-specific cysteine rich peptide, NCR169, abolishes symbiotic nitrogen fixation in the *Medicago truncatula dnf7* mutant**. *Proc. Natl. Acad. Sci. USA* 2015, **112**:15232-15237.

Huang S, Chen S, Liang Z, Zhang C, Yan M, Chen J, Xu G, Fan X, Zhang Y: **Knockdown of the partner protein OsNAR2.1 for high-affinity nitrate transport represses lateral root formation in a nitrate-dependent manner**. *Sci. Rep.* 2015, **5**:18192.

Huault E, Laffont C, Wen J, Mysore KS, Ratet P, Duc G, Frugier F: **Local and systemic regulation of plant root system architecture and symbiotic nodulation by a receptor-like kinase**. *PLOS Genet.* 2014, **10**:e1004891.

Ito Y, Nakanomyo I, Motose H, Iwamoto K, Sawa S, Dohmae N, Fukuda H: **Dodeca-CLE peptides as suppressors of plant stem cell differentiation**. *Science* 2006, **313**:842-845.

Ito Y, Nishizawa-Yokoi A, Endo M, Mikami M, Toki S: **CRISPR/Cas9-mediated mutagenesis of the *RIN* locus that regulates tomato fruit ripening**. *Biochem. Biophys. Res. Commun.* 2015, **467**:76-82.

Jeudy C, Ruffel S, Freixes S, Tillard P, Santoni AL, Morel S, Journet E-P, Duc G, Gojon A, Lepetit M, et al.: **Adaptation of *Medicago truncatula* to nitrogen limitation is modulated via local and systemic nodule developmental responses**. *New Phytol.* 2010, **185**:817-828.

Karimi M, Inzé D, Depicker A: **GATEWAY™ vectors for *Agrobacterium*-mediated plant transformation**. *Trends Plant Sci.* 2002, **7**:193-195.

Kato K, Kanahama K, Kanayama Y: **Involvement of nitric oxide in the inhibition of nitrogenase activity by nitrate in *Lotus* root nodules**. *J. Plant Physiol.* 2010, **167**:238-241.

Kawaguchi M: ***Lotus japonicus* `Miyakojima' MG-20: an early-flowering accession suitable for indoor handling**. *J. Plant Res.* 2000, **113**:507-509.

Kawaguchi M, Imaizumi-Anraku H, Koiwa H, Niwa S, Ikuta A, Syono K, Akao S: **Root, root hair, and symbiotic mutants of the model legume *Lotus japonicus***. *Mol. Plant Microbe Interact.* 2002, **15**:17-26.

Konishi M, Yanagisawa S: **Roles of the transcriptional regulation mediated by the nitrate-responsive cis-element in higher plants**. *Biochem. Biophys. Res. Commun.* 2011, **411**:708-713.

Konishi M, Yanagisawa S: **Arabidopsis NIN-like transcription factors have a central role in nitrate signalling**. *Nat. Commun.* 2013, **4**:1617.

Konishi M, Yanagisawa S: **Emergence of a new step towards understanding the molecular mechanisms underlying nitrate-regulated gene expression**. *J. Exp. Bot.* 2014, **65**:5589-5600.

Kosslak RM, Bohlool BB: **Suppression of nodule development of one side of a split-root system of soybeans caused by prior inoculation of the other side.** *Plant Physiol.* 1984, **75**:125-130.

Kouchi H, Imaizumi-Anraku H, Hayashi M, Hakoyama T, Nakagawa T, Umehara Y, Suganuma N, Kawaguchi M: **How many peas in a pod? Legume genes responsible for mutualistic symbioses underground**. *Plant Cell Physiol.* 2010, **51**:1381-1397.

Krouk G: **Nitrate signalling: Calcium bridges the nitrate gap**. *Nat. Plants* 2017, **3**:17095.

Krouk G, Lacombe B, Bielach A, Perrine-Walker F, Malinska K, Mounier E, Hoyerova K, Tillard P, Leon S, Ljung K, et al.: **Nitrate-regulated auxin transport by NRT1.1 defines a mechanism for nutrient sensing in plants**. *Dev. Cell* 2010, **18**:927-937.

Krusell L, Krause K, Ott T, Desbrosses G, Krämer U, Sato S, Nakamura Y, Tabata S, James EK, Sandal N, et al.: **The sulfate transporter SST1 is crucial for symbiotic nitrogen fixation in *Lotus japonicus* root nodules**. *Plant Cell* 2005, **17**:1625-1636.

Krusell L, Madsen LH, Sato S, Aubert G, Genua A, Szczyglowski K, Duc G, Kaneko T, Tabata S, de Bruijn F, et al.: **Shoot control of root development and nodulation is mediated by a receptor-like kinase**. *Nature* 2002, **420**:422-426.

Krusell L, Sato N, Fukuhara I, Koch BEV, Grossmann C, Okamoto S, Oka-Kira E, Otsubo Y, Aubert G, Nakagawa T, et al.: **The *Clavata2* genes of pea and *Lotus japonicus* affect autoregulation of nodulation**. *Plant J.* 2011, **65**:861-871.

Kumagai H, Hakoyama T, Umehara Y, Sato S, Kaneko T, Tabata S, Kouchi H: **A novel ankyrin-repeat membrane protein, IGN1, is required for persistence of nitrogen-fixing symbiosis in root nodules of *Lotus japonicus***. *Plant Physiol.* 2007, **143**:1293-1305.

Langmead B, Salzberg SL: **Fast gapped-read alignment with Bowtie 2**. *Nat. Methods* 2012, **9**:357-359.

Lawlor DW, Lemaire G, Gastal F: **Nitrogen, plant growth and crop yeld**. *Plant Nitrogen*. Springer Berlin Heidelberg; 2001:343-367.

Lei Y, Lu L, Liu H-Y, Li S, Xing F, Chen L-L: **CRISPR-P: a web tool for synthetic single-guide RNA design of CRISPR-system in plants**. *Mol. Plant* 2014, **7**:1494-1496.

Lerouge P, Roche P, Faucher C, Maillet F, Truchet G, Promé JC, Dénarié J: **Symbiotic host-specificity of *Rhizobium meliloti* is determined by a sulphated and acylated glucosamine oligosaccharide signal**. *Nature* 1990, **344**:781.

Li H, Handsaker B, Wysoker A, Fennell T, Ruan J, Homer N, Marth G, Abecasis G, Durbin R: **The Sequence Alignment/Map format and SAMtools**. *Bioinformatics* 2009, **25**:2078-2079.

Ligero F, Caba JM, Lluch C, Olivares J: **Nitrate inhibition of nodulation can be overcome by the ethylene inhibitor aminoethoxyvinylglycine.** *Plant Physiol.* 1991, **97**:1221-1225.

Limpens E, Mirabella R, Fedorova E, Franken C, Franssen H, Bisseling T, Geurts R: **Formation of organelle-like N2-fixing symbiosomes in legume root nodules is controlled by *DMI2***. *Proc. Natl. Acad. Sci. USA* 2005, **102**:10375-10380.

Liu K-h, Niu Y, Konishi M, Wu Y, Du H, Sun Chung H, Li L, Boudsocq M, McCormack M, Maekawa S, et al.: **Discovery of nitrate–CPK–NLP signalling in central nutrient–growth networks**. *Nature* 2017, **545**:311-316.

Liu K-H, Tsay Y-F: **Switching between the two action modes of the dual-affinity nitrate transporter CHL1 by phosphorylation**. *EMBO J.* 2003, **22**:1005-1013.

Liu KH, Huang CY, Tsay YF: **CHL1 is a dual-affinity nitrate transporter of Arabidopsis involved in multiple phases of nitrate uptake**. *Plant Cell* 1999, **11**:865-874.

Maekawa T, Kusakabe M, Shimoda Y, Sato S, Tabata S, Murooka Y, Hayashi M: **Polyubiquitin promoter-based binary vectors for overexpression and gene silencing in *Lotus japonicus***. *Mol. Plant Microbe Interact.* 2008, **21**:375-382.

Magori S, Oka-Kira E, Shibata S, Umehara Y, Kouchi H, Hase Y, Tanaka A, Sato S, Tabata S, Kawaguchi M: ***TOO MUCH LOVE*, a root regulator associated with the long-distance control of nodulation in *Lotus japonicus***. *Mol. Plant Microbe Interact.* 2009, **22**:259-268.

Małolepszy A, Urbański DF, James EK, Sandal N, Isono E, Stougaard J, Andersen SU: **The deubiquitinating enzyme AMSH1 is required for rhizobial infection and nodule organogenesis in *Lotus japonicus***. *Plant J.* 2015, **83**:719-731.

Marchive C, Roudier F, Castaings L, Bréhaut V, Blondet E, Colot V, Meyer C, Krapp A: **Nuclear retention of the transcription factor NLP7 orchestrates the early response to nitrate in plants**. *Nat. Commun.* 2013, **4**:1713.

Marsh JF, Rakocevic A, Mitra RM, Brocard L, Sun J, Eschstruth A, Long SR, Schultze M, Ratet P, Oldroyd GED: ***Medicago truncatula NIN*** **is essential for rhizobial-independent nodule organogenesis induced by autoactive calcium/calmodulin-dependent protein kinase**. *Plant Physiol.* 2007, **144**:324-335.

Matamoros MA, Baird LM, Escuredo PR, Dalton DA, Minchin FR, Iturbe-Ormaetxe I, Rubio MC, Moran JF, Gordon AJ, Becana M: **Stress-induced legume root nodule senescence. Physiological, biochemical, and structural alterations**. *Plant Physiol.* 1999, **121**:97-111.

Mayer KFX, Schoof H, Haecker A, Lenhard M, Jürgens G, Laux T: **Role of *WUSCHEL* in regulating stem cell fate in the *Arabidopsis* shoot meristem**. *Cell* 1998, **95**:805-815.

Mergaert P, Uchiumi T, Alunni B, Evanno G, Cheron A, Catrice O, Mausset A-E, Barloy-Hubler F, Galibert F, Kondorosi A, et al.: **Eukaryotic control on bacterial cell cycle and differentiation in the *Rhizobium*–legume symbiosis**. *Proc. Natl. Acad. Sci. USA.* 2006, **103**:5230-5235.

Miller AJ, Cramer MD: **Root nitrogen acquisition and assimilation**. *Plant and Soil* 2005, **274**:1-36.

Miller AJ, Fan X, Orsel M, Smith SJ, Wells DM: **Nitrate transport and signalling**. *J Exp Bot.* 2007, **58**:2297-2306.

Minchin FR: **Regulation of oxygen diffusion in legume nodules**. *Soil Biol. Biochem.* 1997, **29**:881-888.

Miyawaki K, Tabata R, Sawa S: **Evolutionarily conserved CLE peptide signaling in plant development, symbiosis, and parasitism**. *Curr. Opin. Plant Biol.* 2013, **16**:598-606.

Miyazawa H, Oka-Kira E, Sato N, Takahashi H, Wu G-J, Sato S, Hayashi M, Betsuyaku S, Nakazono M, Tabata S, et al.: **The receptor-like kinase KLAVIER mediates systemic regulation of nodulation and non-symbiotic shoot development in *Lotus japonicus***. *Development* 2010, **137**:4317-4325.

Mohd-Radzman NA, Laffont C, Ivanovici A, Patel N, Reid D, Stougaard J, Frugier F, Imin N, Djordjevic MA: **Different pathways act downstream of the CEP peptide receptor CRA2 to regulate lateral root and nodule development**. *Plant Physiol.* 2016, **171**:2536

Morère-Le Paven M-C, Viau L, Hamon A, Vandecasteele C, Pellizzaro A, Bourdin C, Laffont C, Lapied B, Lepetit M, Frugier F, et al.: **Characterization of a dual-affinity nitrate transporter MtNRT1.3 in the model legume *Medicago truncatula***. *J. Exp. Bot.* 2011, **62**:5595-5605.

Mortier V, De Wever E, Vuylsteke M, Holsters M, Goormachtig S: **Nodule numbers are governed by interaction between CLE peptides and cytokinin signaling**. *Plant J.* 2012, **70**:367-376.

Mortier V, Den Herder G, Whitford R, Van de Velde W, Rombauts S, D'Haeseleer K, Holsters M, Goormachtig S: **CLE peptides control *Medicago truncatula* nodulation locally and systemically**. *Plant Physiol.* 2010, **153**:222-237

Murray JD: **Invasion by invitation: rhizobial infection in legumes.** *Mol. Plant Microbe. Interact.* 2011, **24**:631-639.

Nacry P, Bouguyon E, Gojon A: **Nitrogen acquisition by roots: physiological and developmental mechanisms ensuring plant adaptation to a fluctuating resource**. *Plant and Soil* 2013, **370**:1-29.

Nakagawa T, Kurose T, Hino T, Tanaka K, Kawamukai M, Niwa Y, Toyooka K, Matsuoka K, Jinbo T, Kimura T: **Development of series of gateway binary vectors, pGWBs, for realizing efficient construction of fusion genes for plant transformation**. *J. Biosci. Bioeng.* 2007, **104**:34-41.

Nishida H, Handa Y, Tanaka S, Suzaki T, Kawaguchi M: **Expression of the *CLE-RS3* gene suppresses root nodulation in *Lotus japonicus***. *J. Plant Res.* 2016, **129**:909-919.

Nishida H, Tanaka S, Handa Y, Ito M, Sakamoto Y, Matsunaga S, Betsuyaku S, Miura K, Soyano T, Kawaguchi M, et al.: **A NIN-LIKE PROTEIN mediates nitrate-induced control of root nodule symbiosis in *Lotus japonicus***. *Nat. Commun.* 2018, **9**:499.

Nishihama R, Ishikawa M, Araki S, Soyano T, Asada T, Machida Y: **The NPK1 mitogen-activated protein kinase kinase kinase is a regulator of cell-plate formation in plant cytokinesis**. *Genes Dev.* 2001, **15**:352-363.

Nishimura R, Hayashi M, Wu GJ, Kouchi H, Imaizumi-Anraku H, Murakami Y, Kawasaki S, Akao S, Ohmori M, Nagasawa M, et al.: **HAR1 mediates systemic regulation of symbiotic organ development**. *Nature* 2002, **420**:426-429.

Nutman PS: **Studies on the physiology of nodule formationIII. experiments on the excision of root-tips and nodules**. *Ann. Bot.* 1952, **16**:79-103.

Ogawa M, Shinohara H, Sakagami Y, Matsubayashi Y: ***Arabidopsis* CLV3 peptide directly binds CLV1 ectodomain**. *Science* 2008, **319**:294.

Ohkubo Y, Tanaka M, Tabata R, Ogawa-Ohnishi M, Matsubayashi Y: **Shoot-to-root mobile polypeptides involved in systemic regulation of nitrogen acquisition**. *Nat. Plants* 2017, **3**:17029.

Oka-Kira E, Kawaguchi M: **Long-distance signaling to control root nodule number**. *Curr. Opin. Plant Biol.* 2006, **9**:496-502.

Oka-Kira E, Tateno K, Miura K-i, Haga T, Hayashi M, Harada K, Sato S, Tabata S, Shikazono N, Tanaka A, et al.: ***klavier* (*klv*), a novel hypernodulation mutant of *Lotus japonicus* affected in vascular tissue organization and floral induction**. *Plant J.* 2005, **44**:505-515.

Okamoto S, Kawaguchi M: **Shoot HAR1 mediates nitrate inhibition of nodulation in *Lotus japonicus***. *Plant Signal. Behav.* 2015, **10**:e1000138.

Okamoto S, Ohnishi E, Sato S, Takahashi H, Nakazono M, Tabata S, Kawaguchi M: **Nod factor/nitrate-induced *CLE* genes that drive HAR1-mediated systemic regulation of nodulation**. *Plant Cell Physiol.* 2009, **50**:67-77.

Okamoto S, Shinohara H, Mori T, Matsubayashi Y, Kawaguchi M: **Root-derived CLE glycopeptides control nodulation by direct binding to HAR1 receptor kinase**. *Nat. Commun.* 2013, **4**:2191.

Okamoto S, Suzuki T, Kawaguchi M, Higashiyama T, Matsubayashi Y: **A comprehensive strategy for identifying long-distance mobile peptides in xylem sap**. *Plant J* 2015, **84**:611-620.

Oldroyd GED: **Speak, friend, and enter: signalling systems that promote beneficial symbiotic associations in plants**. *Nat. Rev. Microbiol.* 2013, **11**:252-263.

Oldroyd GED, Engstrom EM, Long SR: **Ethylene inhibits the Nod factor signal transduction pathway of *Medicago truncatula***. *Plant Cell* 2001, **13**:1835.

Olsson JE, Nakao P, Bohlool BB, Gresshoff PM: **Lack of systemic suppression of nodulation in split root systems of supernodulating Soybean (*Glycine max* [L.] Merr.) mutants**. *Plant Physiol.* 1989, **90**:1347-1352.

Orea A, Pajuelo P, Pajuelo E, Márquez AJ, Romero JM: **Characterisation and expression studies of a root cDNA encoding for ferredoxin-nitrite reductase from *Lotus japonicus***. *Physiol. Plant.* 2001, **113**:193-202.

Ott T, van Dongen JT, Gu¨nther C, Krusell L, Desbrosses G, Vigeolas H, Bock V, Czechowski T, Geigenberger P, Udvardi MK: **Symbiotic leghemoglobins are crucial for nitrogen fixation in legume root nodules but not for general plant growth and development**. *Curr. Biol.* 2005, **15**:531-535.

Peck MC, Fisher RF, Long SR: **Diverse flavonoids stimulate NodD1 binding to *nod* gene promoters in *sinorhizobium meliloti***. *J. Bacteriol.* 2006, **188**:5417-5427.

Pellizzaro A, Clochard T, Cukier C, Bourdin C, Juchaux M, Montrichard F, Thany S, Raymond V, Planchet E, Limami AM, et al.: **The nitrate transporter MtNPF6.8 (MtNRT1.3) transports abscisic acid and mediates nitrate regulation of primary root growth in *Medicago truncatula***. *Plant Physiol.* 2014, **166**:2152-2165.

Penmetsa RV, Cook DR: **A legume ethylene-insensitive mutant hyperinfected by its rhizobial symbiont**. *Science* 1997, **275**:527.

Peters NK, Frost JW, Long SR: **A plant flavone, luteolin, induces expression of *Rhizobium meliloti* nodulation genes**. *Science* 1986, **233**:977.

Pierce M, Bauer WD: **A rapid regulatory response governing nodulation in soybean.** *Plant Physiol.* 1983, **73**:286-290.

Prosser IM, Massonneau A, Smyth AJ, Waterhouse RN, Forde BG, Clarkson DT: **Nitrate assimilation in the forage legume *Lotus japonicus* L.** *Planta* 2006, **223**:821-834.

Rahayu YS, Walch-Liu P, Neumann G, Römheld V, von Wirén N, Bangerth F: **Root-derived cytokinins as long-distance signals for $NO3^-$-induced stimulation of leaf growth**. *J. Exp. Bot.* 2005, **56**:1143-1152.

Reid DE, Ferguson BJ, Gresshoff PM: **Inoculation- and nitrate-induced CLE peptides of soybean control NARK-dependent nodule formation**. *Mol. Plant Microbe Interact.* 2011, **24**:606-618.

Reid DE, Li D, Ferguson BJ, Gresshoff PM: **Structure–function analysis of the *Gm*RIC1 signal peptide and CLE domain required for nodulation control in soybean**. *J. Exp. Bot.* 2013, **64**:1575-1585.

Remans T, Nacry P, Pervent M, Filleur S, Diatloff E, Mounier E, Tillard P, Forde BG, Gojon A: **The *Arabidopsis* NRT1.1 transporter participates in the signaling pathway triggering root colonization of nitrate-rich patches**. *Proc Natl Acad Sci U S A* 2006, **103**:19206.

Ruffel S, Freixes S, Balzergue S, Tillard P, Jeudy C, Martin-Magniette ML, van der Merwe MJ, Kakar K, Gouzy J, Fernie AR, et al.: **Systemic signaling of the plant nitrogen status triggers specific transcriptome responses depending on the nitrogen source in *Medicago truncatula***. *Plant Physiol.* 2008, **146**:2020-2035.

Ruffel S, Krouk G, Ristova D, Shasha D, Birnbaum KD, Coruzzi GM: **Nitrogen economics of root foraging: Transitive closure of the nitrate–cytokinin relay and distinct systemic signaling for N supply vs. demand**. *Proc. Natl. Acad. Sci. USA* 2011, **108**:18524-18529.

Saito A, Tanabata S, Tanabata T, Tajima S, Ueno M, Ishikawa S, Ohtake N, Sueyoshi K, Ohyama T: **Effect of nitrate on nodule and root growth of soybean (*Glycine max* (L.) Merr.)**. *Int. J. Mol. Sci.* 2014, **15**:4464-4480.

Sasaki T, Suzaki T, Soyano T, Kojima M, Sakakibara H, Kawaguchi M: **Shoot-derived cytokinins systemically regulate root nodulation**. *Nat. Commun.* 2014, **5**:4983.

Sato S, Nakamura Y, Kaneko T, Asamizu E, Kato T, Nakao M, Sasamoto S, Watanabe A, Ono A, Kawashima K, et al.: **Genome structure of the legume, *Lotus japonicus***. *DNA Res.* 2008, **15**:227-239.

Sato T, Maekawa S, Konishi M, Yoshioka N, Sasaki Y, Maeda H, Ishida T, Kato Y, Yamaguchi J, Yanagisawa S: **Direct transcriptional activation of *BT* genes by NLP transcription factors is a key component of the nitrate response in Arabidopsis**. *Biochem. Biophys. Res. Commun.* 2017, **483**:380-386.

Schauser L, Roussis A, Stiller J, Stougaard J: **A plant regulator controlling development of symbiotic root nodules**. *Nature* 1999, **402**:191-195.

Schauser L, Wieloch W, Stougaard J: **Evolution of NIN-like proteins in *Arabidopsis*, rice, and *Lotus japonicus***. *J. Mol. Evol.* 2005, **60**:229-237.

Schnabel E, Journet E-P, Carvalho-Niebel dF, Duc G, Frugoli J: **The *Medicago truncatula SUNN* gene encodes a *CLV1*-like leucine-rich repeat receptor kinase that regulates nodule number and root length**. *Plant Mol. Biol.* 2005, **58**:809-822.

Schoof H, Lenhard M, Haecker A, Mayer KFX, Jürgens G, Laux T: **The stem cell population of *Arabidopsis* shoot meristems is maintained by a regulatory loop between the *CLAVATA* and *WUSCHEL* genes**. *Cell* 2000, **100**:635-644.

Searle IR, Men AE, Laniya TS, Buzas DM, Iturbe-Ormaetxe I, Carroll BJ, Gresshoff PM: **Long-distance signaling in nodulation directed by a CLAVATA1-like receptor kinase**. *Science* 2003, **299**:109-112.

Signora L, De Smet I, Foyer CH, Zhang H: **ABA plays a central role in mediating the regulatory effects of nitrate on root branching in *Arabidopsis***. *Plant J.* 2001, **28**:655-662.

Soyano T, Hirakawa H, Sato S, Hayashi M, Kawaguchi M: **NODULE INCEPTION creates a long-distance negative feedback loop involved in homeostatic regulation of nodule organ production**. *Proc. Natl. Acad. Sci. USA* 2014, **111**:14607-14612.

Soyano T, Kouchi H, Hirota A, Hayashi M: **NODULE INCEPTION directly targets *NF-Y* subunit genes to regulate essential processes of root nodule development in *Lotus japonicus***. *PLOS Genet.* 2013, **9**:e1003352.

Soyano T, Shimoda Y, Hayashi M: **NODULE INCEPTION antagonistically regulates gene expression with nitrate in *Lotus japonicus***. *Plant Cell Physiol.* 2015, **56**:368-376.

Stahl Y, Grabowski S, Bleckmann A, Kühnemuth R, Weidtkamp-Peters S, Pinto Karine G, Kirschner Gwendolyn K, Schmid Julia B, Wink René H, Hülsewede A, et al.: **Moderation of *Arabidopsis* root stemness by CLAVATA1 and ARABIDOPSIS CRINKLY4 receptor kinase complexes**. *Curr. Biol.* 2013, **23**:362-371.

Stahl Y, Wink RH, Ingram GC, Simon R: **A signaling module controlling the stem cell niche in *Arabidopsis* root meristems**. *Curr. Biol.* 2009, **19**:909-914.

Streeter J, Wong PP: **Inhibition of legume nodule formation and N_2 fixation by nitrate**. *Crit. Rev. Plant Sci.* 1988, **7**:1-23.

Suganuma N, Nakamura Y, Yamamoto M, Ohta T, Koiwa H, Akao S, Kawaguchi M: **The *Lotus japonicus Sen1* gene controls rhizobial differentiation into nitrogen-fixing bacteroids in nodules**. *Mol. Genet. Genomics* 2003, **269**:312-320.

Sun C-H, Yu J-Q, Hu D-G: **Nitrate: A Crucial Signal during Lateral Roots Development**. *Front Plant Sci.* 2017, **8**.

Suzaki T, Ito M, Yoro E, Sato S, Hirakawa H, Takeda N, Kawaguchi M: **Endoreduplication-mediated initiation of symbiotic organ development in *Lotus japonicus***. *Development* 2014, **141**:2441-2445.

Suzaki T, Kim CS, Takeda N, Szczyglowski K, Kawaguchi M: ***TRICOT* encodes an AMP1-related carboxypeptidase that regulates root nodule development and shoot apical meristem maintenance in *Lotus japonicus***. *Development* 2013, **140**:353-361.

Suzaki T, Toriba T, Fujimoto M, Tsutsumi N, Kitano H, Hirano H-Y: **Conservation and diversification of meristem maintenance mechanism in *Oryza sativa*: function of the *FLORAL ORGAN NUMBER2* gene**. *Plant Cell Physiol.* 2006, **47**:1591-1602.

Suzaki T, Yano K, Ito M, Umehara Y, Suganuma N, Kawaguchi M: **Positive and negative regulation of cortical cell division during root nodule development in *Lotus japonicus* is accompanied by auxin response**. *Development* 2012, **139**:3997-4006.

Suzaki T, Yoro E, Kawaguchi M: **Leguminous plants: inventors of root nodules to accommodate symbiotic bacteria.** *Int. Rev. Cell Mol. Biol.* 2015, 316:111-158.

Suzuki A, Hara H, Kinoue T, Abe M, Uchiumi T, Kucho K-i, Higashi S, Hirsch AM, Arima S: **Split-root study of autoregulation of nodulation in the model legume *Lotus japonicus***. *J. Plant Res.* 2008, **121**:245-249.

Suzuki W, Konishi M, Yanagisawa S: **The evolutionary events necessary for the emergence of symbiotic nitrogen fixation in legumes may involve a loss of nitrate responsiveness of the NIN transcription factor**. *Plant Signal. Behav.* 2013, **8**:e25975.

Tabata R, Sumida K, Yoshii T, Ohyama K, Shinohara H, Matsubayashi Y: **Perception of root-derived peptides by shoot LRR-RKs mediates systemic N-demand signaling**. *Science* 2014, **346**:343-346.

Takahara M, Magori S, Soyano T, Okamoto S, Yoshida C, Yano K, Sato S, Tabata S, Yamaguchi K, Shigenobu S, et al.: **TOO MUCH LOVE, a novel kelch repeat-containing F-box protein, functions in the long-distance regulation of the legume–*rhizobium* symbiosis**. *Plant Cell Physiol.* 2013, **54**:433-447.

Tian Q, Chen F, Liu J, Zhang F, Mi G: **Inhibition of maize root growth by high nitrate supply is correlated with reduced IAA levels in roots**. *J. Plant Physiol.* 2008, **165**:942-951.

Tian Q-Y, Sun P, Zhang W-H: **Ethylene is involved in nitrate-dependent root growth and branching in *Arabidopsis thaliana***. *New Phytol.* 2009, **184**:918-931.

Tjepkema JD, Winship LJ: **Energy requirement for nitrogen fixation in actinorhizal and legume root nodules**. *Science* 1980, **209**:279-281.

Tsay Y-F, Schroeder JI, Feldmann KA, Crawford NM: **The herbicide sensitivity gene CHL1 of arabidopsis encodes a nitrate-inducible nitrate transporter**. *Cell* 1993, **72**:705-713.

Undurraga SF, Ibarra-Henríquez C, Fredes I, Álvarez JM, Gutiérrez RA: **Nitrate signaling and early responses in Arabidopsis roots**. *J. Exp. Bot.* 2017, **68**:2541-2551.

Van de Velde W, Zehirov G, Szatmari A, Debreczeny M, Ishihara H, Kevei Z, Farkas A, Mikulass K, Nagy A, Tiricz H, et al.: **Plant peptides govern terminal differentiation of bacteria in symbiosis**. *Science* 2010, **327**:1122-1126.

van Noorden GE, Verbeek R, Dinh QD, Jin J, Green A, Ng JLP, Mathesius U: **Molecular signals controlling the inhibition of nodulation by nitrate in *Medicago truncatula***. *Int. J. Mol. Sci.* 2016, **17**:1060.

Vance CP: **Symbiotic nitrogen fixation and phosphorus acquisition. Plant nutrition in a world of declining renewable resources**. *Plant Physiol.* 2001, **127**:390-397.

Vernié T, Kim J, Frances L, Ding Y, Sun J, Guan D, Niebel A, Gifford ML, de Carvalho-Niebel F, Oldroyd GED: **The NIN transcription factor coordinates diverse nodulation programs in different tissues of the *Medicago truncatula* root**. *Plant Cell* 2015, **27**:3410-3424.

Vessey JK, Waterer J: **In search of the mechanism of nitrate inhibition of nitrogenase activity in legume nodules: Recent developments**. *Physiol. Plant.* 1992, **84**:171-176.

Walch-Liu P, Neumann G, Bangerth F, Engels C: **Rapid effects of nitrogen form on leaf morphogenesis in tobacco**. *J. Exp. Bot.* 2000, **51**:227-237.

Wang D, Griffitts J, Starker C, Fedorova E, Limpens E, Ivanov S, Bisseling T, Long S: **A nodule-specific protein secretory pathway required for nitrogen-fixing symbiosis**. *Science* 2010, **327**:1126-1129.

Wang R, Liu D, Crawford NM: **The *Arabidopsis* CHL1 protein plays a major role in high-affinity nitrate uptake**. *Proc. Natl. Acad. Sci. USA* 1998, **95**:15134-15139.

Wang R, Tischner R, Gutiérrez RA, Hoffman M, Xing X, Chen M, Coruzzi G, Crawford NM: **Genomic analysis of the nitrate response using a nitrate reductase-null mutant of Arabidopsis**. *Plant Physiol.* 2004, **136**:2512.

Wang R, Xing X, Wang Y, Tran A, Crawford NM: **A genetic screen for nitrate regulatory mutants captures the nitrate transporter gene *NRT1.1***. *Plant Physiol.* 2009, **151**:472.

Wang Y, Wang L, Zou Y, Chen L, Cai Z, Zhang S, Zhao F, Tian Y, Jiang Q, Ferguson BJ, et al.: **Soybean miR172c targets the repressive AP2 transcription factor NNC1 to activate *ENOD40* expression and regulate nodule initiation**. *Plant Cell* 2014, **26**:4782-4801.

Wopereis J, Pajuelo E, Dazzo FB, Jiang Q, Gresshoff PM, De Bruijn FJ, Stougaard J, Szczyglowski K: **Short root mutant of *Lotus japonicus* with a dramatically altered symbiotic phenotype**. *Plant J.* 2000, **23**:97-114.

Yadav RK, Perales M, Gruel J, Girke T, Jönsson H, Reddy GV: **WUSCHEL protein movement mediates stem cell homeostasis in the *Arabidopsis* shoot apex**. *Genes Dev.* 2011, **25**:2025-2030.

Yan D, Easwaran V, Chau V, Okamoto M, Ierullo M, Kimura M, Endo A, Yano R, Pasha A, Gong Y, et al.: **NIN-like protein 8 is a master regulator of nitrate-promoted seed germination in *Arabidopsis***. *Nat. Commun.* 2016, **7**:13179.

Yano K, Tansengco ML, Hio T, Higashi K, Murooka Y, Imaizumi-Anraku H, Kawaguchi M, Hayashi M: **New nodulation mutants responsible for infection thread development in *Lotus japonicus***. *Mol. Plant Microbe Interact.* 2006, **19**:801-810.

Yashima H, Fujikake H, Sato T, Ohtake N, Sueyoshi K, Ohyama T: **Systemic and local effects of long-term application of nitrate on nodule growth and N_2 fixation in soybean (*Glycine max* [L.] Merr.)**. *Soil Sci. Plant Nutr.* 2003, **49**:825-834.

Yoro E, Suzaki T, Toyokura K, Miyazawa H, Fukaki H, Kawaguchi M: **A positive regulator of nodule organogenesis, NODULE INCEPTION, acts as a negative regulator of Rhizobial infection in *Lotus japonicus***. *Plant Physiol.* 2014, **165**:747-758.

Yu P, Li X, Yuan L, Li C: **A novel morphological response of maize (*Zea mays*) adult roots to heterogeneous nitrate supply revealed by a split-root experiment**. *Physiol. Plant.* 2014, **150**:133-144.

Yuan S, Zhang Z-W, Zheng C, Zhao Z-Y, Wang Y, Feng L-Y, Niu G, Wang C-Q, Wang J-H, Feng H, et al.: ***Arabidopsis* cryptochrome 1 functions in nitrogen regulation of flowering**. *Proc. Natl. Acad. Sci. USA* 2016, **113**:7661-7666.

Zhang H, Jennings A, Barlow PW, Forde BG: **Dual pathways for regulation of root branching by nitrate**. *Proc. Natl. Acad. Sci. USA* 1999, **96**:6529-6534.